JHR 91: 83–183 (2022)
doi: 10.3897/jhr.91.83318
https://jhr.pensoft.net

RESEARCH ARTICLE

JOURNAL OF Hymenoptera RESEARCH
A peer-reviewed open-access journal
The International Society of Hymenopterists

Open access in a taxonomic sense: a morphological and molecular guide to Western Palaearctic *Dusona* (Hymenoptera, Ichneumonidae)

Noah Meier[1], Karin Urfer[1,2], Håkon Haraldseide[3], Hege Vårdal[4], Seraina Klopfstein[1,5]

1 *Naturhistorisches Museum Basel, Augustinergasse 2, CH-4001 Basel, Switzerland* **2** *Naturmuseum St. Gallen, Rorschacher Strasse 263, CH-9016 St. Gallen, Switzerland* **3** *Ålavikvegen 4, 4250 Kopervik, Norway* **4** *Naturhistoriska Riksmuseet, Box 50007, 104 05 Stockholm, Sweden* **5** *Institute of Ecology and Evolution, University of Bern, Baltzerstr. 6, CH-3012 Bern, Switzerland*

Corresponding author: Noah Meier (noah.meier@bs.ch)

Academic editor: Gavin Broad | Received 8 March 2022 | Accepted 6 June 2022 | Published 30 June 2022

https://zoobank.org/430AC937-9D0E-4EC1-8D45-D2FEE73D5E68

Citation: Meier N, Urfer K, Haraldseide H, Vårdal H, Klopfstein S (2022) Open access in a taxonomic sense: a morphological and molecular guide to Western Palaearctic *Dusona* (Hymenoptera, Ichneumonidae). Journal of Hymenoptera Research 91: 83–183. https://doi.org/10.3897/jhr.91.83318

Abstract

In the present time of biodiversity crisis, assessing species diversity by accurate and accessible taxonomic revisions is more crucial than ever. Parasitoid wasps are considered as both one of the most diverse and under-studied groups in the tree of life. *Dusona* Cameron, 1901 (Ichneumonidae, Campopleginae) is with 442 species one of the most species - rich genera of Darwin wasps, but despite the existence of recent keys, species identification has proven difficult to impossible to non-specialists. In this study, we examined about 1,500 *Dusona* specimens from recent and historical collections in Sweden and Switzerland. We provide a photographic guide to diagnostic characters and detailed plates for 57 out of 125 Western Palaearctic *Dusona* species, facilitating species identification based on existing keys. We add 11 and 3 species to the faunistic records of Sweden and Switzerland, respectively. Furthermore, we reconstruct the phylogeny of European *Dusona* based on four standard markers (COI, CAD, ITS2, 28S) for 45 species, complemented with a reliable reference barcode library for 46 species. Even though we can identify several morphologically distinct clades, we do not propose any new subgenera due to prevalent homoplasy of characters. While most species are well separated by barcodes, several morphologically distinct species have barely discriminatory barcode sequences (p-distances < 2%) or are even paraphyletic in this marker,

Copyright *Noah Meier et al.* This is an open access article distributed under the terms of the Creative Commons Attribution License (CC BY 4.0), which permits unrestricted use, distribution, and reproduction in any medium, provided the original author and source are credited.

indicating limitations in the applicability of barcodes for Darwin wasps. This study reveals severe gaps in the inventories of neglected taxa even for well-studied countries such as Sweden and Switzerland. As this study makes species determination for Western Palaearctic *Dusona* more accessible, we encourage more people, including non-specialists, to work with this genus.

Keywords
barcode library, Bayesian phylogenetic analysis, dark taxa, identification, standard markers

Introduction

Incomplete biodiversity data

Biodiversity loss is undoubtedly one of the most urgent problems of the present time. Key drivers of this crisis are rather well known - and as habitat change, pollution, climate change, invasive species and overexploitation of natural resources (Mazor et al. 2018). In order to counteract this biodiversity crisis, the UN declared the protection of biodiversity on land and in water as two of the 17 sustainable development goals (United Nations 2015). It is obvious that comprehensive knowledge of biodiversity is a fundamental basis for conservation approaches. Studies have shown that only between 10–20% of the true species diversity has been discovered and described up to today (~1.2 Million species) and that most undescribed species are expected within insects (Mora et al. 2011). In order to achieve a robust knowledge base about biodiversity and how to protect it, two fundamental steps are necessary. First, we should aim to complete taxon inventories with species occurrence data and speed up the description of new species. Second, we need to make taxonomic knowledge accessible to a wider audience, not only to experts for a specific group, but also for example to students, naturalists and ecologists. By closing this link between taxonomists and a wider audience, we get the opportunity to collect large amounts of distributional and ecological information and will obtain a powerful tool in the fight against biodiversity loss. One outstanding example in biodiversity research is the Swedish Taxonomy Initiative (STI), an all–taxa biodiversity inventory that has the goal to identify all multi-cellular organisms in Sweden (Karlsson et al. 2020b). The Swedish Malaise Trap Project (SMTP) is funded by the STI and is known as one of the most ambitious insect inventories in the world. The main focus of the SMTP are species-rich groups like Diptera and parasitoid Hymenoptera, which are known to be particularly under-researched (Karlsson et al. 2020a, Ronquist et al. 2020).

The diversity of Darwin wasps

Darwin wasps (Ichneumonidae) are believed to have one of the largest gaps between described species (~25,000) (Yu et al. 2016) and expected species diversity (~60,000) (Townes 1969a; Klopfstein et al. 2019a). The enormous diversity of Darwin wasps is certainly connected with their parasitoid life history and corresponding adaptation to certain host species and the physiology and ecology of the latter. The reproductive strategies of Darwin wasps can be rather complex and sometimes include several levels

of parasitism, e.g., Mesochorinae are invariably obligate hyperparasitoids (Broad et al. 2018). It can be assumed that their adaptation to specific hosts makes parasitoid wasps especially vulnerable to environmental changes which affect the latter, and it has been shown that biodiversity loss across trophic levels can have tremendous impacts on entire ecosystems (Cardinale et al. 2012). However, almost no attention has been paid to the conservation of parasitoid wasps due to the lack of taxonomic and ecological knowledge for this group (Shaw and Hochberg 2001).

Campopleginae

Campopleginae belong to the clade of the higher Ophioniformes within Ichneumonidae (Bennett et al. 2019; Klopfstein et al. 2019b) and consist of 65 genera worldwide, of which 43 occur in the Western Palaearctic (Yu et al. 2016). The morphology of Campopleginae is considered as relatively homogenous. Hence, finding apomorphies to differentiate species and genera is often difficult. As a result, the subfamily as a whole and many of its genera are lacking modern taxonomic revisions (Broad et al. 2018). A study focusing on the ribosomal gene 28S retrieved unstable relationships between the different Campopleginae genera (Quicke et al. 2009). Common morphological traits of Campopleginae are: 1) propleuron with an elongated lobe reaching posteriorly to cover part of the fore coxa; 2) subapically notched dorsal valve of ovipositor; 3) petiolate first tergite; 4) clypeus weakly separated from the face; 5) laterally compressed metasoma 6) iridescent compound eyes (Broad et al. 2018).

Taxonomic history of *Dusona*

Dusona Cameron, 1901 is the most species-rich genus within Campopleginae, with 442 species worldwide and 125 species in the Western Palaearctic (Yu et al. 2016), and one of the most species-rich genera among all Darwin wasps. *Dusona* species can be easily recognised on genus level due to some very distinct diagnostic characters: 1) elongated, oval or slit-shaped propodeal spiracle; 2) very strongly compressed metasoma; 3) closed areolet; 4) petiolar suture often obliterated or positioned very low anteriorly. As *Dusona* includes the Campopleginae species with the largest body sizes of up to more than 20 mm, e.g., in *D. falcator* (Fabricius, 1775), it is not surprising that they received the attention of entomologists early on in the 19th century (e.g., Holmgren 1872; Thomson 1887) and the 20th century (e.g., Teunissen 1947). Perhaps for the same reason, *Dusona* attracted the focus of Rolf Hinz and Klaus Horstmann, who were the first to prepare extensive species descriptions, conduct taxonomic revisions and compile keys for the Eastern and Western Palaearctic *Dusona* species (Hinz 1963, 1977, 1985, 1990, 1994; Horstmann 1995, 2009, 2011; Hinz and Horstmann 2004). Undoubtedly, the revisions of the Palaearctic *Dusona* set an excellent basis to work with the genus (Shaw et al. 2016). However, despite the keys, species identification remains rather challenging for *Dusona*, because there are hardly any drawings and no photographs included, and the morphological terminology is sometimes inadequately explained (Hinz and Horstmann 2004; Horstmann 2009). Some of the Palaearctic

Dusona with occurrence in Korea were illustrated by Choi and Lee (2014), but this work only covers 25 species. The application of several characters that are hardly used for other genera of Darwin wasps, such as the shape of the antennal carina or the junction of the epicnemial and transverse carinae on the mesopleuron, further decreases the accessibility of the keys. Hence, it is not surprising that the quality of species determinations in natural history collections is very inconsistent, and misidentifications are rather frequent in the genus (pers. observation, N. Meier).

Ecology

Compared to other Campopleginae, *Dusona* have an even more strongly laterally compressed metasoma. It is possible that this strong compression is an ecological adaptation to hot temperatures and arid habitats, as it minimizes the exposure to sunlight. Indeed, Darwin wasps with laterally compressed metasomata, such as Campopleginae and Anomaloninae, are more likely to be found in the middle of the day than those with dorso-ventral compression or cylindrical metasomal shape (pers. observation, S. Klopfstein). Another hypothesis suggests that the lateral compression of the metasoma is an adaptation for ovipositing in lepidopteran hosts with especially long setae (Broad et al. 2018). Admittedly, other subfamilies such as Ophioninae also share laterally compressed metasomata but are neither active during daytime nor specialized on lepidopteran larvae with long setae. Hence, further research is required to understand the significance of the various factors that contribute to this metasomal shape. Rearing studies have shown that lepidopterans (mostly Geometridae, Noctuidae, Nolidae, Drepanidae, Erebidae and Notodontidae) are the main hosts of *Dusona* (Horstmann 2011; Shaw et al. 2016); only one species, *Dusona minor* (Provancher, 1879), has been reported as a parasitoid of a sawfly of the family Diprionidae, *Monoctenus juniperi* (Linnaeus, 1758), although this record needs independent confirmation (Horstmann 2011). However, for many *Dusona* species, host records are still missing or presumably incomplete. Finding further host records would be a fundamental step towards understanding the ecology and host adaptation of the genus, but it is rarely done, as taxonomic knowledge for both the parasitoid and the host species is required. Collaborations between specialists for both hosts and parasitoids could be an efficient approach to obtain new host records. Host adaptations are often phylogenetically linked, as for instance in spider parasitoids in Pimplinae (Matsumoto 2016). Hence, a molecular phylogeny of *Dusona* could help to further understand the evolutionary processes behind ecology and speciation of the genus (Tschopp et al. 2013).

Molecular taxonomy

In addition, a phylogeny of *Dusona* could help to split the genus into subgenera that reflect its evolution and help to compartmentalize identification and potentially simplify the application of the species keys. Earlier attempts to divide *Dusona* into species groups were often based on homoplastic characters (Hinz 1977), such as the shape of the epicnemial carina or the presence of light yellow colouration on the metasoma

or hind tibia. Hence, Hinz and Horstmann (2004) doubted that these groupings are monophyletic. So far, no molecular methods have been used to reconstruct the intrageneric phylogeny of *Dusona*, which could be very helpful to properly evaluate the significance of these species groups and to define subgenera. Numerous sequences attributed to this genus have been published both on GenBank (n = 850) and BOLD Systems (n = 1900). More than three quarters of these sequences are only determined to genus level, mainly involving specimens from Canada and Costa Rica. The remaining sequences cover COI barcodes for 44 mainly Nearctic and Palaearctic species and very few ribosomal 18S and 28S sequences (Quicke et al. 2009). In order to facilitate ecological studies with *Dusona*, a reliable reference barcode library would be needed (Lue et al. 2021).

The aim of this study is to make *Dusona* available to a wide audience of professional taxonomists, layman entomologists, and ecologists. In order to achieve this, we provide a detailed photographic guide to diagnostic characters and species and supplement the limited faunistic data of *Dusona* in Sweden and Switzerland. Furthermore, we lay the foundation for a reference barcode library for the Western Palaearctic, based on carefully identified voucher specimens deposited in public collections. Finally, we build a phylogenetic framework based on four standard markers, which can be easily expanded in the future.

Materials and methods

Material

In order to do phylogenetic analyses based on molecular data, the availability of recently collected material was crucial for this study. Hence, we mainly used material collected by the SMTP (collection period: 2003–2006). In total, we examined a subsample of ~6,000 Campopleginae (~1/3 of the available SMTP material) including 465 *Dusona* specimens originating from 55 traps dispersed over the country. In addition to the SMTP material, we examined material from various Swedish, Swiss, and Norwegian collections (Table 1).

Table 1. Specimens studied and their depositories. The number of *Dusona* individuals used for morphological (rounded) and molecular analysis is indicated for each source. *In the collection of the NHRS, a total of 500 *Dusona* specimens are available, but only 30 specimens were examined for this study.

Institute / Collection	Acronym	Morphological analysis	Molecular analysis
Musée Cantonale de Zoologie, Lausanne (CH)	MZL	100	0
Naturhistorisches Museum, Basel (CH)	NMB	350	20
Naturhistorisches Museum, Bern (CH)	NMBE	50	0
Naturhistoriska Riksmuseet, Stockholm (SE)	NHRS	30*	0
Naturmuseum, St. Gallen (CH)	NMSG	6	1
Private collection of Hakon Haraldseide, Kopervik (NO)	HH	49	49
Private collection of Niklas Johansson, Habo (SE)	NJ	200	0
Swedish Malasie Trap Project, Skogsby (SE)	SMTP	465	58
Zoologische Staatssammlung, München (DE)	ZSM	50	0
Total		1300	128

Morphological analysis

We used the keys of Hinz and Horstmann (2004) and Horstmann (2009) for species determination. Furthermore, nearly all determined species were checked against either type material or specimens determined by R. Hinz or K. Horstmann from the MZL and ZSM. In this study, we generally follow the terminology of R. Hinz and K. Horstmann for morphological characters, in order to directly refer to their keys. However, in some cases, they deviate from commonly accepted terminology for Darwin wasp morphology (Broad et al. 2018). In these cases, we followed the terminology of Broad et al. (2018). Discrepancies in the keys for *Dusona* (Hinz and Horstmann 2004; Horstmann 2009) from the generally accepted morphological terminology (Broad et al. 2018) are listed in Table 2.

Table 2. Overview of the discrepancies in the terminology used in the *Dusona* keys (Hinz and Horstmann 2004, Horstmann 2009), compared to the commonly accepted terminology (Broad et al. 2018).

Terminology in *Dusona* keys	Terminology in Broad et al. (2018)
Oral carina	Hypostomal carina
Prepectus, Prepectal carina	Epicnemium, Epicnemial carina
Costula	Anterior transverse carina (lateral part of)
Epipleurite	Laterotergite
Mesopleurum	Mesopleuron
Propodeum: Median longitudinal carina	Latero-median longitudinal carina

Imaging and drawings

In order to improve the accessibility of the keys for *Dusona* (Hinz and Horstmann 2004; Horstmann 2009), we produced images of all species in our sample. The images were taken with the photosystem *Keyence VHX 6000*. Both stitching and stacking techniques were used to enhance image quality. Habitus images were taken with 100× magnification (150× for small specimens), while character close-ups were taken with 150× magnification (200× for small specimens). Images were then arranged in plates, each consisting of a habitus image (female, or if not available, male) and six character close-ups. Furthermore, we created a photographic guide for seven diagnostic characters (with four to six character states each). Image processing and figure alignment was made with Adobe Photoshop and InDesign. Additional elements, such as coloured line fragments and arrows, were used to show length ratios or mark hidden characters. In order to improve the understanding of the shape of the epicnemial and the transverse carina, line drawings were made with Adobe Photoshop and placed next to the photographs. Full resolution figure plates are uploaded to Zenodo, DOIs are given in the figure captions.

Faunistic analysis

All specimen data from SMTP was digitized using a preformatted table provided by the Station Linné (Suppl. material 1, https://doi.org/10.5281/zenodo.6535195). Studied

material that was recently collected from Switzerland was digitized in a separate table (Suppl. material 2, https://doi.org/10.5281/zenodo.6535211). Barplots and a species accumulation curve were drawn in R (R Core Team 2017) using the function "specaccum" from the R package VEGAN (Oksanen et al. 2020). We calculated the mean species accumulation curve and corresponding standard deviation based on random permutations of the data. Maps with the trap distribution, the species diversity and species distribution were created in the open-source software QGIS3 (v.3.4; QGIS.org 2022) using the OpenStreetMap as background layer. Where needed, points on the map which represent trap locations were slightly shifted in order to prevent overlapping.

Laboratory protocol

We collected data from the barcoding portion of Cytochrome Oxidase Subunit 1 (COI) as a reference library and from three additional standard markers for phylogenetic reconstruction (28S rRNA, ITS2 rRNA, and the carbamoyl phosphate synthase domain CAD). We used samples of 128 *Dusona* specimens for molecular analysis that were less than 20 years old. As *Dusona* might be the sister genus to the remaining Campopleginae or at least branches off early in the tree (Sharanowski et al. 2021), we chose eight outgroup species representing the entire diversity of the subfamily (Suppl. material 3, https://doi.org/10.5281/zenodo.6535230). Extractions and PCR reactions took place at the University of Basel (Section of Conservation Biology, NLU). DNA extracts are stored at NMB, vouchers are stored in the same place or at NHRS. Of each specimen, one leg with coxa was used to extract DNA. Extractions were done with the DNeasy blood and tissue kit from Qiagen according to the standard protocol, but with a prolonged digestion step over night at 56 °C and two elusion steps with only 50 µl each. The PCR conditions are reported in Suppl. material 4, https://doi.org/10.5281/zenodo.6535284. We used previously published primers for COI (Folmer et al. 1994), 28S (Belshaw and Quicke 1997; Mardulyn and Whitfield 1999), and ITS2 (Quicke et al. 2006). For CAD, we used the forward primer for Ichneumonidae from Klopfstein et al. (2013) (forward – CADfor9s: ATG AAR AGY GTN GGN GAR GTR ATG GC) but modified it by resolving ambiguous positions according to a preliminary alignment including several Campopleginae sequences (new primer for9sB: ATG AAG AGC GTT GGT GAA GTT ATG GC). As the reverse primer, we newly designed a primer (reverse – CADIchnRb1B: ACC AAT GAC CAT CGT GTA ATT TCC). The PCRs for CAD were run at an annealing temperature of 52 °C. Two additional internal primers for degenerated COI sequences were used; forward FA336 and reverse RA435 (Johansson and Klopfstein 2020), these primers were combined with LCO/HCO and run on an annealing temperature at 50 °C. The quality of the PCR products was then checked on a 2% agarose electrophoresis gel and they were sent for cleanup and sequencing to Macrogen Europe in the Netherlands. COI data from Norway was produced by the Barcoding of Life consortium in Guelph, following their standard protocols.

Molecular analyses

Sequence cleaning and alignments of the protein-coding genes were done with MEGA7 (Kumar et al. 2016), while the two ribosomal genes were aligned using the E-INS-i strategy on the MAFFT web server (Katoh et al. 2019). No gaps or stop codons were detected in COI and CAD. Uncorrected p-distances for COI were calculated in MEGA7, using pairwise deletions. For the phylogenetic analysis, we combined all four markers into a concatenated alignment, while only including specimens that had at least 1,000 bp of sequence data in total. Phylogenies were reconstructed under Bayesian inference with MrBayes (Ronquist et al. 2012), both for each gene individually and for the four genes concatenated. We partitioned the protein-coding genes into 1st and 2nd versus 3rd codon positions, while no partitioning was applied to the ribosomal genes. We let MrBayes sample over the complete GTR model space and used a separate gamma distribution and proportion of invariant sites for each partition to model among-site rate variation. We ran 10 million generations, sampling every 1,000 generations and using a burn - in of 50% (for input files of MrBayes, see Suppl. material 5, https://doi.org/10.5281/zenodo.6535309). All phylogenetic analyses were run on the UBELIX Cluster of the University of Bern. Nodes with support values below 50% are indicated as polytomies. Phylogenetic trees were drawn with FigTree (v.1.4.4) and species groups were indicated on the trees using Adobe Illustrator. We plotted character states on the genus tree in order to find morphologically distinct species groups as candidates for subgenus divisions.

Results

Assessment and illustration of diagnostic characters

Horstmann (2009) used several characters not commonly used for identification in Darwin wasps. We here assess and illustrate the seven most important characters in detail (ordered from anterior to posterior), covering the shape of the antennal carina (I), the junction of the genal and hypostomal carinae (II), the shape of the epicnemial and transverse carinae (III), the sculpture of the mesopleuron (IV), the shape and sculpture of the propodeum (V), the shape and sculpture of the first tergite (VI) and the separation of the third laterotergite (VII). These characters were chosen because they are either especially important for the identification of *Dusona* species or their states are sometimes difficult to assess based on the key couplets (Hinz and Horstmann 2004; Horstmann 2009).

The shape of the antennal carina (I)

The antennal carina (*sensu* Hinz and Horstmann 2004) equals the rim surrounding the antennal sockets. This character is rarely used in other ichneumonid genera, in

which the antennal carina is usually flat and narrow (Fig. 1a). This is also the case in most *Dusona* species; however, in several species, the antennal carina shows a large diversity of dorsal extensions (Fig. 1c–f). In some species they appear as nose-like bulges (Fig. 1c, d), while in other species, the rim of the antennal sockets is extended into an ear-like crescent-shaped plate (Fig. 1f), sometimes also called auricles (Broad et al. 2018), such as in *Tryphon latrator* (Fabricius, 1781), or just slightly raised (Fig. 1e). These dorsal extensions are often accompanied by some sort of transverse striation (Fig. 1d, e). Furthermore, some species show a strong longitudinal carina between the antennal sockets (Fig. 1b). In specimens, where the scape is positioned parallel to the frons pointing upwards, the examination of the antennal carina can be difficult. In certain cases, it is necessary to either relax the specimen in water and shift one antenna or to separate one antenna from the antennal socket in order to identify the species.

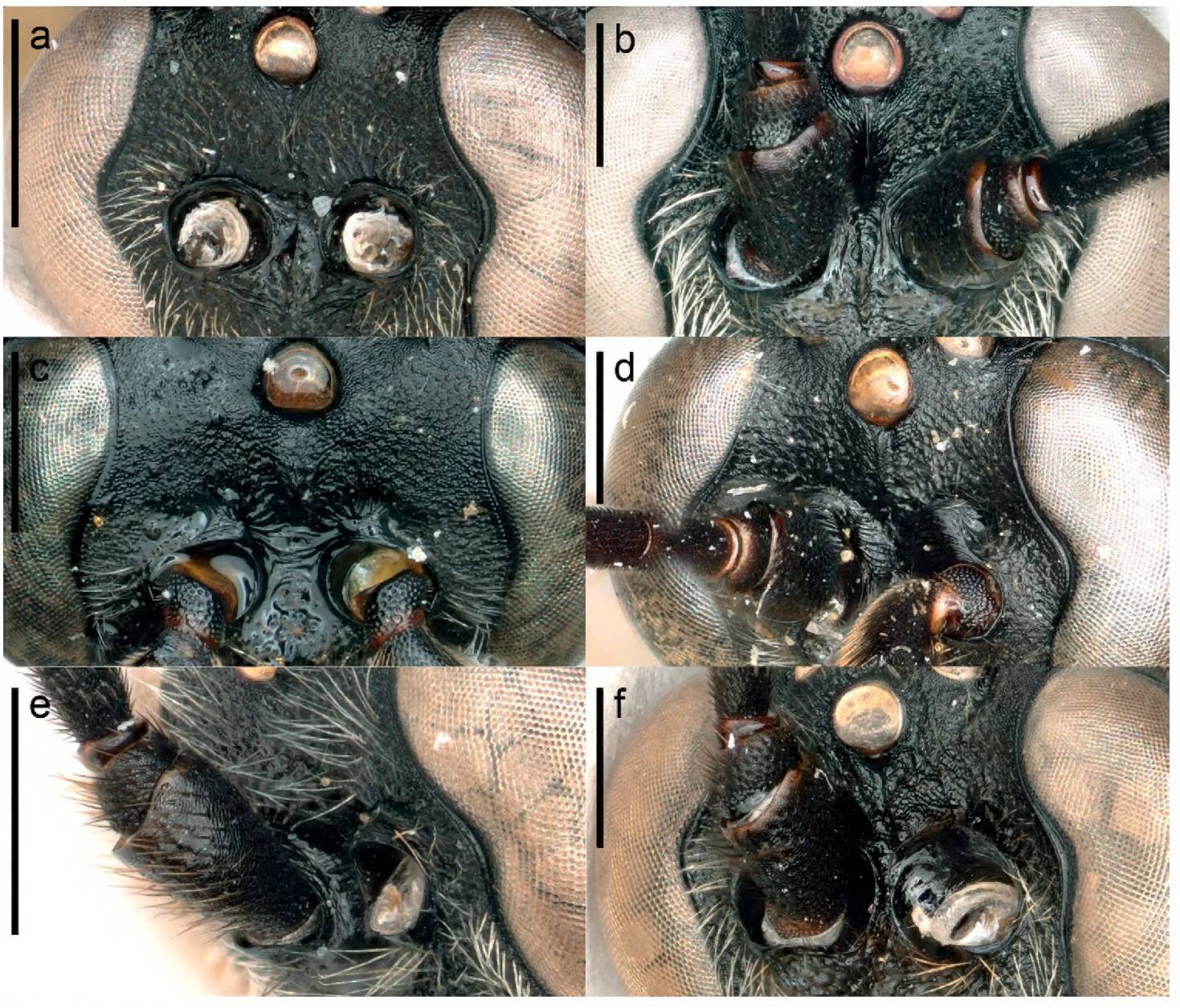

Figure 1. Shape of the antennal carina. **a** antennal carina narrow and flat (*D. blanda*) **b** antennal carina narrow and flat, frons with a strong median longitudinal keel (*D. carinifrons*) **c** antennal carina widened dorsally to a rather inconspicuous nose-like projection (*D. stygia*) **d** antennal carina widened dorsally to a large nose-like projection with transverse striae (*D. pineticola*) **e** antennal carina slightly raised dorsally and transverse striate (*D. sobolicida*) **f** antennal carina raised and strongly bent upwards forming an ear-like, crescent-shaped plate (*D. infesta*). Scale bars: 0.5 mm. https://doi.org/10.5281/zenodo.6340012.

This character is used in more than 20 couplets throughout the keys of Hinz and Horstmann (2004) and Horstmann (2009). Our molecular analysis reveals no phylogenetic relationship between species that show any of these dorsal extensions of the antennal carina (see section *molecular analysis*).

The junction of the genal and hypostomal carinae (II)

The genal carina (continuous with the more dorsal occipital carina) separates the gena from the occiput. The hypostomal carina separates the occiput from the hypostoma. The junction of the genal carina and the hypostomal carina is usually either at the base of the mandible or positioned more dorsally. The genal index describes the ratio of the distance between the junction of the genal and the hypostomal carinae and the base of the mandibles (green line in Fig. 2) to the basal width of the mandibles (blue line in Fig. 2). In some species the genal carina can be slightly obliterated ventrally, which makes it difficult to identify the position of the junction with the hypostomal carina (Fig. 2c). Furthermore, in some species the junction of the genal and the hypostomal carina can be distinctly raised, forming a lopsided triangular pyramid (Fig. 2d, e), *sensu* Hinz and Horstmann (2004). In specimens where the head is closely positioned to the mesosoma, the examination of this character can be tricky. In certain cases it is necessary to either relax the specimen in water and shift the head slightly in its position or separate the head from the rest of the body for proper examination of this character.

Hinz and Horstmann (2004) and Horstmann (2009) both use this character in more than a dozen couplets of their keys. Our phylogenetic analysis reveals that the species that possess a lopsided triangular pyramid constitute the monophyletic *mercator*-group as it was previously proposed by Hinz and Horstmann (2004), see also section *molecular analysis*. In addition, a genal index of zero is one of the diagnostic characters for the *flagellator* group and the *angustifrons* group; however, it also occurs in several other species, such as *D. thomsoni* Hinz, 1963 and *D. pulchripes* (Holmgren, 1872).

The shape of the epicnemial and transverse carinae (III)

The epicnemial carina separates the mesopleuron from the epicnemium, while the transverse carina separates the ventral part of the epicnemium from its pleural part. The former is present in nearly all ichneumonids, while the latter is very rare outside *Dusona*. The epicnemial carina is divided into a ventral part and pleural part. These two parts are separated at the junction of the epicnemial carina with the transverse carina. In some *Dusona*, the pleural part of the epicnemial carina is complete and merges dorsally with the anterior edge of the mesopleuron (Fig. 3c), such as in *D. xenocampta* (Förster, 1868). However, in many species the pleural part of the epicnemial carina can be replaced or covered by wrinkles (Fig. 3a, b) and be obliterated dorsally (Fig. 3b), such as in *D. tenuis* (Förster, 1868) or even

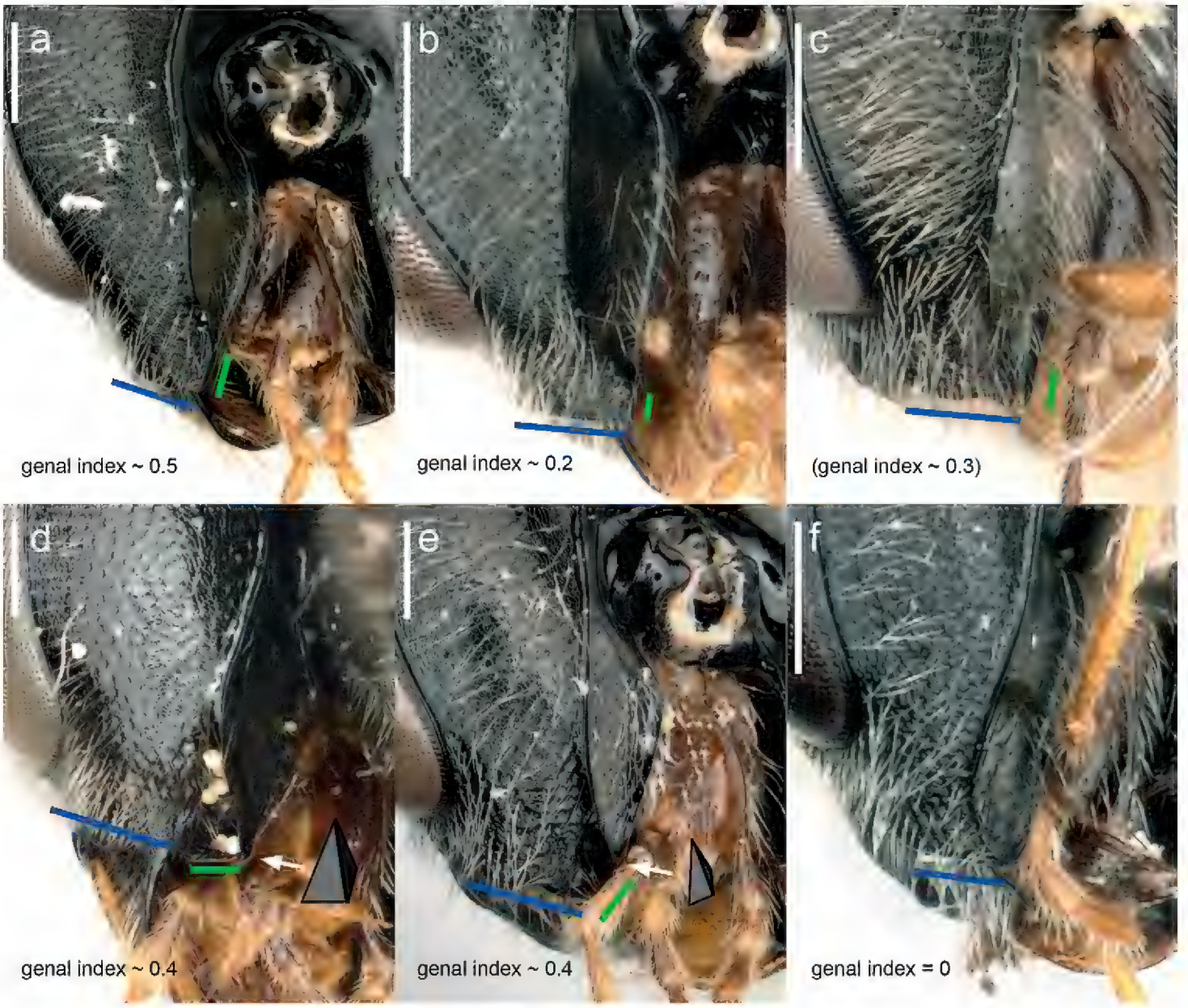

Figure 2. Junction of the genal and the hypostomal carinae. **a, b** genal carina meets the hypostomal carina clearly above the base of the mandible (**a** *D. blanda*; **b** *D. rubidatae*) **c** genal carina meets hypostomal carina clearly above the base of the mandible, occipital carina obliterated close to the junction (*D. tenuis*) **d, e** genal and hypostomal carina distinctly raised, their junction forming a lopsided triangular pyramid (**d** *D. mercator* **e** *D. aurita*) **f** genal carina meets the hypostomal carina at the base of the mandibles (*D. flagellator*). Genal index = distance between the base of the mandibles and the junction of the genal and hypostomal carina (green bars) / the basal length of the mandibles (blue bars). Scale bars: 0.25 mm. https://doi.org/10.5281/zenodo.6362512.

completely obliterated (Fig. 3d), such as in *D. juvenilis* (Förster, 1868). In the latter case, the pleural part of the epicnemium is completely fused with the mesopleuron (Fig. 3d).

Hinz and Horstmann (2004) and Horstmann (2009) both use this character in more than a dozen couplets of their keys. They propose that the ventral part of the epicnemial carina can either merge with the transverse carina or the pleural part of the epicnemial carina. This description can be misleading, as the ventral part of the epicnemial carina merges usually with both the pleural part and the transverse carina (except when one of these is obliterated). Nevertheless, it is pos-

sible to judge which half of these couplets to follow by comparing the height of the transverse carina and the pleural part of the epicnemial carina, which is usually described as secondary characters in these couplets. Our molecular analysis suggests that individual character states of epicnemial and transverse carina do not reflect phylogenetic relationships in *Dusona*. On the contrary, this character appears highly homoplastic; for instance, the strongly raised transverse carina occurs in the whole *flagellator* group, the *mercator* group, some members of the *angustifrons* group, and in *D. tenuis* (Fig. 3b).

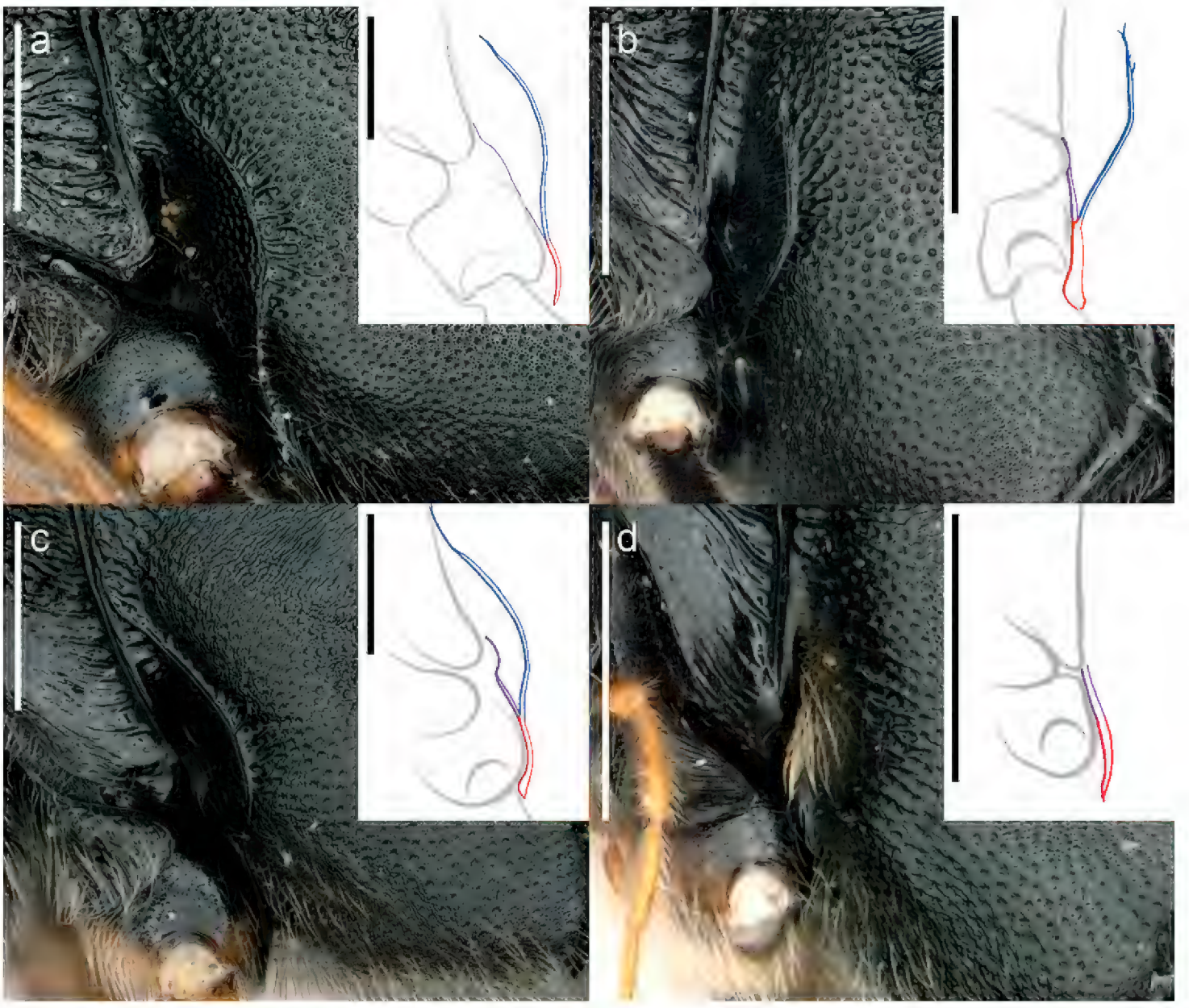

Figure 3. Shape of the epicnemial and transverse carinae. **a** ventral part of the epicnemial carina merging with the pleural part, both carinae low, transverse carina indistinct (*D. bicoloripes*) **b** ventral part of the epicnemial carina distinctly raised, merging with the transverse carina, pleural part of the epicnemial carina low and dorsally obliterated (*D. tenuis*) **c** ventral part of the epicnemial carina only slightly raised, merging with the pleural part or the transverse carina, pleural part of the epicnemial carina dorsally complete and merging with anterior edge of the mesopleuron (*D. xenocampta*) **d** ventral part of the epicnemial carina slightly raised, merging with the transverse carina, pleural part of the epicnemial carina completely obliterated (*D. juvenilis*). red = ventral part of the epicnemial carina. blue = pleural part of the epicnemial carina. purple = transverse carina. Structures in grey are for orientation purposes. Scale bars: 0.5 mm. https://doi.org/10.5281/zenodo.6362741.

The sculpture of the mesopleuron (IV)

The sculpture of the mesopleuron shows a rather broad range of variability within *Dusona*. It can be very shiny in some species (Fig. 4a) or appear rather dull due to a coriaceous background (Fig. 4d–f). Many species have a strong punctation on the mesopleuron, which can be dense (puncture diameter > interspace between punctures; Fig. 4b), rather dense (puncture diameter = interspace between punctures; Fig. 4d), or dispersed (puncture diameter < interspace between punctures; Fig. 4e). Only a few species have an irregularly wrinkled mesopleuron, instead of the punctation (Fig. 4f). The sculpture of the depression in front of the speculum can either be wrinkled (Fig. 4a), finely striate (Fig. 4b), granulate strigose or coriaceous (Fig. 4c). There are several couplets in Horstmann (2009) asking whether the longitudinal striae merge anteriorly with the punctation or with an area without punctation. This character is difficult to assess in our opinion. We rather suggest checking whether the punctation is distinct on the anterior dorsal part of the mesopleuron (Fig. 4d), such as in *D. blanda* (Förster, 1868) or if the punctures are very small and dispersed or obliterated (Fig. 4e), such as in *D. humilis* (Förster, 1868).

This character is used in more than 20 couplets throughout the keys of Hinz and Horstmann (2004) and Horstmann (2009). Our molecular analysis suggests that the sculpture of the mesopleuron is not useful to separate species groups at basal nodes in the phylogeny of *Dusona*. However, the sculpture of the mesopleuron usually shows less intraspecific variability than other characters and is thus useful for differentiation at species level.

The shape and sculpture of the propodeum (V)

The propodeum of Darwin wasps carries many systematically relevant characters. In *Dusona*, mainly three types of characters of the propodeum are used for species identification: the general shape (e.g., central depression), the carination, and the sculpture of the surface. The propodeum in *Dusona* can either be weakly depressed (Fig. 5a), broadly and shallowly depressed (Fig. 5b, c), narrowly but deeply depressed to a longitudinal furrow (Fig. 5d, e), or broadly and deeply depressed (Fig. 5f). The propodeal carination can be obliterated to a variable extent (Fig. 5a, b), or almost complete with a distinct anterior transverse carina and lateromedian longitudinal carinae (Fig. 5c, less distinct in Fig. 5f). The surface sculpture of the propodeum is usually either wrinkled or coriaceous (often anteriorly). Especially in species with a deep and narrow median longitudinal furrow, the furrow can be expected to have distinct short (Fig. 5d) or long (Fig. 5e) transverse wrinkles. In some species, in which the propodeum is often only weakly depressed, the propodeal sculpture is very irregularly wrinkled (Fig. 5a).

The propodeum is described in nearly all terminal couplets in Hinz and Horstmann (2004) and Horstmann (2009). Our molecular analysis suggests that the shape and sculpture of the propodeum is not very useful to separate species groups at basal nodes

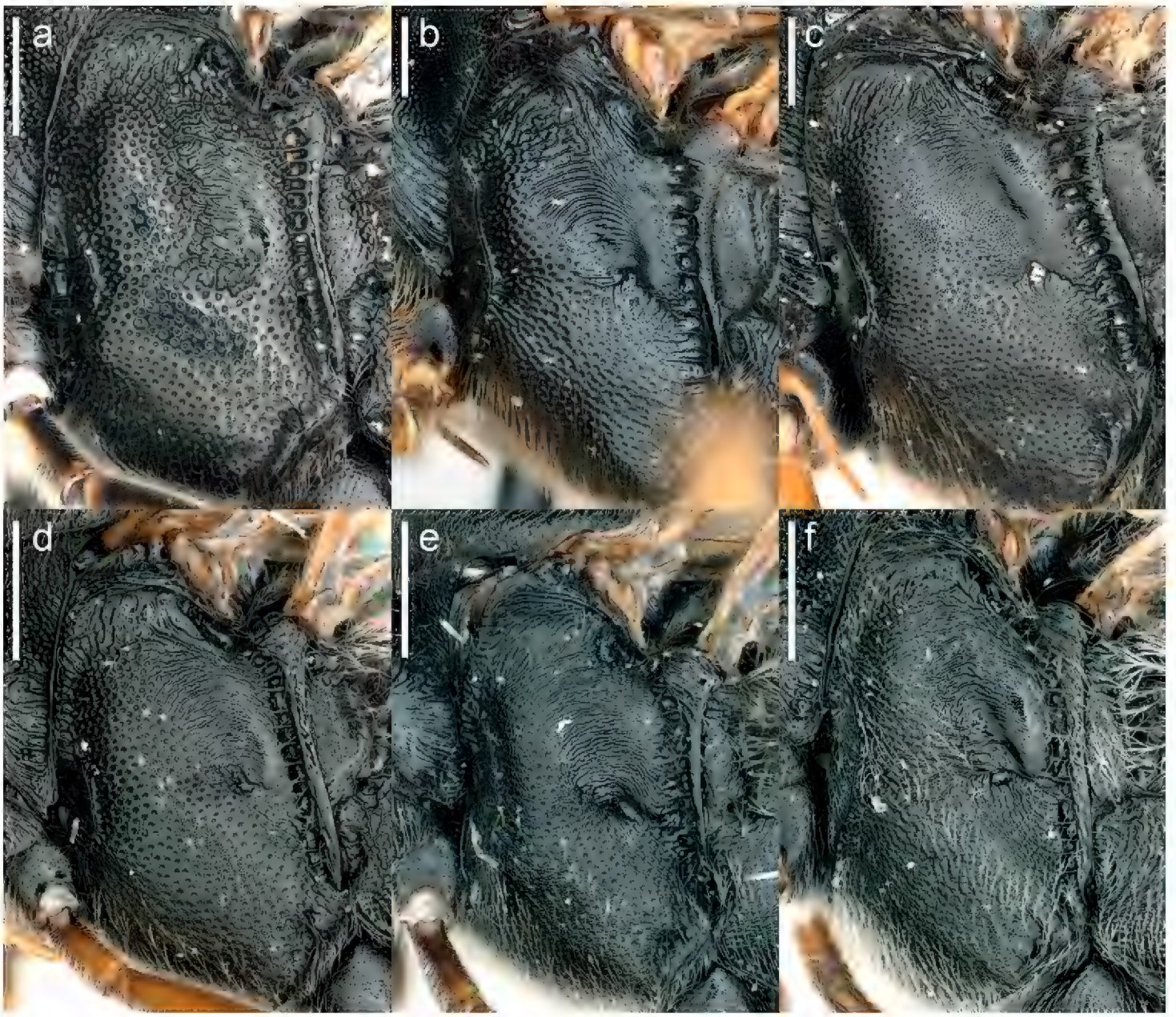

Figure 4. Sculpture of the mesopleuron. **a** mesopleuron with a distinct and dense or rather dense punctation on a smooth background, depression in front of speculum wrinkled (*D. bucculenta*) **b** mesopleuron with a dense punctation, background slightly coriaceous and shining, depression in front of speculum with fine longitudinal striae (*D. falcator*) **c** mesopleuron with a rather dense to dense punctation, background coriaceous and slightly shining, depression in front of the speculum with a few longitudinal striae dorsally and granulate-strigose ventrally (*D. obliterata*) **d** mesopleuron with a distinct and rather dense punctation, background distinctly coriaceous, slightly shining, depression in front of the speculum with longitudinal striae merging with the punctation anteriorly (*D. blanda*) **e** mesopleuron with a rather dispersed punctation, background distinctly coriaceous and dull, depression in front of the speculum granulate-strigose or with some longitudinal striae that merge with an area without punctation (*D. humilis*) **f** mesopleuron with wrinkles centrally, rugose punctate dorsally and ventrally, rather dull (*D. leptogaster*). Scale bars: 0.5 mm. https://doi.org/10.5281/zenodo.6368561.

in the phylogeny of *Dusona*. Even though the characters of the propodeum often show some intraspecific variability, they are in many cases the best or even only character to differentiate closely related species. One such example are males of *D. flagellator* (Fabricius, 1793), which are best separated from *D. notabilis* (Förster, 1868) by the distinctly depressed propodeum with long transverse wrinkles (Figs 5e, 47e). While

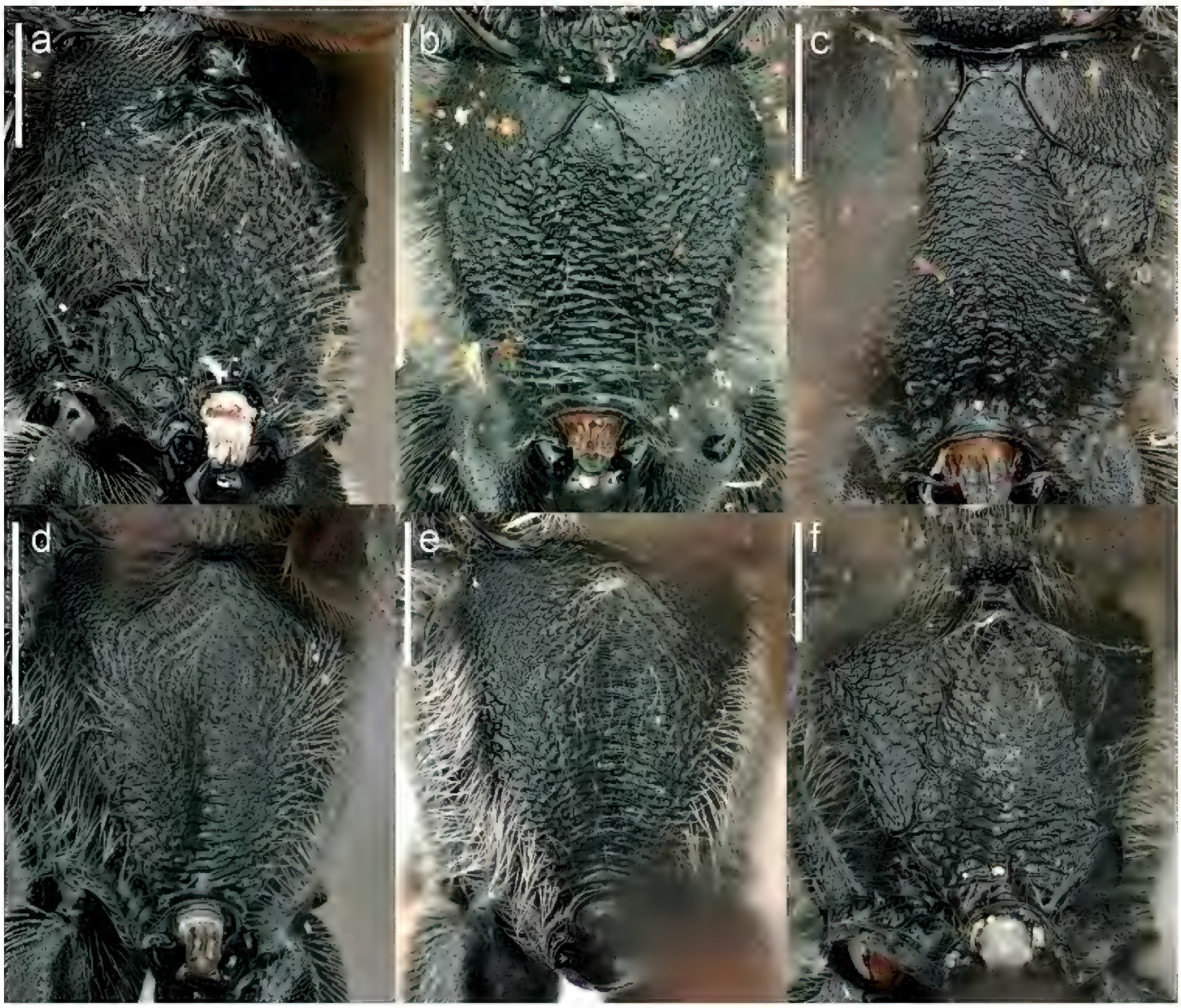

Figure 5. Shape and sculpture of the propodeum. **a** propodeum hardly depressed with irregular wrinkles (*D. bicoloripes*) **b** propodeum broadly and shallowly depressed, irregularly wrinkled anteriorly and with transverse wrinkles medially and posteriorly (*D. stygia*) **c** propodeum broadly and shallowly depressed, rugose or irregularly wrinkled with some short transverse wrinkles posteriorly and a rather complete carination (*D. terebrator*) **d** propodeum narrowly and deeply depressed with short transverse wrinkles in the sulcus (*D. angustifrons*) **e** propodeum narrowly and deeply depressed with long transverse wrinkles in the sulcus (*D. flagellator*) **f** propodeum rather broadly and deeply depressed with distinct transverse wrinkles posteriorly and medially (*D. stragifex*). Scale bars: 0.5 mm. https://doi.org/10.5281/zenodo.6368594.

the degree of depression of the propodeum as it is used in Horstmann (2009) can be difficult to judge, determining the presence and prevalence of transverse wrinkles is usually much easier.

The shape and sculpture of the first tergite (VI)

The first tergite is commonly used to characterize Darwin wasps and can even be diagnostic at subfamily-level, for example the presence of the glymma or the position of the spiracle (Broad et al. 2018). In *Dusona*, however, the presence and size of the glymma

is highly variable between different species, ranging from large glymma (Fig. 6a, b), to medium-sized or small glymma (Fig. 6c–d), to glymma absent (Fig. 6e, f). In front of the glymma, some *Dusona* species show distinct sculpture in the form of short, transverse grooves (Fig. 6a) such as *D. insignita* (Förster, 1868), or long transverse wrinkles (Fig. 6b) such as *D. nidulator* (Fabricius, 1804). The lateral sides of the first tergite can be bordered by variably distinct longitudinal carinae. The area between these carinae (if present) often has a different surface sculpture from the rest of the tergite, e.g., coriaceous instead of smooth (Fig. 6a–e).

This character is used in many couplets throughout the keys of Hinz and Horstmann (2004) and Horstmann (2009). Our molecular analysis suggests that characters concerning the first tergite, such as the presence of the glymma, lateral areas and sculpture, are hardly conserved in any of the groupings within the phylogeny of *Dusona*.

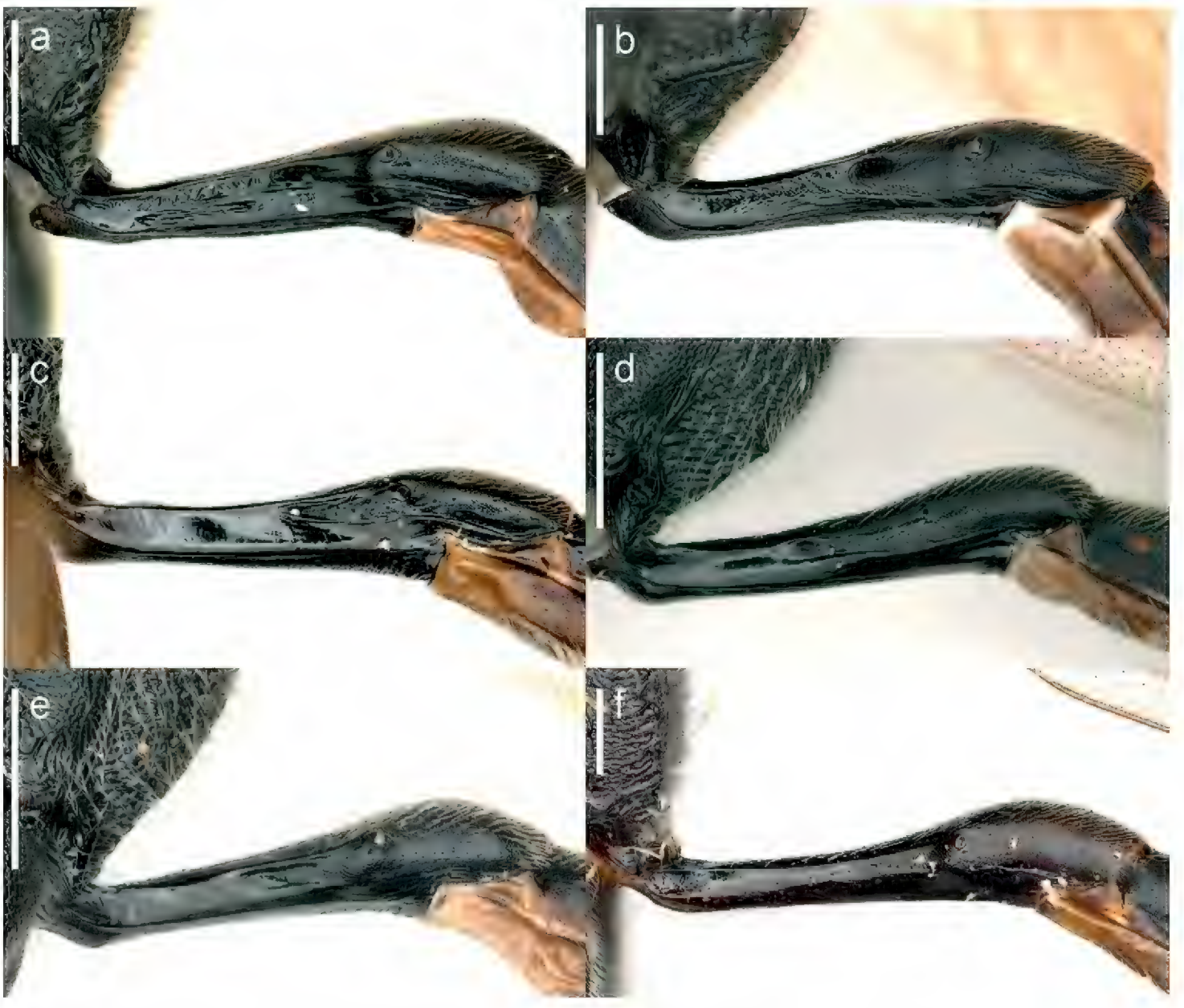

Figure 6. Shape and sculpture of the first tergite. **a** petiole with long row of short transverse wrinkles in front of a large glymma (*D. insignita*) **b** petiole with long row of long transverse wrinkles in front of a large glymma (*D. nidulator*) **c** petiole very fine sculpture in front of a large glymma (*D. bicoloripes*) **d** petiole with a small glymma at the anterior edge of narrow lateral areas (*D. angustifrons*) **e** petiole without a glymma but narrow lateral areas (*D. limnobia*) **f** petiole with indistinct glymma or lateral areas (*D. pineticola*). Scale bars: 0.5 mm. https://doi.org/10.5281/zenodo.6368627.

Furthermore, these characters are sometimes also subject to intraspecific variability, e.g., the presence or absence of small glymmae within species of the *flagellator* group (see also Horstmann 2009).

The separation of the third laterotergite (VII)

In the Western Palaearctic *Dusona* species, the second laterotergite is always completely separated from the tergite by a crease, while the fourth laterotergite is always completely fused with the tergite. In contrast, the third laterotergite shows a broad range of interspecific variability, from completely fused with the tergite to separated from the tergite by a crease of variable length. This crease can be seen as a thickened straight line and is often marked with black (Fig. 7e). However, also species with a

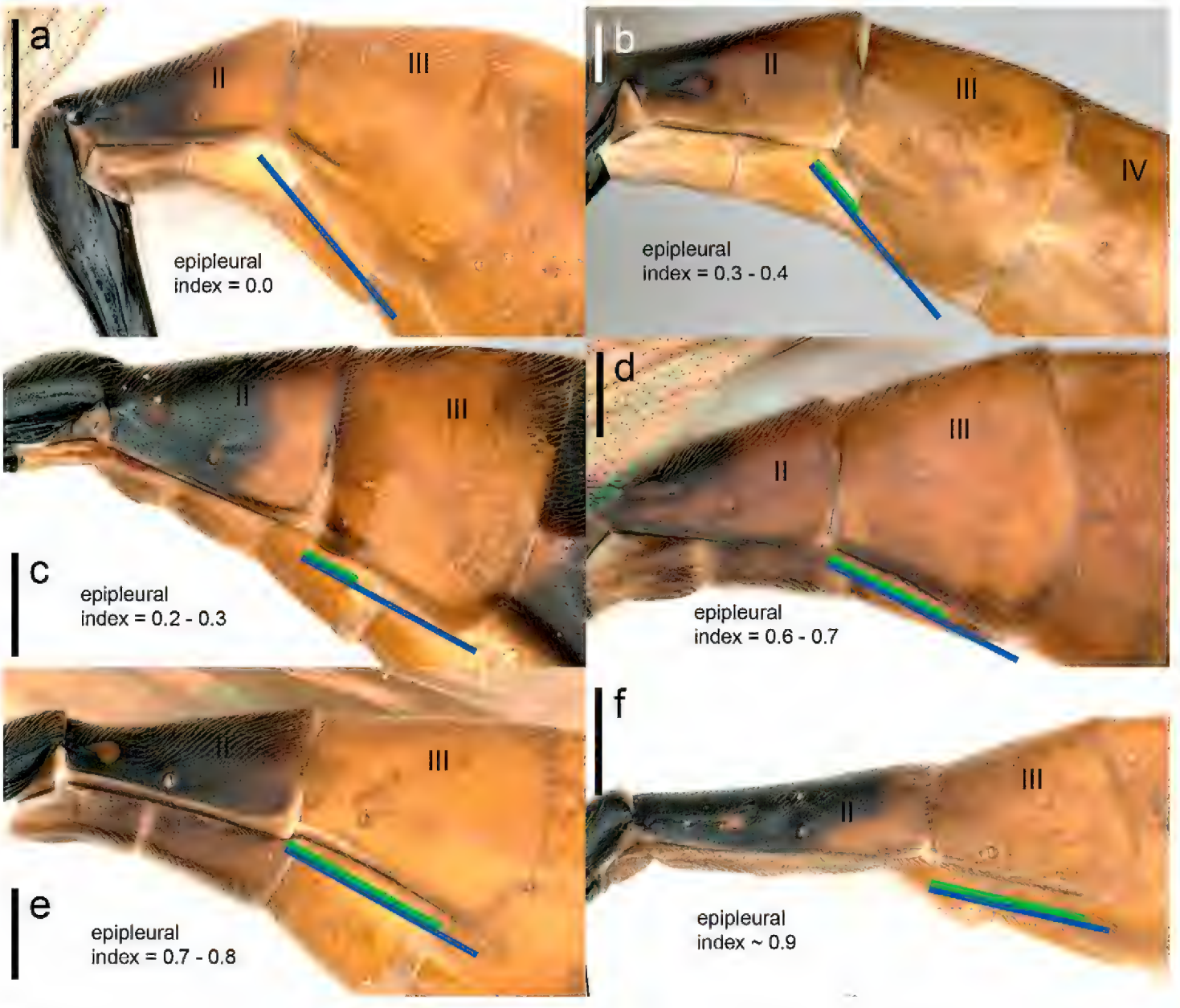

Figure 7. Separation of third laterotergite. **a** laterotergite completely fused with the tergite, its ventral edge thin and curved (*D. sobolicida*) **b–f** laterotergite folded in anteriorly, separated from the tergite by a crease, mind that the crease is secondarily folded back in *D insignita* **b** *D. pugillator* **c** *D. insignita* **d** *D. stragifex* **e** *D. nidulator* **f** *D. leptogaster*. Blue bars indicate the lateral length of the third tergite. Green bars indicate the length of the crease separating the laterotergite from the tergite. Epipleural index = length of the crease / lateral length of the tergite. Scale bars: 0.5 mm. https://doi.org/10.5281/zenodo.6368663.

completely fused third laterotergite can have a black longitudinal mark on this tergite, called "black lateral stripe" in Hinz and Horstmann (2004), which is then well separated from the thin and curved ventrolateral edge of the tergite (Fig. 7a). The epipleural index describes the ratio of the length of the crease to the lateral length of the third tergite. In some species, such as *D. insignita* (Fig. 7c), the third laterotergite is separated from the tergite by a crease but secondarily folded back. In such cases, only the length of the crease anterior to the secondary fold back is measured for the epipleural index.

This character is used in both keys for Eastern (Hinz and Horstmann 2004) and Western Palaearctic *Dusona* (Horstmann 2009) as the first couplet, thus dividing *Dusona* species into 2 large groups. Our molecular analysis (see below) reveals that this character is in part correlated to phylogenetic relationships (see section *molecular analysis*).

Faunistic analysis

Among the ~6,000 examined Campopleginae from the SMTP material, we have found 465 *Dusona* specimens (Suppl. material 1, https://doi.org/10.5281/zenodo.6535195). This means that *Dusona*, the most species rich genus within Campopleginae, comprised almost 8% of the studied sample. In total, the 465 specimens were identified to 42 different species, of which 9 new for Sweden and 31 among the 54 *Dusona* species previously recorded for Sweden. 23 of the previously recorded species for Sweden have been found in our sample. In 41 out of 55 Malaise traps, at least one *Dusona* species was collected (Fig. 8). Habitat and species diversity correlations could not be analysed quantitatively because the habitat of each trap was described individually. However, the three traps with the highest species diversity are described as follows: Trap 7: Uppland, Älvkarleby kommun, Båtfors; dry meadow with birch, field of fire (16 species). Trap 22: Öland, Mörbylånga kommun, Gamla Skogsby (Kalkstad); nemoral grove (12 species). Trap 1008: Småland, Nybro kommun, Alsterbro/Alsterån; mixed forest (10 species). *D. bicoloripes* (Ashmead, 1906) was the species that was collected by the highest number of traps (n = 19), followed by *D. blanda* (n = 15) and *D. circumspectans* (Förster, 1868) (n = 9). In contrast to these apparently common and widespread species, there were also 10 species for which only a single specimen was found in the SMTP sample. We have found no clear trends in the number of *Dusona* species and individuals on the latitudinal axis (Fig. 10a, b). However, the seven northern-most traps (>63°N) have each only caught very few specimens and species. Apparently, some of the new species for Sweden were more likely to be found in southern or coastal areas (Fig. 9). The sample-based species accumulation curve is not yet saturated (Fig. 10). Hence, it is very likely that more species would be found, if a larger sample were examined.

We report 11 *Dusona* species new to the faunistic records of Sweden and 3 *Dusona* species new to the faunistic records of Switzerland (Yu et al. 2016; Klopfstein et al. 2019c; Dyntaxa 2022). While most of the newly recorded species for

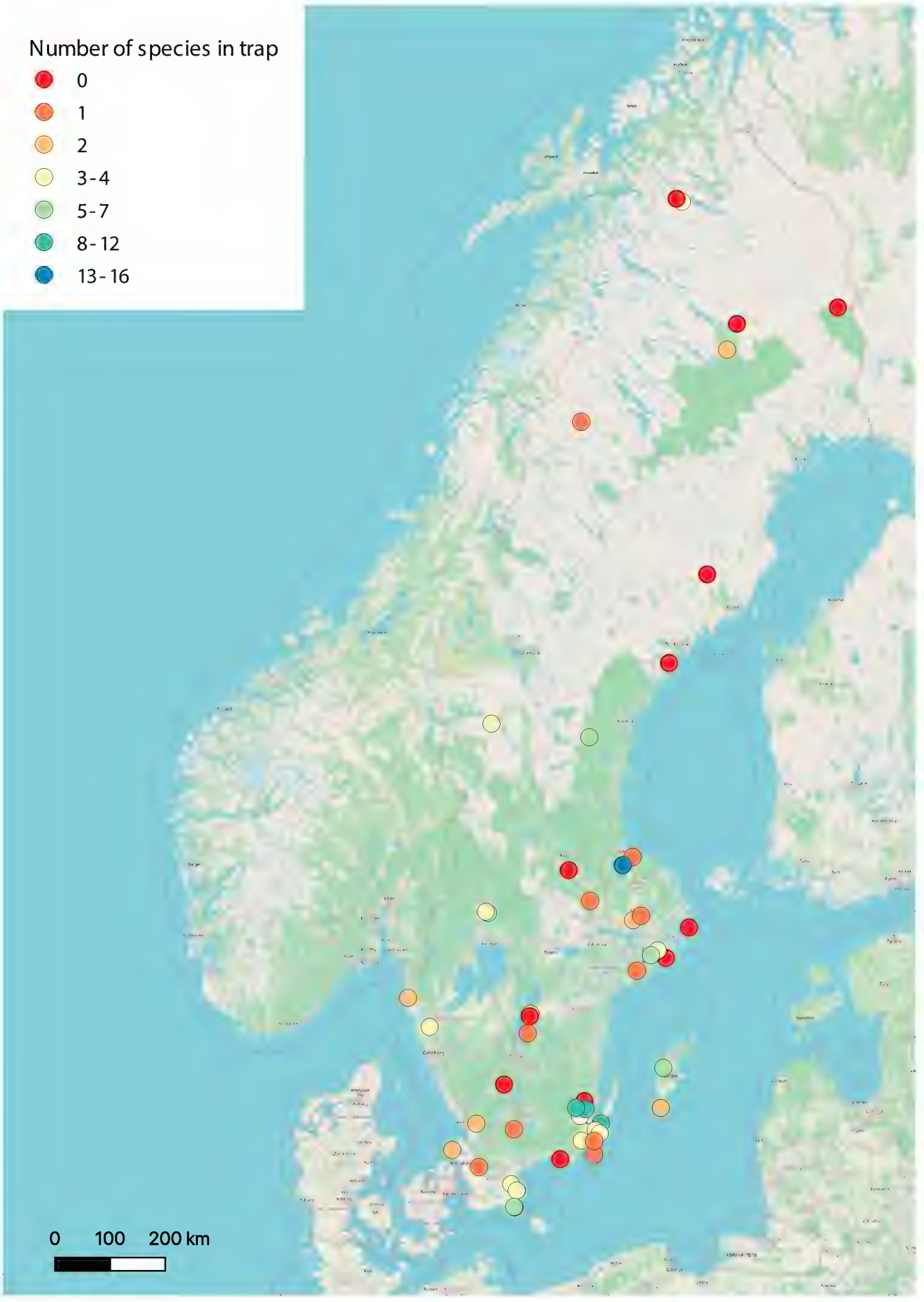

Figure 8. Map with number of *Dusona* species per trap. In 41 out of 55 traps, one or more *Dusona* species were found. Some points were slightly shifted in order to prevent overlap. Background map: OpenStreetMap.

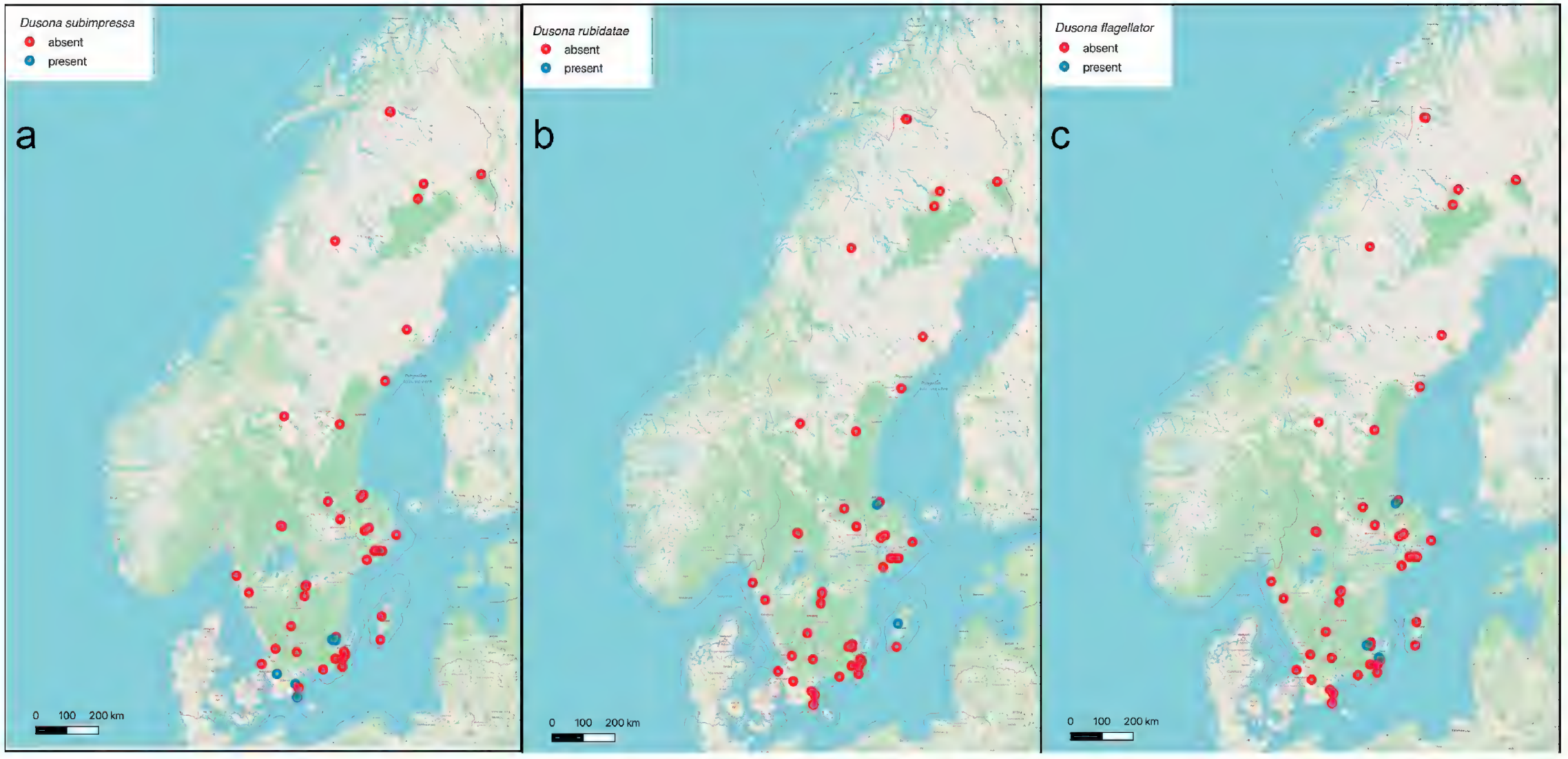

Figure 9. The distribution of the three most abundant *Dusona* species in the SMTP sample without earlier records in Sweden. blue dots = traps where the species was found. red dots = traps where the species was not found **a** *D. subimpressa* **b** *D. rubidatae* **c** *D. flagellator*. background map: OpenStreetMap.

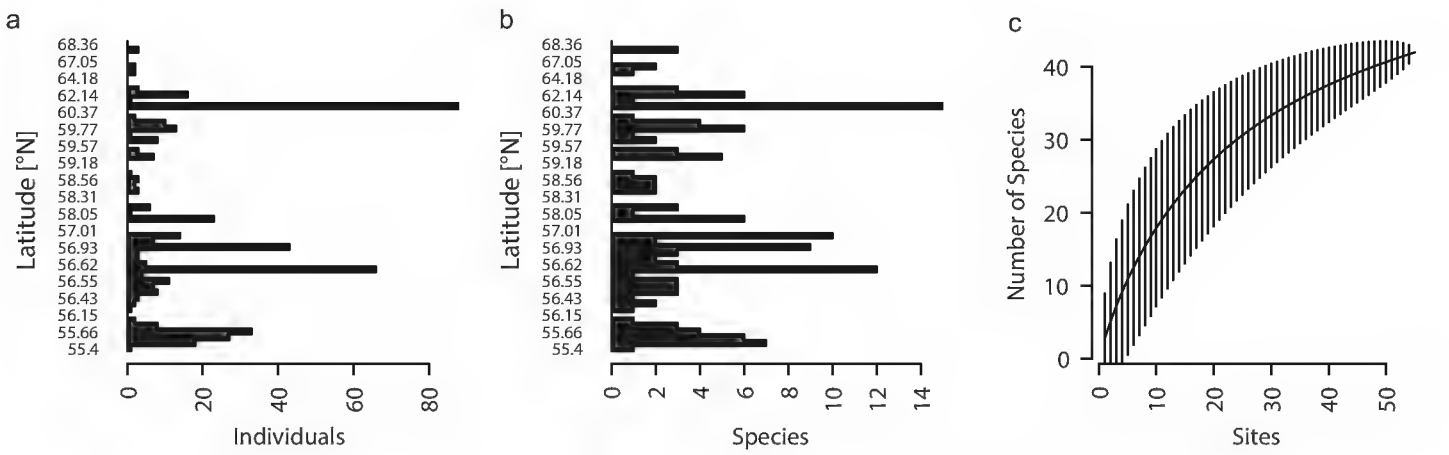

Figure 10. Faunistic analyses. **a** number of *Dusona* individuals in the SMTP material on the latitudinal axis (axis not numerical) **b** number of *Dusona* individuals in the SMTP material on the latitudinal axis (axis not numerical) **c** species accumulation curve (sites = Malaise traps, the curved line indicates the mean species accumulation curve, error bars indicate the SD).

Sweden were found in the extensive collection of the SMTP, several species were already deposited in the collection of the NHRS, e.g., *Dusona libertatis* (Teunissen, 1947) or were found in the collection NJ, e.g., *Dusona stygia* (Förster, 1868). An up-to-date checklist of Swedish *Dusona* will be available on www.artfakta.se, the follow-up website of www.dyntaxa.se. We provided the website operators with the according information.

Species treatments

In the following, we report locality data for newly recorded species from both Sweden and Switzerland, observations regarding unknown intraspecific variation and their possible taxonomic implications. For each of the newly recorded species, only one location is reported here, the remaining locality data being given in Suppl. materials 1, 2 (Suppl. material 1, https://doi.org/10.5281/zenodo.6535195 and Suppl. material 2, https://doi.org/10.5281/zenodo.6535211). For species without new records, no locality data is listed below, but morphological variations are sometimes discussed. In the end of this section, illustrative plates for all species available to our study (n = 57) are shown (Figs 11–67).

Dusona admontina (Speiser, 1908) (Fig. 11)

Sweden • 1♂; Skåne, Simrishamns kommun, Stenshuvuds nationalpark, Svabeholmsskog (malaise trap ID 40); hornbeam forest; 55.6613830°N, 14.2687330°E; 2005.iv.22–2005.v.22.

The species has not previously been recorded for Sweden (Dyntaxa 2022). The recorded distribution range mainly covers countries in northern and eastern Europe: Austria, Belgium, Germany, Netherlands, Norway, Poland, Romania, Russia and United Kingdom (Horstmann 2011; Yu et al. 2016).

Dusona aemula (Förster, 1868) (Fig. 12)

Switzerland • 1 ♀; GR, Sur, NE Sur; forest (pine, larch), river stream; 46.52419°N, 9.63425°E; 2006.vii.19–27; malaise trap; S. Klopfstein, H. Baur leg.

A single specimen of this species from Graubünden (CH) was included for this study. This specimen indicates that the species is slightly more variable than described by Hinz and Horstmann (2004) in terms of the leg colouration: front legs yellow from the trochanter, mid leg yellow from the apex of the trochanter, hind tibia yellowish medially, narrowly marked with black basally, rather broadly marked with black apically. All tarsi are darkened apically. Specimens with this colour pattern resemble *Dusona carpathica* (Szépligeti 1916) in many characters. However, they differ from *D. carpathica* by having the pleural part of the epicnemial carina complete dorsally and merging with the anterior margin of the mesopleuron (obliterated dorsally in *carpathica*) and the propodeum being rather deeply depressed and transverse striate (slightly depressed and irregularly wrinkled but with a median longitudinal keel posteriorly in *carpathica*). The species has not previously been recorded for Switzerland (Klopfstein et al. 2019c). However, the current records suggest that the distribution covers the entire Palaearctic: Austria, Azerbaijan, Belgium, Bulgaria, Croatia, Czech Republic, Finland, France, Germany, Hungary, Italy, Kazakhstan, Moldova, Netherlands, Norway, Poland, Romania, Russia, Spain, Sweden, Tunisia, Turkey, Ukraine and United Kingdom (Horstmann 2011; Yu et al. 2016).

Dusona alpina (Strobl, 1904) (Fig. 13)

Sweden • 1♀; Värmland, Munkfors kommun, Ransäter, Rudstorp (malaise trap ID 1002); 59.7729560°N, 13.4737140°E; sandy railway embankment through pastureland; 2005.vii.23–2005.viii.12.

The species has not previously been recorded for Sweden (Dyntaxa 2022). The recorded distribution range mainly covers countries in central and eastern Europe: Austria, Czech Republic, Germany, Norway, Poland, Romania and Ukraine (Horstmann 2011; Yu et al. 2016).

Dusona aurita (Kreichbaumer, 1883) (Fig. 18)

Switzerland • 1 ♂; BE, Bern, Bremgartenwald; opening, mixed forest; 46.95962°N, 7.41565°E; 2006.vii.21–28, S. Klopfstein leg.

The species has not previously been recorded for Switzerland (Klopfstein et al. 2019c). However, the current records suggest that the distribution covers the entire Palaearctic: Austria, Belarus, France, Georgia, Germany, Italy, Japan, Latvia, Moldova, Mongolia, Netherlands, Poland, Romania, Russia, Spain, Ukraine and United Kingdom (Horstmann 2011; Di Giovanni et al. 2015; Yu et al. 2016).

Dusona baueri Hinz, 1973 (Fig. 19)

Sweden • 2 ♂♂; Öland, Mörbylånga kommun, Gamla Skogsby (Kalkstad) (malaise trap ID 22); 56.6167000°N, 16.5076170°E; meadow with shrub vegetation; 2005.iv.25–2005.vi.28.

This species has not previously been recorded for Sweden (Dyntaxa 2022). The recorded distribution range covers mainly countries in northern Europe: Belgium, Finland, Germany, Poland, Russia (Horstmann 2011; Yu et al. 2016). The species appears to be quite rare (with only two specimens from Sweden in the dataset) but misidentification of the genus could also be an issue for this rather atypical species. The propodeal spiracle is small and oval (2× longer than wide), not strongly elongate as in other *Dusona* species.

Dusona bicoloripes (Ashmead, 1906) (Fig. 21)

Sweden • 5 ♀♀; Öland, Mörbylånga kommun, Västerstads almlund (malaise trap ID 3002); 56.4273070°N, 16.4219420°E; almlund; 2014.v.15–2014.vi.09.

This species has been recorded in Sweden (Dyntaxa 2022), even though Sweden is not included in the distribution range for *D. bicoloripes* in Yu et al. (2016) and Horstmann (2011). However, the current records suggest that the distribution covers the entire Palaearctic: Algeria, Armenia, Austria, Azerbaijan, Belarus, Belgium, Bulgaria, Croatia, Czech Republic, Finland, France, Georgia, Germany, Greece, Ireland, Italy, Japan, Kazakhstan, Korea, Kyrgyzstan, Moldova, Netherlands, Norway, Poland, Romania, Russia, Slovakia, Slovenia, Spain, Switzerland, Turkey, Ukraine and United Kingdom (Horstmann 2011; Yu et al. 2016; Varga 2021). The species has been found in large quantities in the SMTP material, as well as in the collection of the NHRS and the collection NJ. The species probably has been overlooked in many main collections due to misidentification of the species as *D. pugillator* (Linnaeus 1758; pers. observation G. Broad). This confusion was also observed in the collections NHRS and NMB. Furthermore, we found COI-sequences on BOLD and GenBank that were determined as *D. pugillator* and clustered with our sequences for *D. bicoloripes* (the corresponding authors were contacted and asked to recheck their species identifications and eventually to correct the taxon ID). Hinz and Horstmann (2004) have already mentioned the high variability of this species. Our study included a large series of *D. bicoloripes* specimens from Sweden, revealing an enormous intraspecific variability, especially in size (7.5–14 mm), the number of flagellar segments (44–54), and the colouration of the legs and metasoma. The hind tibiae are usually darkish brown or black. However, there was one very small specimen (20–197; barcode: OM912351; total length = 7.5 mm) in the SMTP material with yellowish-red hind tibia. The remaining characters of specimen 20–197 fit well with *D. bicoloripes* and it clusters together with other specimens of *D. bicoloripes* in the phylogenetic analysis (Figs 68, 69). The species can be differentiated from the similar species *D. stragifex* (Förster, 1868) and *D. bellipes* (Holmgren, 1872) by the weakly depressed propodeum lacking transverse wrinkles (see also Horstmann 2009).

Dusona carpathica (Szépligeti, 1916) (Fig. 26)

Material from Switzerland and the collection NJ fits the descriptions for *D. carpathica* by Hinz and Horstmann (2004). A single specimen from the SMTP determined as cf. *carpathica* (20–142) appears to have completely reddish hind legs. The proportion of reddish colour on the hind legs was already reported to be rather variable in *D. carpathica* with the femur being usually black, but reddish in some specimens (Hinz and Horstmann 2004). However, as the specimen 20–142 clusters slightly apart from the other specimens of *D. carpathica*, but still within the *angustifrons* group, its taxonomic identity raises questions. This specimen clearly differs from closely related species within the *angustifrons* group, *D. angustifrons* (Förster 1868) and *D. minor*, as they have completely blackish hind legs and low ventral parts of the epicnemial carina (see also p-distances between these species in the section *molecular analysis*). In order to properly assess the taxonomic status of specimen 20–142, additional specimens with similar traits are needed. Even though we examined all the material that was collected at this locality (SMTP, trap ID 7), no other matching specimens were found.

Dusona calceata (Brauns, 1895) (Fig. 24)

Switzerland • 4 ♂♂; BE, Biel, Bözingen; 1915.v.16; T. Steck leg.

D. calceata was discovered in the collection of the Naturhistorisches Museum in Basel, misidentified as *D. angustata*, from which it differs by the genal carina only being slightly raised (strongly raised in *D. angustata*) and the second metasomal tergite being almost completely black (broadly yellow laterally in *D. angustata*). The species has not previously been recorded for Switzerland (Klopfstein et al. 2019c). The species is currently known from countries of central and southern Europe: Austria, Bulgaria, Czech Republic, France, Greece, Hungary, Italy, Macedonia, Romania, Slovakia, Turkey and Ukraine (Horstmann 2011; Yu et al. 2016).

Dusona flagellator (Fabricius, 1793) (Fig. 34)

Sweden • 1 ♂, 2 ♀♀; Småland, Nybro kommun, Alsterbro/Alsterån (malaise trap ID 1008); 56.9365360°N, 15.9201670°E; mixed forest; 2006.vii.04–2006.vii.10.

This species was recorded in Sweden (Dyntaxa 2022). However, Sweden is not included in the distribution range for *D. flagellator* in Yu et al. (2016) and Horstmann (2011). Besides 6 specimens in the SMTP material, the species was also found in the collection NJ and the main collection of the NHRS. Current records of the species suggest that the distribution covers the entire Palaearctic: Andorra, Armenia, Austria, Azerbaijan, Belgium, Bulgaria, Croatia, Czech Republic, Finland, France, Georgia, Germany, Hungary, Italy, Kazakhstan, Kyrgyzstan, Moldova, Netherlands, Norway, Poland, Romania, Russia, Slovakia, Spain, Switzerland, Turkey, Ukraine and United Kingdom (Horstmann 2011; Yu et al. 2016; Varga 2021)

Dusona inermis (Förster, 1868) (Fig. 36)

In addition to the reddish colour pattern described by Hinz and Horstmann (2004), the petiole is also marked with red posteriorly in several specimens from the SMTP material. This character state also occurred in specimens in main collection of the MZL (det. by Hinz).

Dusona libertatis (Teunissen, 1947) (Fig. 41)

Sweden • 1 ♀; Blekinge; NHRS-HEVA000015885

This species has not previously been recorded for Sweden (Dyntaxa 2022). However, the current records suggest that the distribution covers the entire Western Palaearctic: Austria, France, Georgia, Germany, Italy, Lithuania, Netherlands, Poland, Romania, Russia, Ukraine, United Kingdom (Horstmann 2011; Yu et al. 2016).

Dusona cf. *nebulosa* Horstmann, 2004 (Fig. 45)

Sweden • 1 ♂; Uppland, Älvkarleby kommun, Marma skjutfält (malaise trap ID 6); 60.5242670°N, 17.4514830°E; dry meadow with birch (field of fire); 2003.viii.26–2003.ix.09.

A single specimen from the SMTP material fits the description of *D. nebulosa*, but has only 44 flagellar segments. It is plausible that the intraspecific variability for this species is higher than mentioned in the first description (46–47 flagellar segments, in Hinz and Horstmann 2004). Horstmann (2011) mentioned that the few males which are known from *D. nebulosa* (no females are known) could be an aberrant form of another species. In contrast to this suggestion, the single male which was examined in this study appears to have a rather unique barcode sequence (COI), clearly separating it from morphologically similar species such as *D. humilis* or *D. rubidatae*. However, as we were not able to examine further specimens of *D. nebulosa* (types or material determined by R. Hinz or K. Horstmann), we maintain the species identification as *D.* cf. *nebulosa* according to the recommendations by Sigovini et al. (2016). This species has not previously been recorded for Sweden (Dyntaxa 2022). So far, the species is only recorded from Germany, Russia and Ukraine (Horstmann 2011; Yu et al. 2016; Varga 2021).

Dusona opaca (Thomson, 1887) (Fig. 49)

Sweden • 1 ♂; Värmland, Munkfors kommun, Ransäter, Ransbergs Herrgård (malaise trap ID 1003); 59.7904420°N, 13.4151690°E; old mixed deciduous forest in stream ravine; 2005.vi.18–2005.vi.27.

This species has not previously been recorded for Sweden (Dyntaxa 2022). The current records suggest that the distribution covers the entire Palaearctic: Austria, Bel-

gium, Bulgaria, Czech Republic, Finland, France, Georgia, Germany, Hungary, Kazakhstan, Netherlands, Poland, Romania, Russia, Switzerland, Turkey, Ukraine and United Kingdom (Horstmann 2011; Yu et al. 2016).

Dusona pineticola (Holmgren, 1872) (Fig. 51)

Within this species, two colour varieties can be observed; a darker one with black or dark brown hind tibiae and fifth tergite which is distributed in Siberia and Northern Europe and a lighter one with red hind tibiae and fifth tergite which is distributed in central Europe (Hinz 1963). The former was originally described as a subspecies *D. p. siberica* (Hinz 1985; Hinz and Horstmann 2004) but was later synonymized again because the lectotype of *D. pineticola* from Skåne in southern Sweden (Hinz 1963) is intermediate between these two colour variations (Horstmann 2009). In this study, a single specimen from the main collection of the NMB collected in Bern (CH) was included, for which the colour fits the description of *D. p. pineticola* (Hinz 1963; see also Fig. 51). The significance of this wide variation in colouration remains unclear, but it should be considered that the two subspecies might represent true biological species, given their parapatric or even partly overlapping distribution. Yet, we were not able to study the darker colour variant in this study. In the future, the two colour variants should be examined for further discriminative characters, both morphological and genetic, in order to solve this taxonomic riddle.

Dusona recta (Thomson, 1887) (Fig. 56)

Sweden • 1 ♀; Östergötland, Rodga; E. Haglund leg.; NHRS-HEVA000015975 • 1 ♀; Ög, Rinna, Björneberg inäga; 58.19549°N, 14.91032°E; Malaise trap; Old mixed forest, meadow; 2019.vii.27–2019.viii.21; N. Johansson leg.; collection NJ.

This species has not previously been recorded for Sweden (Dyntaxa 2022). The current records suggest a distribution in the northern regions of the Western Palaearctic: Czech Republic, Finland, Germany, Latvia, Poland, Russia and United Kingdom (Horstmann 2011; Yu et al. 2016).

Dusona rubidatae Horstmann, 2009 (Fig. 57)

Sweden • 1 ♂; Gotland, Gotlands kommun, Roleks (malaise trap ID 28); 57.5367830°N, 18.3378830°E; border between mixed pine forest and open grazed calcareous pasture; 2004.ix.21–2005.iv.01.

This species has not previously been recorded for Sweden (Dyntaxa 2022). The current records suggest that the distribution covers the entire Western Palaearctic: Austria, Bulgaria, Czech Republic, France, Germany, Hungary, Netherlands, Russia, Switzerland and United Kingdom (Horstmann 2011; Yu et al. 2016). The species has just recently been split from *D. limnobia* (Thomson, 1887) by Horstmann (2009).

Hence, the recorded distribution range for this species still must be considered largely unknown. Specimens determined as *D. limnobia* before 2009 should be checked again. *Dusona rubidatae* differs from *D. limnobia* by more numerous flagellomeres (>=44 in *rubidatae*; <=44 in *limnobia*) and the slightly raised and transversely striate antennal carina. *Dusona rubidatae* was also found in the collection NJ.

Dusona spinipes (Thomson, 1887) (Fig. 59)

Sweden • 1 ♀; Småland, Nybro kommun, Alsterbro/Alsterån (Malaise trap ID 1008); 56.9365360°N, 15.9201670°E; mixed forest; 2006.vii.10–2006.vii.16.

This species has not previously been recorded for Sweden (Dyntaxa 2022). The current records suggest that the distribution covers the entire Palaearctic: Austria, Belarus, Belgium, Bulgaria, Croatia, Czech Republic, Finland, France, Germany, Hungary, Italy, Japan, Moldova, Netherlands, Norway, Poland, Romania, Russia, Spain, Switzerland, Ukraine and United Kingdom (Horstmann 2011; Haraldseide 2015; Yu et al. 2016). *Dusona spinipes* was also found in the collection NJ.

Dusona stygia (Förster, 1868) (Fig. 61)

Sweden • 1 ♀ 1 ♂; Västergötland, Aspåsen, Gustaf Adolf, Habo; RT90:x-6430518.y-448802; sweep net; Sandy meadow, deciduous forest; 2017.v.20; N. Johansson leg.; collection NJ.

This species has not previously been recorded for Sweden (Dyntaxa 2022). The current records suggest that the distribution covers the entire Palaearctic: Algeria, Armenia, Austria, Belgium, Bulgaria, Cyprus, Czech Republic, France, Germany, Greece, Hungary, Iran, Italy, Kazakhstan, Moldova, Morocco, Netherlands, Poland, Romania, Spain, Tunisia, Turkey, Turkmenistan, Ukraine and United Kingdom (Horstmann 2011; Yu et al. 2016). The raised antennal carina with a nose-like projection is in many specimens rather inconspicuous. Specimens lacking this character can be differentiated from the similar *D. bucculenta* (Holmgren 1860) by the mesopleuron being distinctly coriaceous, which is very smooth between the punctures in *D. bucculenta*.

Dusona subimpressa (Förster, 1868) (Fig. 62)

Sweden • 2 ♂♂; Skåne, Klippans kommun, Skäralid, dal (malaise trap ID 37); 56.027217°N, 13.223433°E; rich beech forest; 2005.vii.07–2005.viii.09.

This species has not previously been recorded for Sweden (Dyntaxa 2022). The current records suggest that the distribution covers the entire Western Palaearctic: Austria, Belarus, Belgium, Bulgaria, Czech Republic, Finland, France, Germany, Italy, Japan, Moldova, Netherlands, Norway, Poland, Romania, Russia, Slovenia, Spain, Switzerland, Ukraine and United Kingdom (Horstmann 2011; Yu et al. 2016; Varga 2021). In addition to more than a dozen specimens in the SMTP material, *D. subimpressa* was also found in the material of the collection NJ.

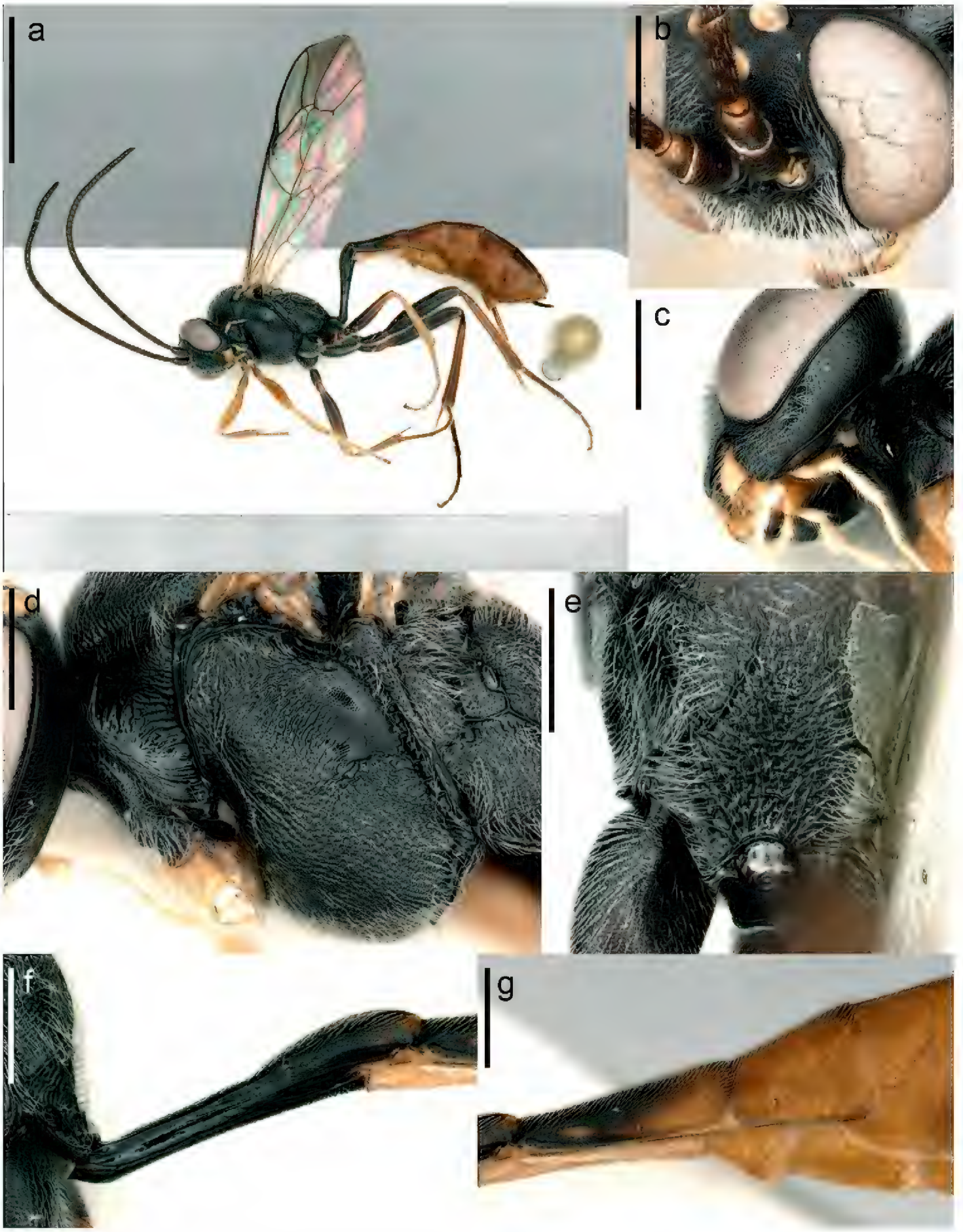

Figure 11. *D. admontina* (Speiser, 1908), ♀ Sweden. **a** habitus **b** antennal carina **c** junction of genal and hypostomal carina **d** mesopleuron **e** propodeum **f** first gastral tergite **g** 2nd and 3rd gastral tergites. Scale bars: 3 mm (**a**); 0.5 mm (**b–g**). https://doi.org/10.5281/zenodo.6046671.

Figure 12. *D. aemula* (Förster, 1868), ♀ Switzerland. **a** habitus **b** antennal carina **c** junction of genal and hypostomal carina **d** mesopleuron **e** propodeum **f** first gastral tergite **g** 2nd and 3rd gastral tergites. Scale bars: 3 mm (**a**); 0.5 mm (**b–g**). https://doi.org/10.5281/zenodo.6333923.

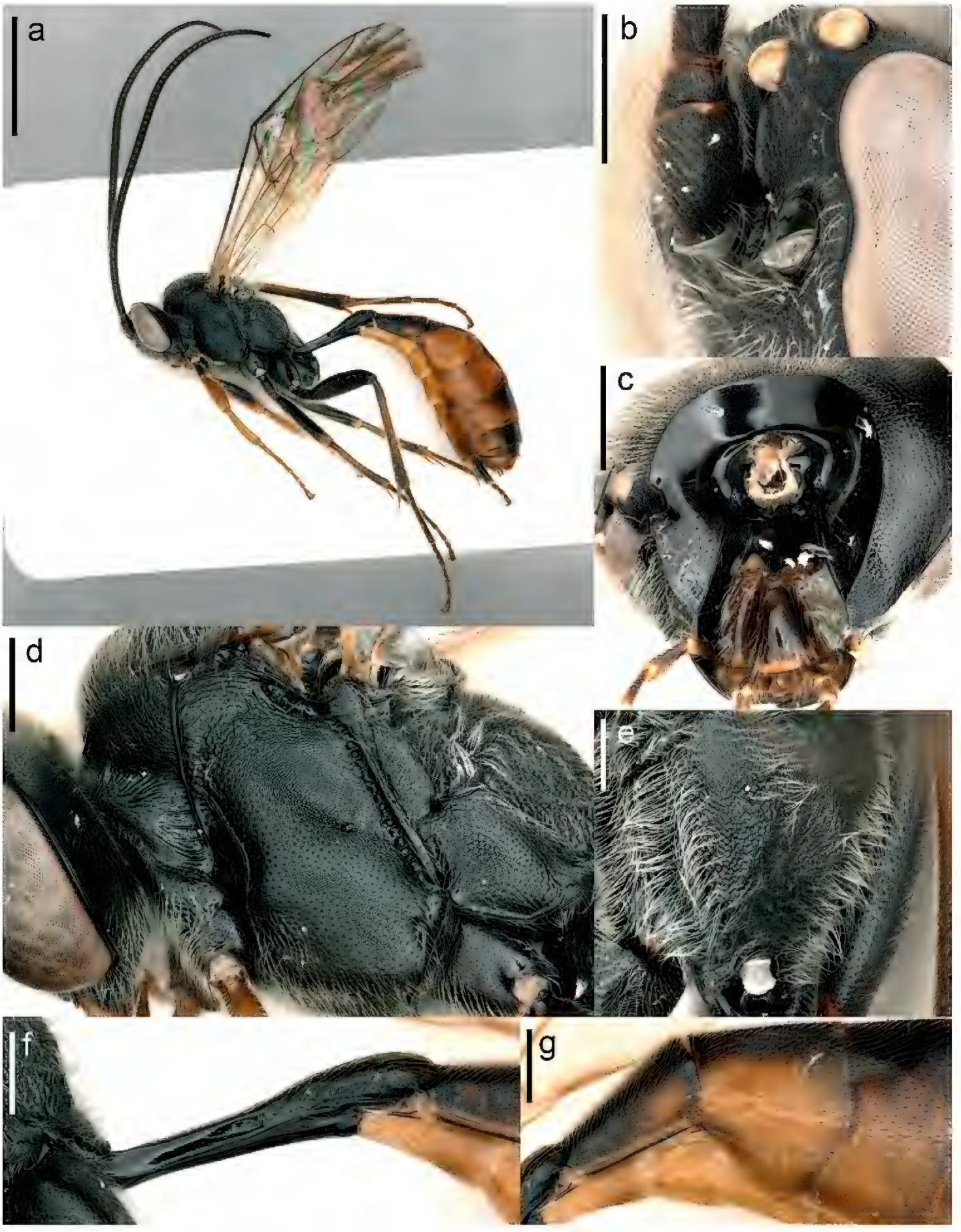

Figure 13. *D. alpina* (Strobl, 1904), ♀ Sweden. **a** habitus **b** antennal carina **c** junction of genal and hypostomal carina **d** mesopleuron **e** propodeum **f** first gastral tergite **g** 2nd and 3rd gastral tergites. Scale bars: 3 mm (**a**); 0.5 mm (**b–g**). https://doi.org/10.5281/zenodo.6368714.

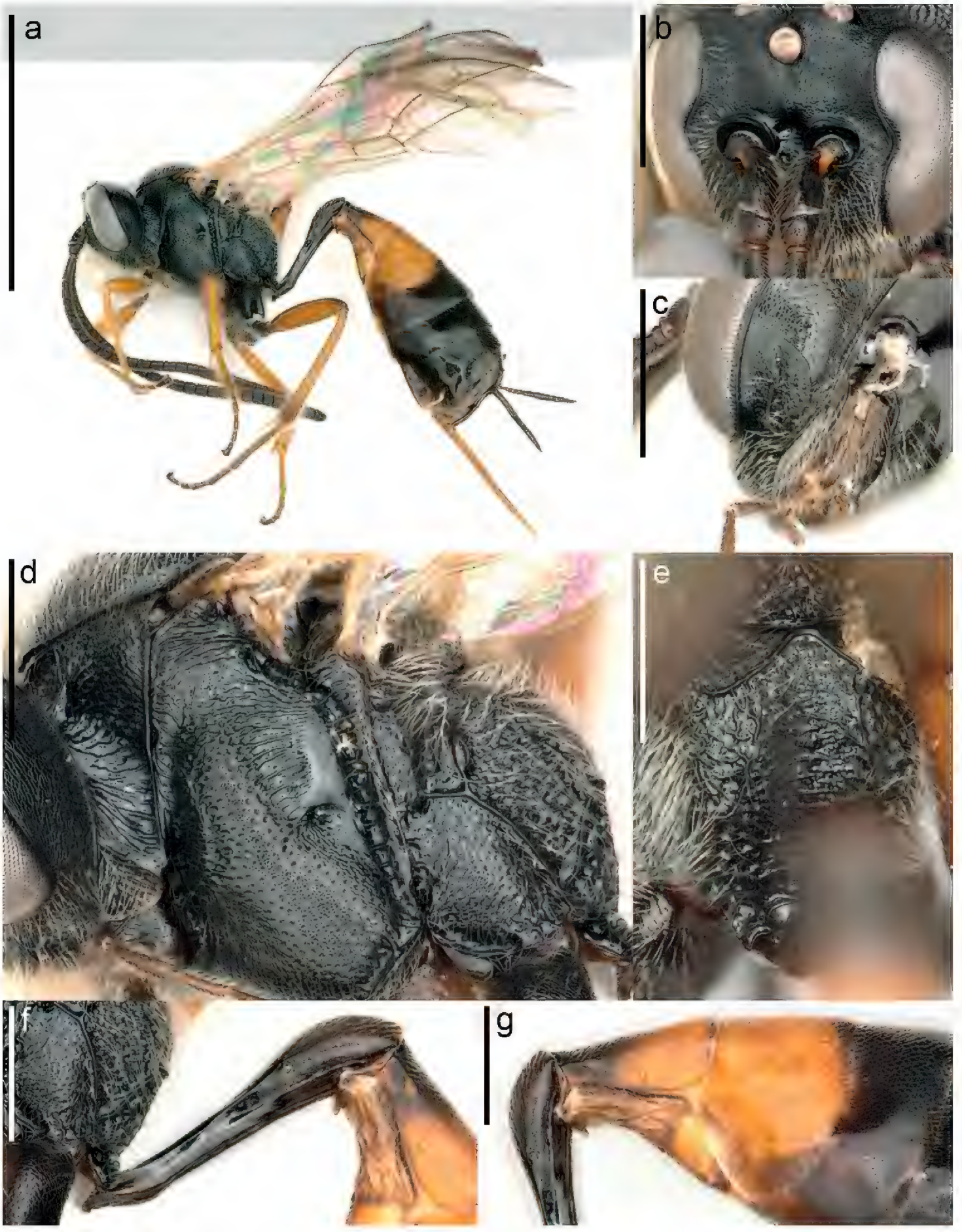

Figure 14. *D. alticola* (Gravenhorst, 1829), ♀ Sweden. **a** habitus **b** antennal carina **c** junction of genal and hypostomal carina **d** mesopleuron **e** propodeum **f** first gastral tergite **g** 2nd and 3rd gastral tergites. Scale bars: 3 mm (**a**); 0.5 mm (**b–g**). https://doi.org/10.5281/zenodo.6368756.

Figure 15. *D. angustata* (Thomson, 1887), ♀ Norway. **a** habitus **b** antennal carina **c** junction of genal and hypostomal carina **d** mesopleuron **e** propodeum **f** first gastral tergite **g** 2nd and 3rd gastral tergites. Scale bars: 3 mm (**a**); 0.5 mm (**b–g**). https://doi.org/10.5281/zenodo.6368773.

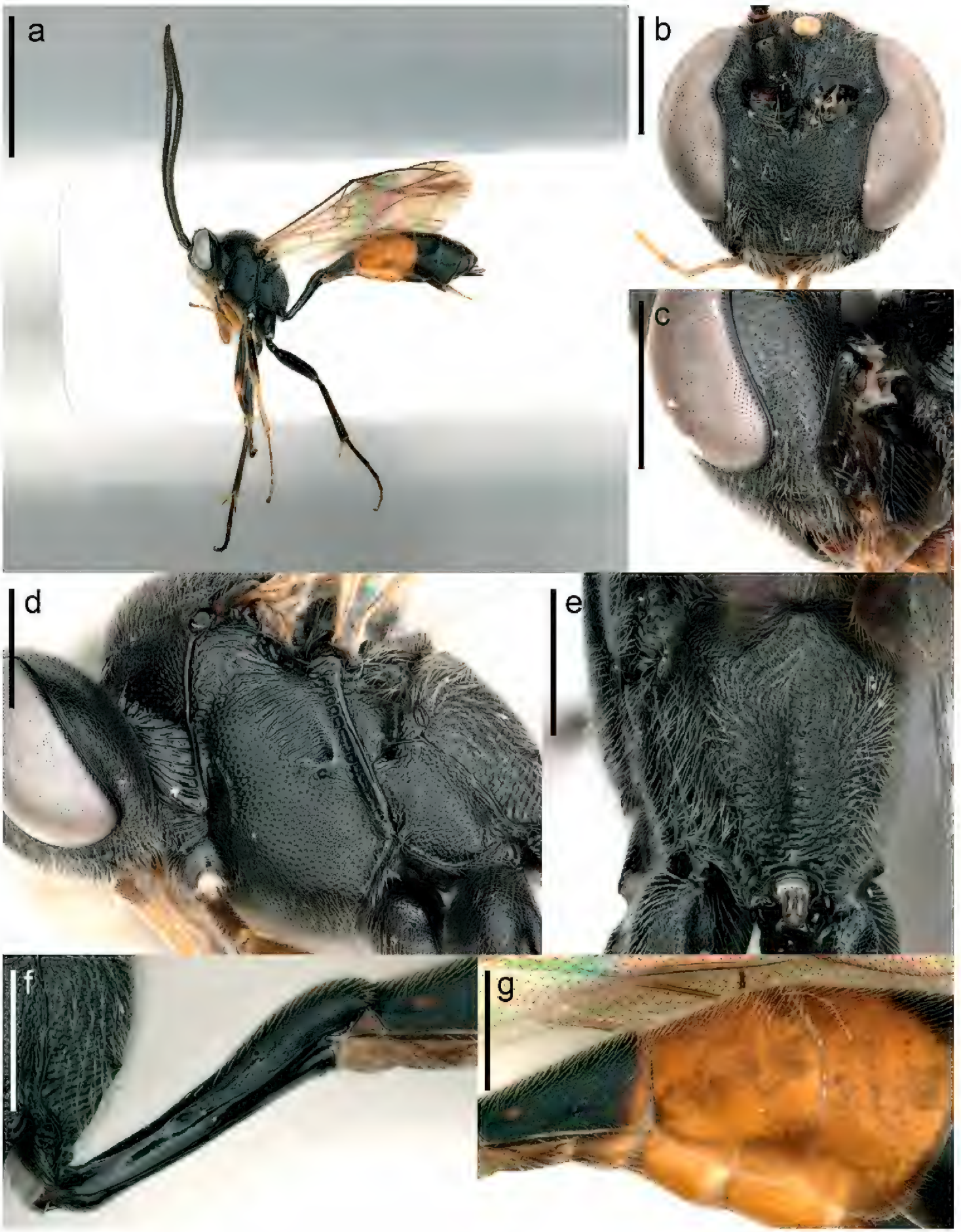

Figure 16. *D. angustifrons* (Förster, 1868), ♀ Sweden. **a** habitus **b** antennal carina **c** junction of genal and hypostomal carina **d** mesopleuron **e** propodeum **f** first gastral tergite **g** 2nd and 3rd gastral tergites. Scale bars: 3 mm (**a**); 0.5 mm (**b–g**). https://doi.org/10.5281/zenodo.6368793.

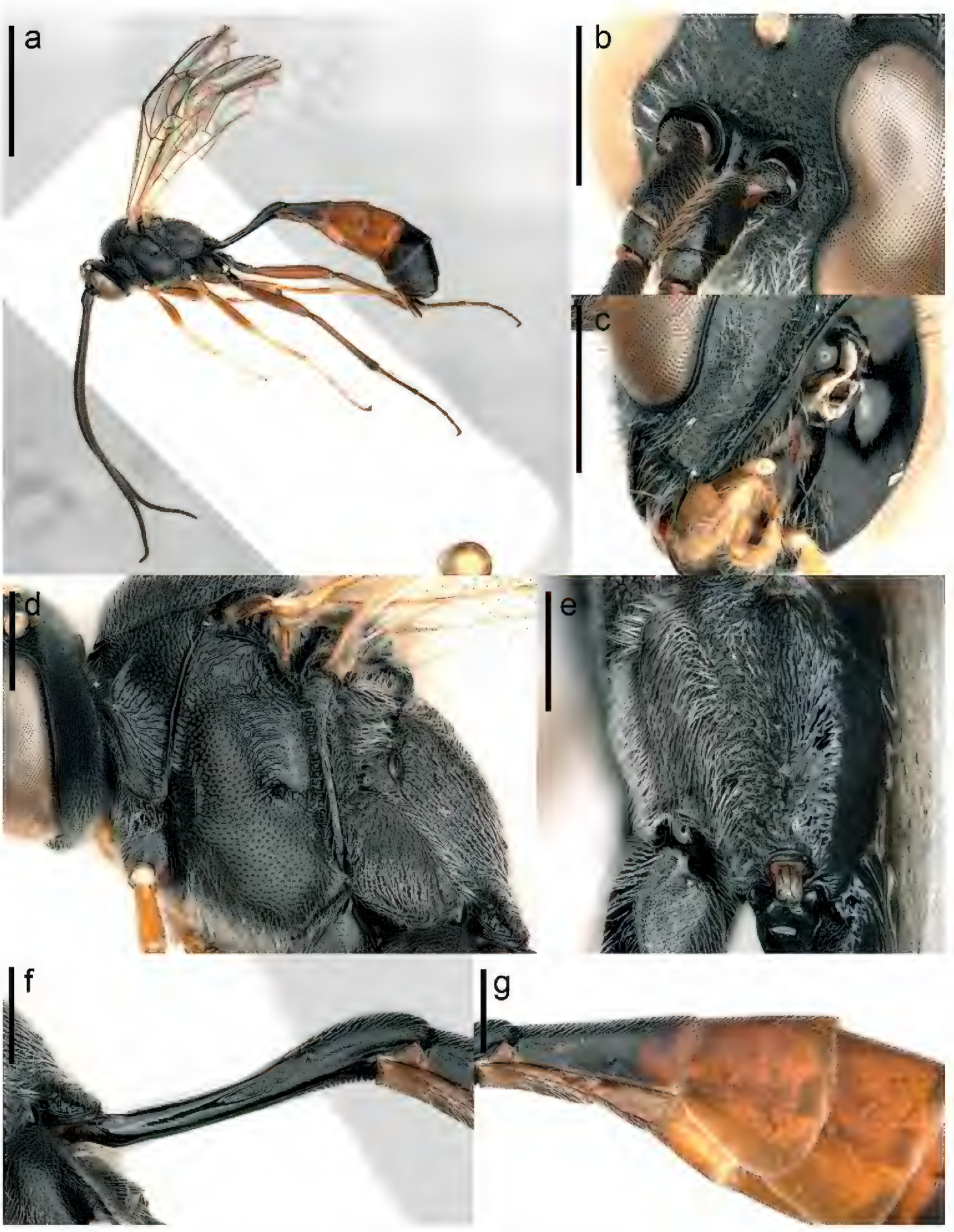

Figure 17. *D. annexa* (Förster, 1868), ♀ Sweden. **a** habitus **b** antennal carina **c** junction of genal and hypostomal carina **d** mesopleuron **e** propodeum **f** first gastral tergite **g** 2nd and 3rd gastral tergites. Scale bars: 3 mm (**a**); 0.5 mm (**b – g**). https://doi.org/10.5281/zenodo.6368862.

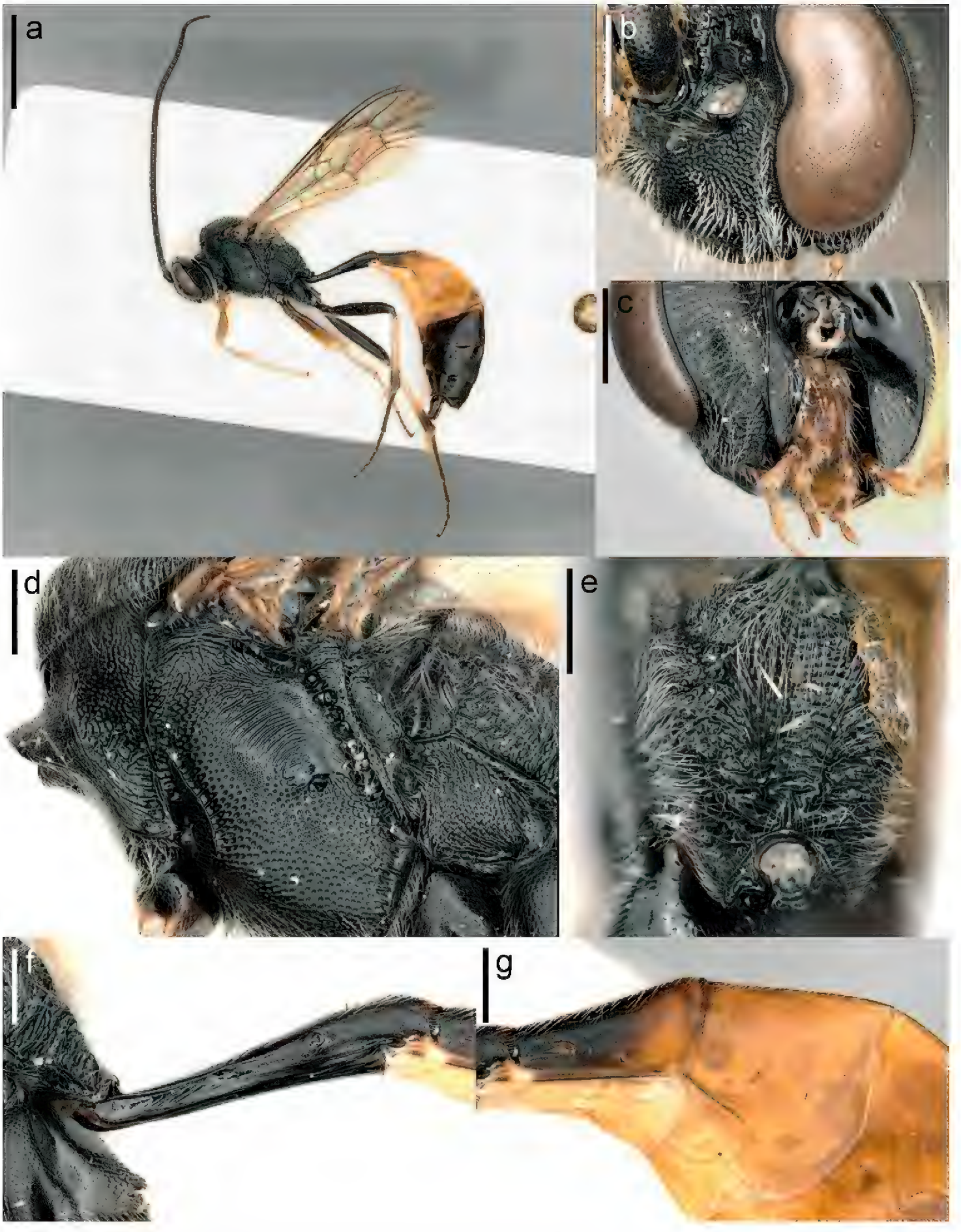

Figure 18. *D. aurita* (Kriechbaumer, 1883), ♂ Switzerland. **a** habitus **b** antennal carina **c** junction of genal and hypostomal carina **d** mesopleuron **e** propodeum **f** first gastral tergite **g** 2nd and 3rd gastral tergites. Scale bars: 3 mm (**a**); 0.5 mm (**b–g**). https://doi.org/10.5281/zenodo.6368911.

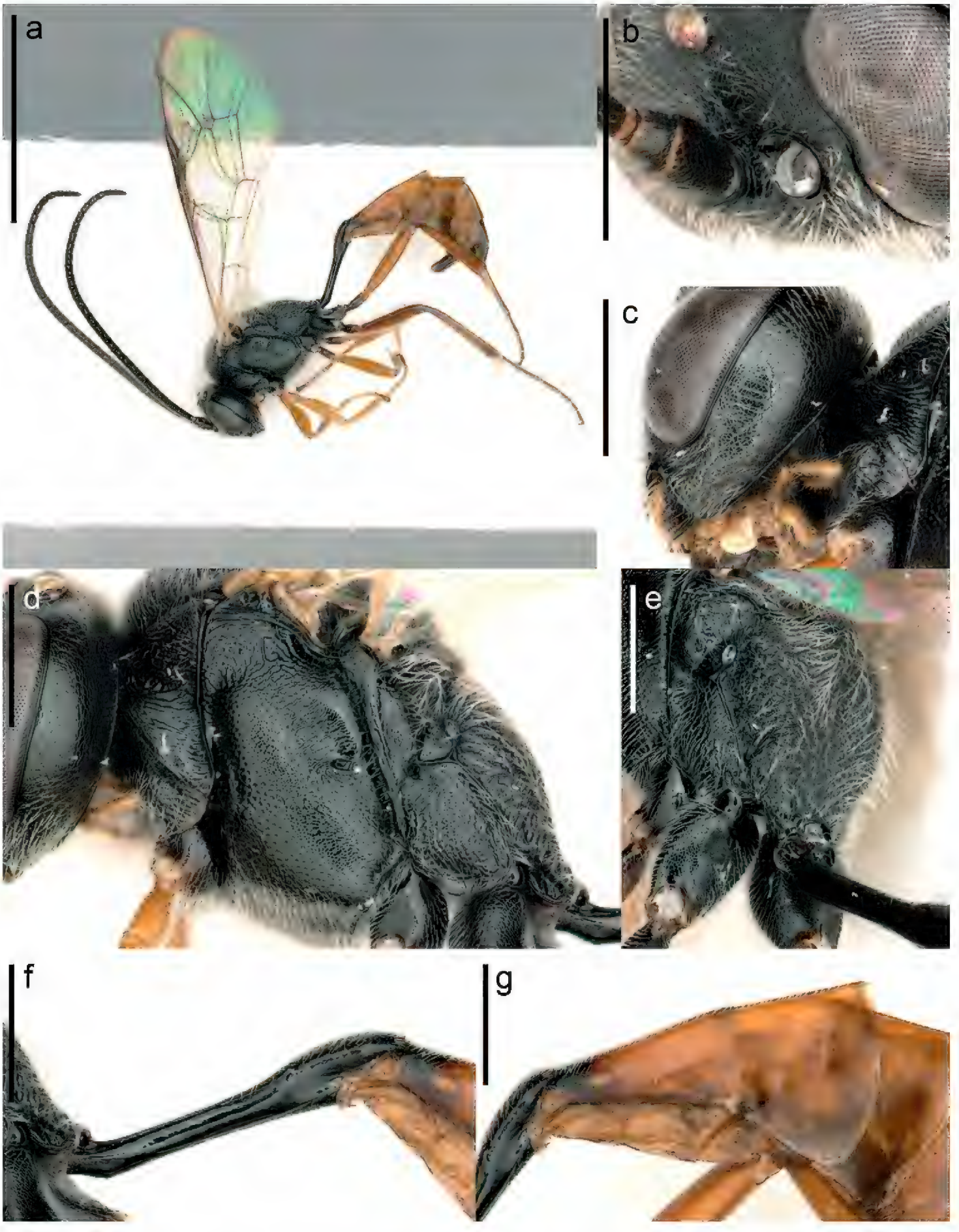

Figure 19. *D. baueri* Hinz, 1973, ♂ Sweden. **a** habitus **b** antennal carina **c** junction of genal and hypostomal carina **d** mesopleuron **e** propodeum **f** first gastral tergite **g** 2nd and 3rd gastral tergites. Scale bars: 1 mm (**a**); 0.5 mm (**b–g**). https://doi.org/10.5281/zenodo.6369124.

Figure 20. *D. bellipes* (Holmgren, 1872), ♀ Sweden. **a** habitus **b** antennal carina **c** junction of genal and hypostomal carina **d** mesopleuron **e** propodeum **f** first gastral tergite **g** 2nd and 3rd gastral tergites. Scale bars: 3 mm (**a**); 0.5 mm (**b–g**). https://doi.org/10.5281/zenodo.6369136.

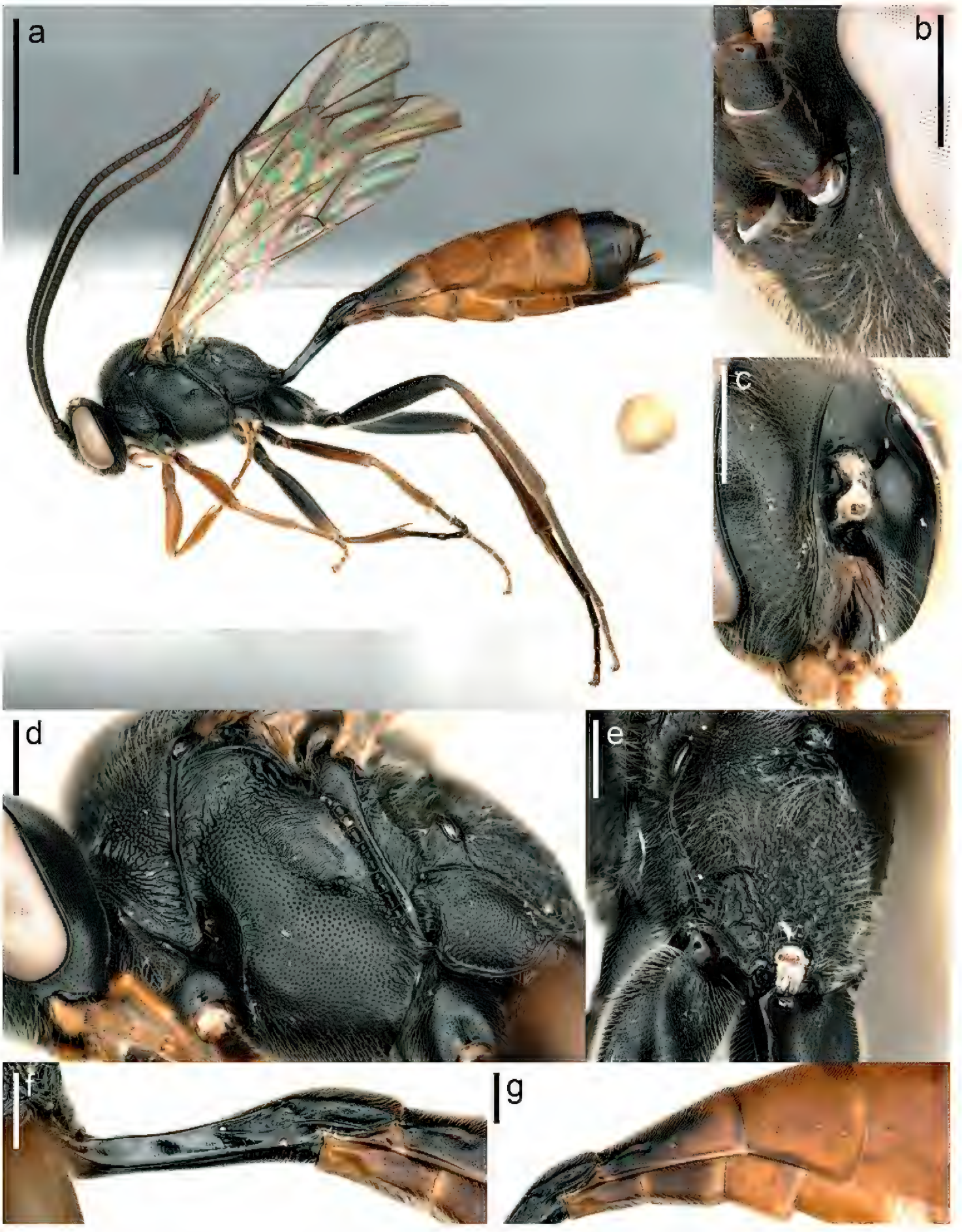

Figure 21. *D. bicoloripes* (Ashmead, 1906), ♀ Sweden. **a** habitus **b** antennal carina **c** junction of genal and hypostomal carina **d** mesopleuron **e** propodeum **f** first gastral tergite **g** 2nd and 3rd gastral tergites. Scale bars: 3 mm (**a**); 0.5 mm (**b–g**). https://doi.org/10.5281/zenodo.6370015.

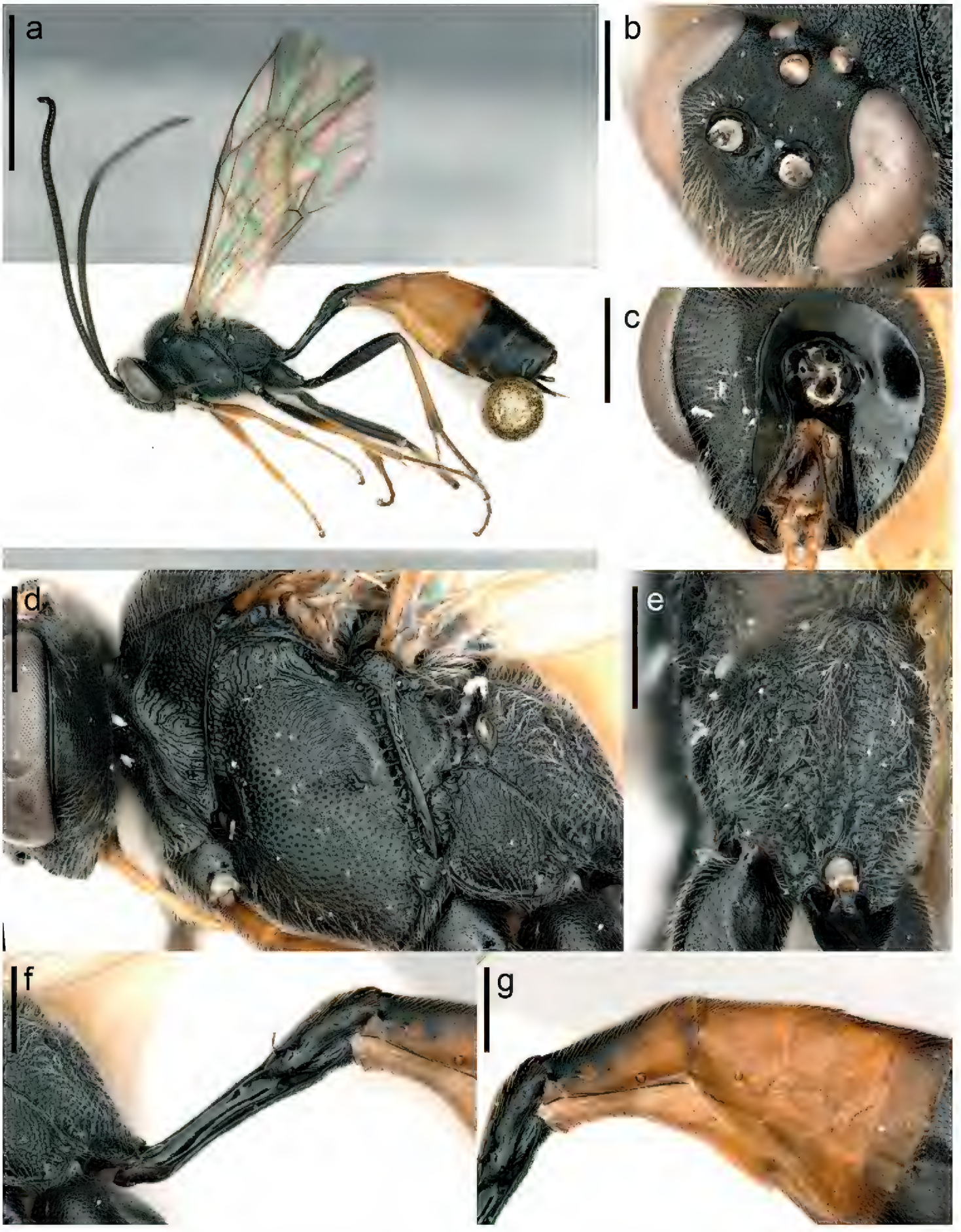

Figure 22. *D. blanda* (Förster, 1868), ♀ Sweden. **a** habitus **b** antennal carina **c** junction of genal and hypostomal carina **d** mesopleuron **e** propodeum **f** first gastral tergite **g** 2nd and 3rd gastral tergites. Scale bars: 3 mm (**a**); 0.5 mm (**b–g**). https://doi.org/10.5281/zenodo.6370029.

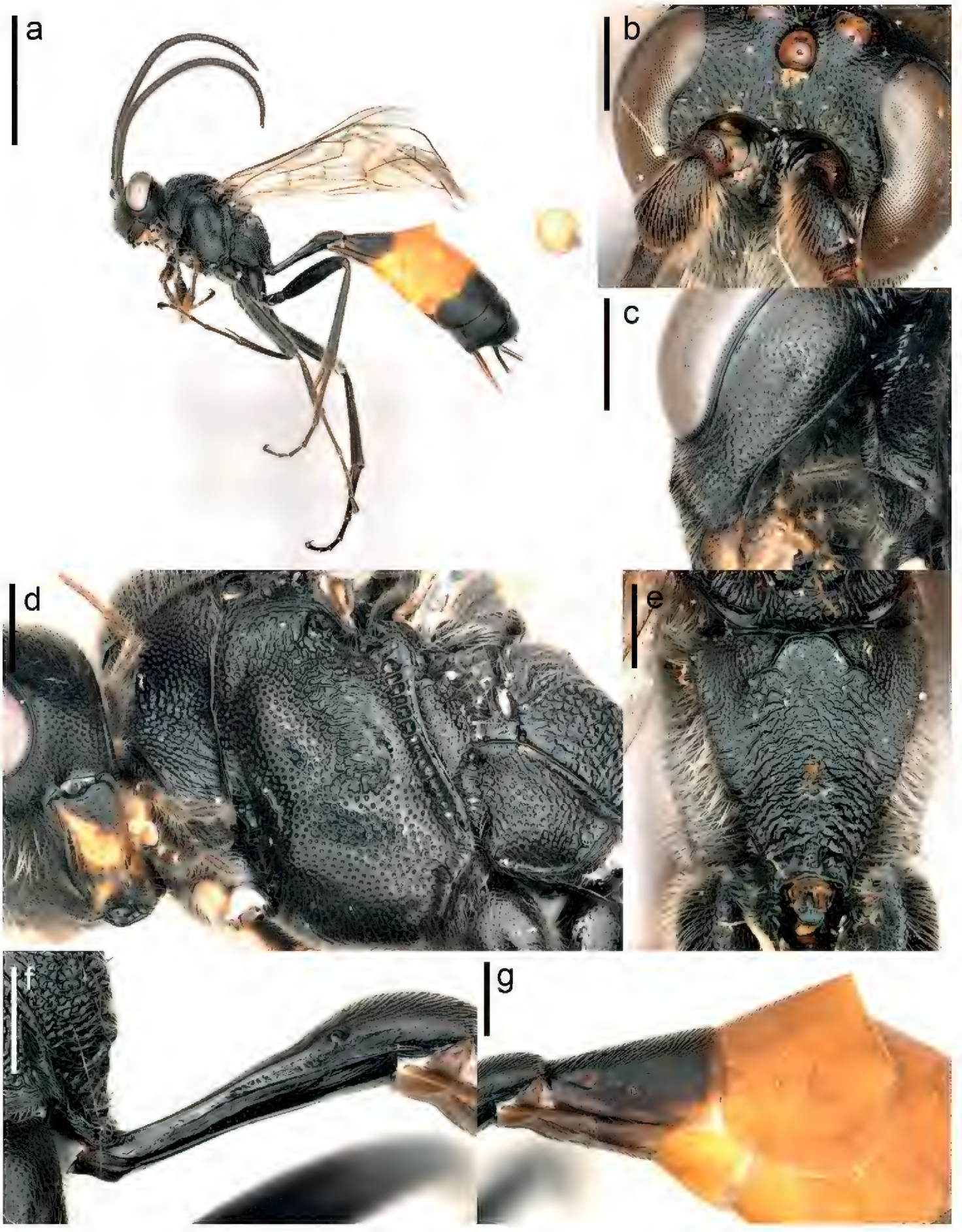

Figure 23. *D. bucculenta* (Holmgren, 1860), ♀ Sweden. **a** habitus **b** antennal carina **c** junction of genal and hypostomal carina **d** mesopleuron **e** propodeum **f** first gastral tergite **g** 2nd and 3rd gastral tergites. Scale bars: 3 mm (**a**); 0.5 mm (**b–g**). https://doi.org/10.5281/zenodo.6370034.

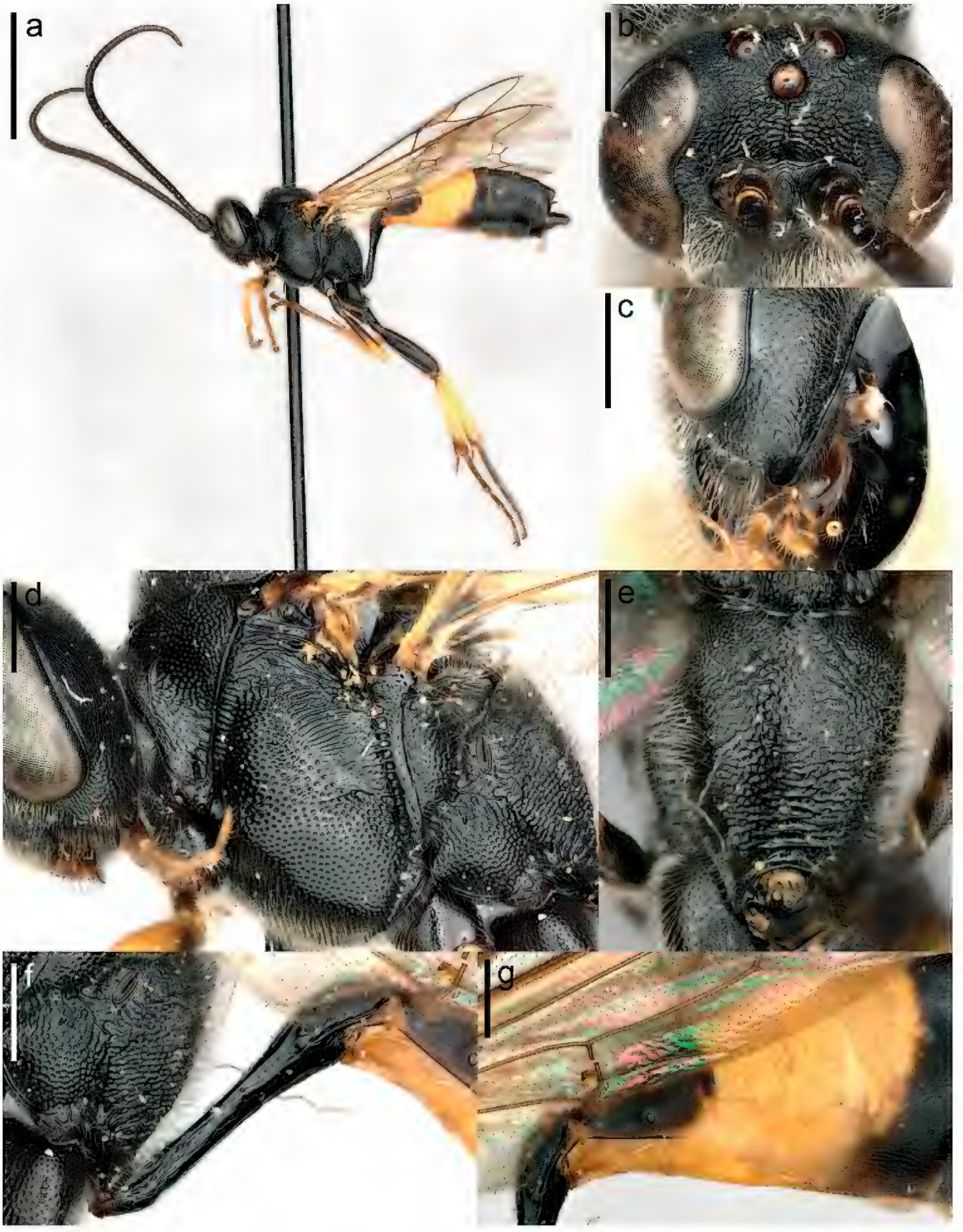

Figure 24. *D. calceata* (Brauns, 1885), ♂ Switzerland. **a** habitus **b** antennal carina **c** junction of genal and hypostomal carina **d** mesopleuron **e** propodeum **f** first gastral tergite **g** 2nd and 3rd gastral tergites. Scale bars: 3 mm (**a**); 0.5 mm (**b–g**). https://doi.org/10.5281/zenodo.6370039.

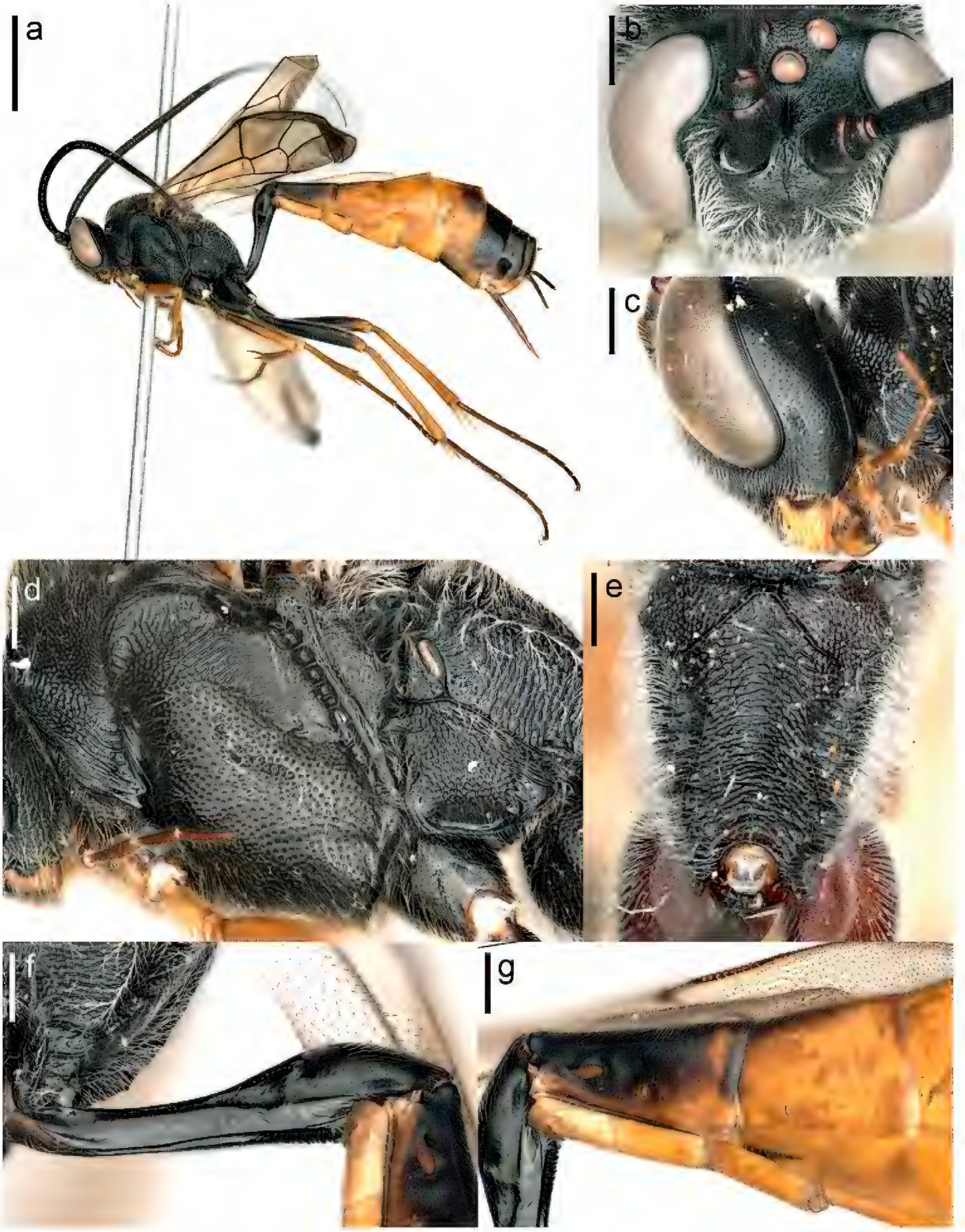

Figure 25. *D. carinifrons* (Holmgren, 1860), ♀ Sweden. **a** habitus **b** antennal carina **c** junction of genal and hypostomal carina **d** mesopleuron **e** propodeum **f** first gastral tergite **g** 2nd and 3rd gastral tergites. Scale bars: 3 mm (**a**); 0.5 mm (**b–g**). https://doi.org/10.5281/zenodo.6370042.

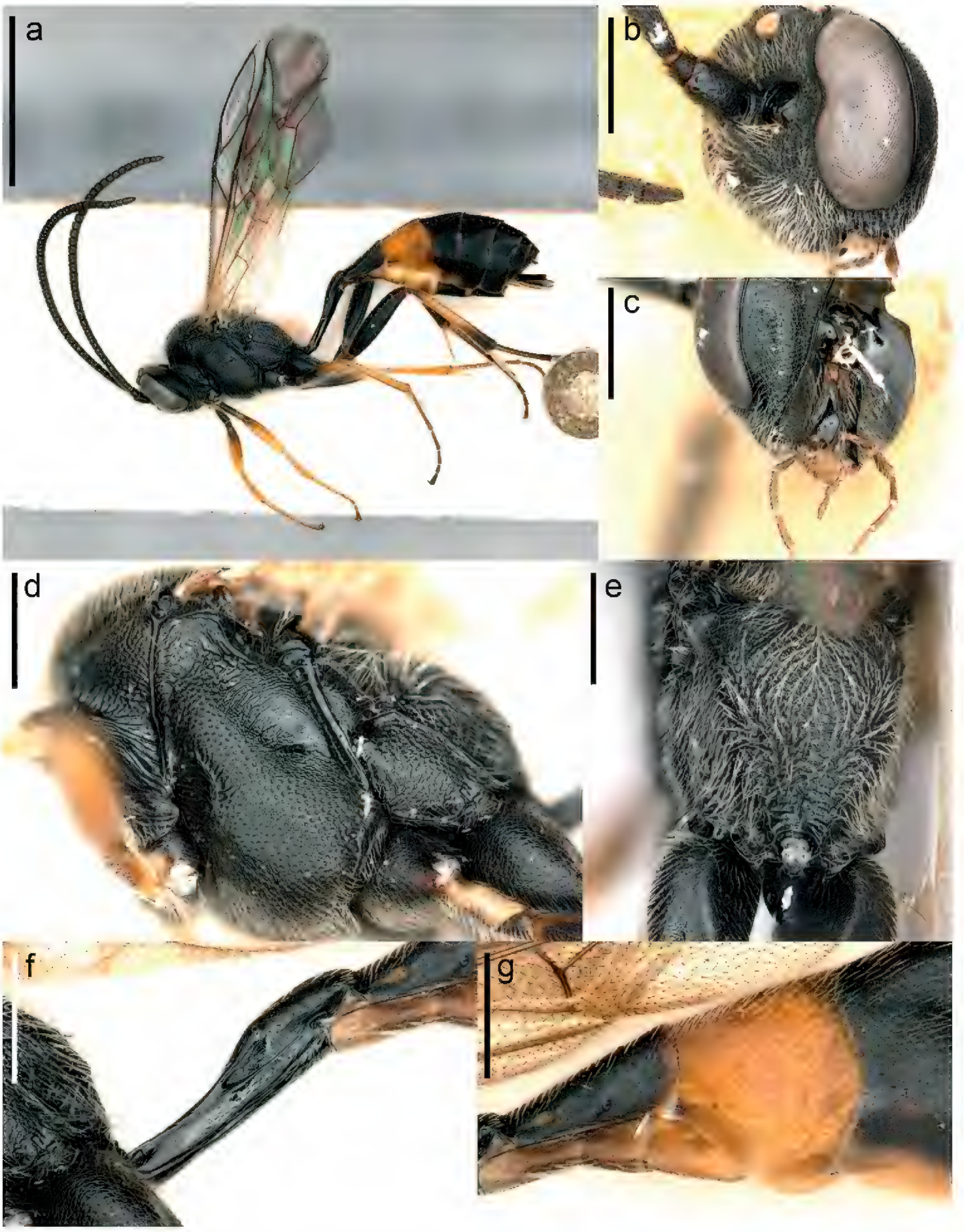

Figure 26. *D. carpathica* (Szépligeti, 1916), ♀ Switzerland. **a** habitus **b** antennal carina **c** junction of genal and hypostomal carina **d** mesopleuron **e** propodeum **f** first gastral tergite **g** 2nd and 3rd gastral tergites. Scale bars: 3 mm (**a**); 0.5 mm (**b–g**). https://doi.org/10.5281/zenodo.6370050.

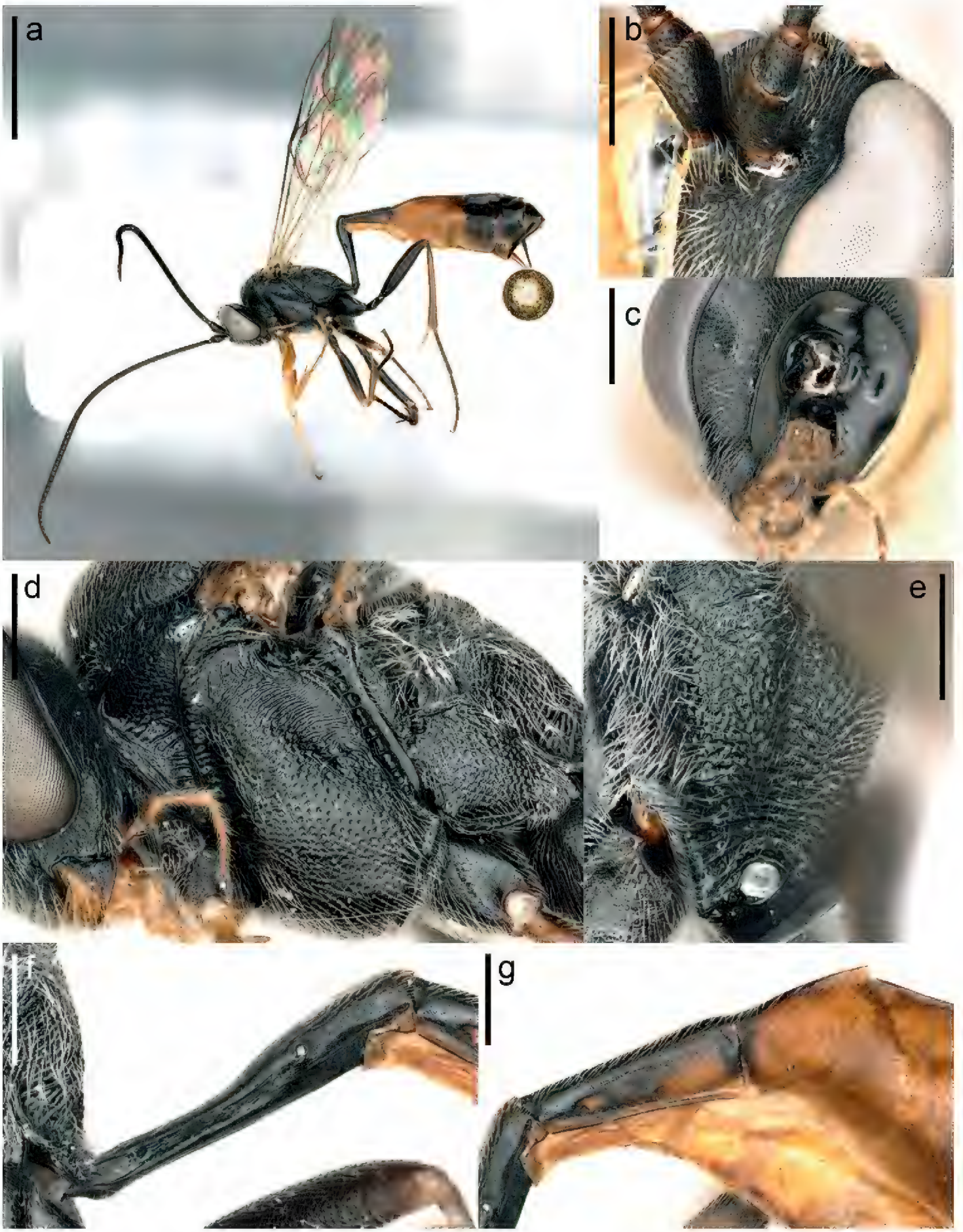

Figure 27. *D. circumcinctus* (Förster, 1868), ♀ Sweden. **a** habitus **b** antennal carina **c** junction of genal and hypostomal carina **d** mesopleuron **e** propodeum **f** first gastral tergite **g** 2nd and 3rd gastral tergites. Scale bars: 3 mm (**a**); 0.5 mm (**b–g**). https://doi.org/10.5281/zenodo.6370053.

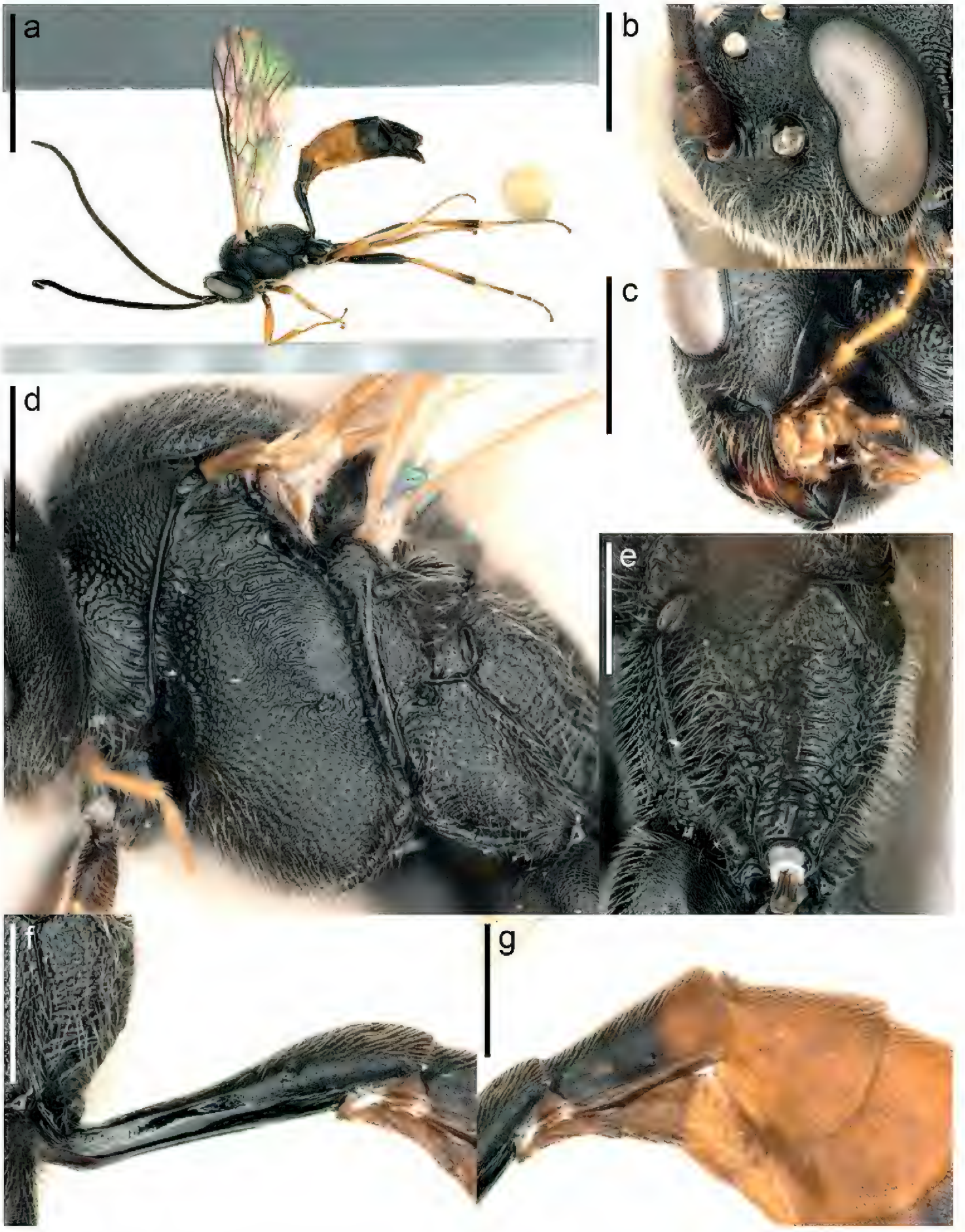

Figure 28. *D. circumspectans* (Förster, 1868), ♂ Sweden. **a** habitus **b** antennal carina **c** junction of genal and hypostomal carina **d** mesopleuron **e** propodeum **f** first gastral tergite **g** 2nd and 3rd gastral tergites. Scale bars: 3 mm (**a**); 0.5 mm (**b–g**). https://doi.org/10.5281/zenodo.6370091.

Figure 29. *D. confusa* (Förster, 1868), ♀ Sweden. **a** habitus **b** antennal carina **c** junction of genal and hypostomal carina **d** mesopleuron **e** propodeum **f** first gastral tergite **g** 2nd and 3rd gastral tergites. Scale bars: 3 mm (**a**); 0.5 mm (**b–g**). https://doi.org/10.5281/zenodo.6370096.

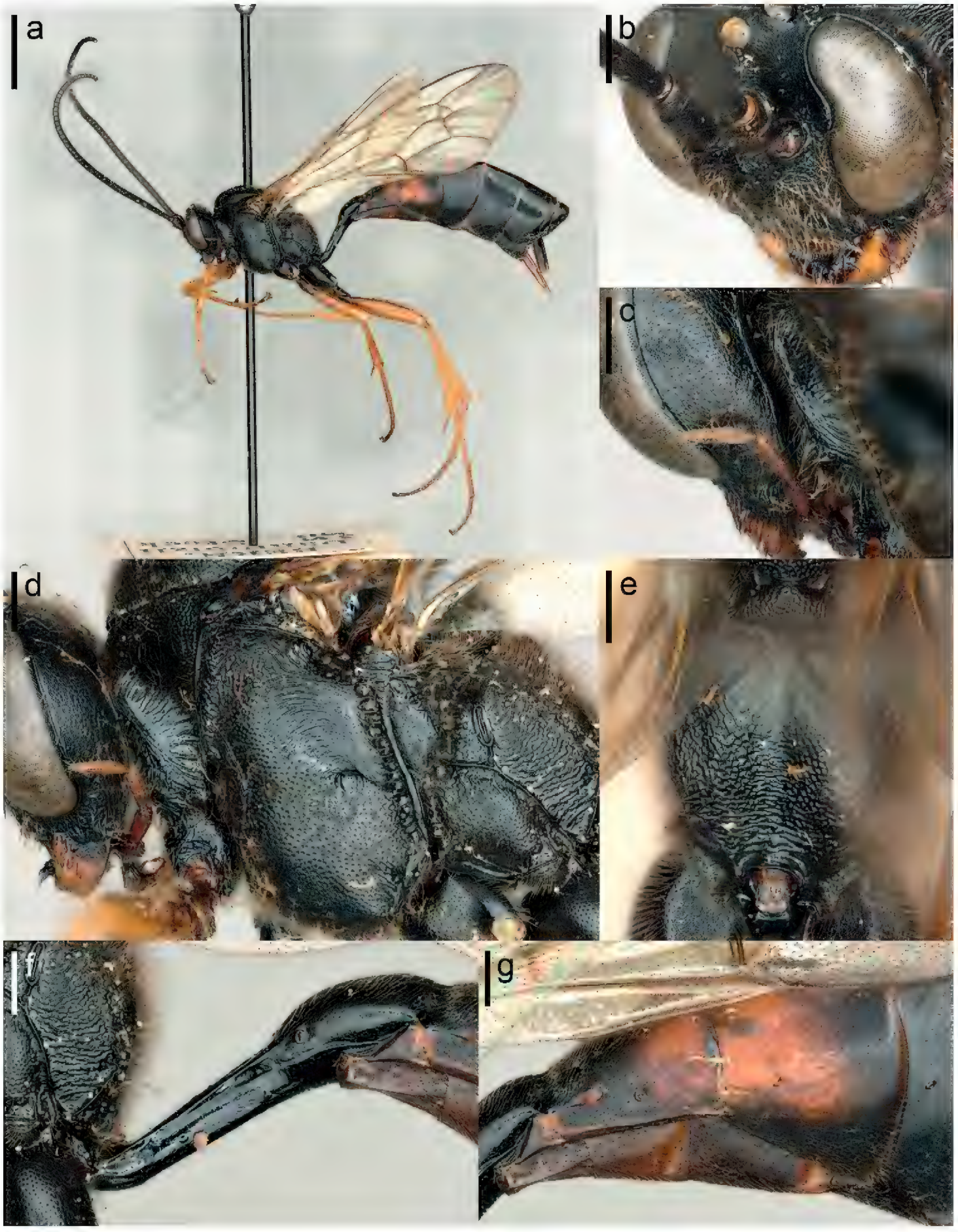

Figure 30. *D. cultrator* (Gravenhorst, 1829), ♀ Switzerland. **a** habitus **b** antennal carina **c** junction of genal and hypostomal carina **d** mesopleuron **e** propodeum **f** first gastral tergite **g** 2nd and 3rd gastral tergites. Scale bars: 3 mm (**a**); 0.5 mm (**b–g**). https://doi.org/10.5281/zenodo.6370126.

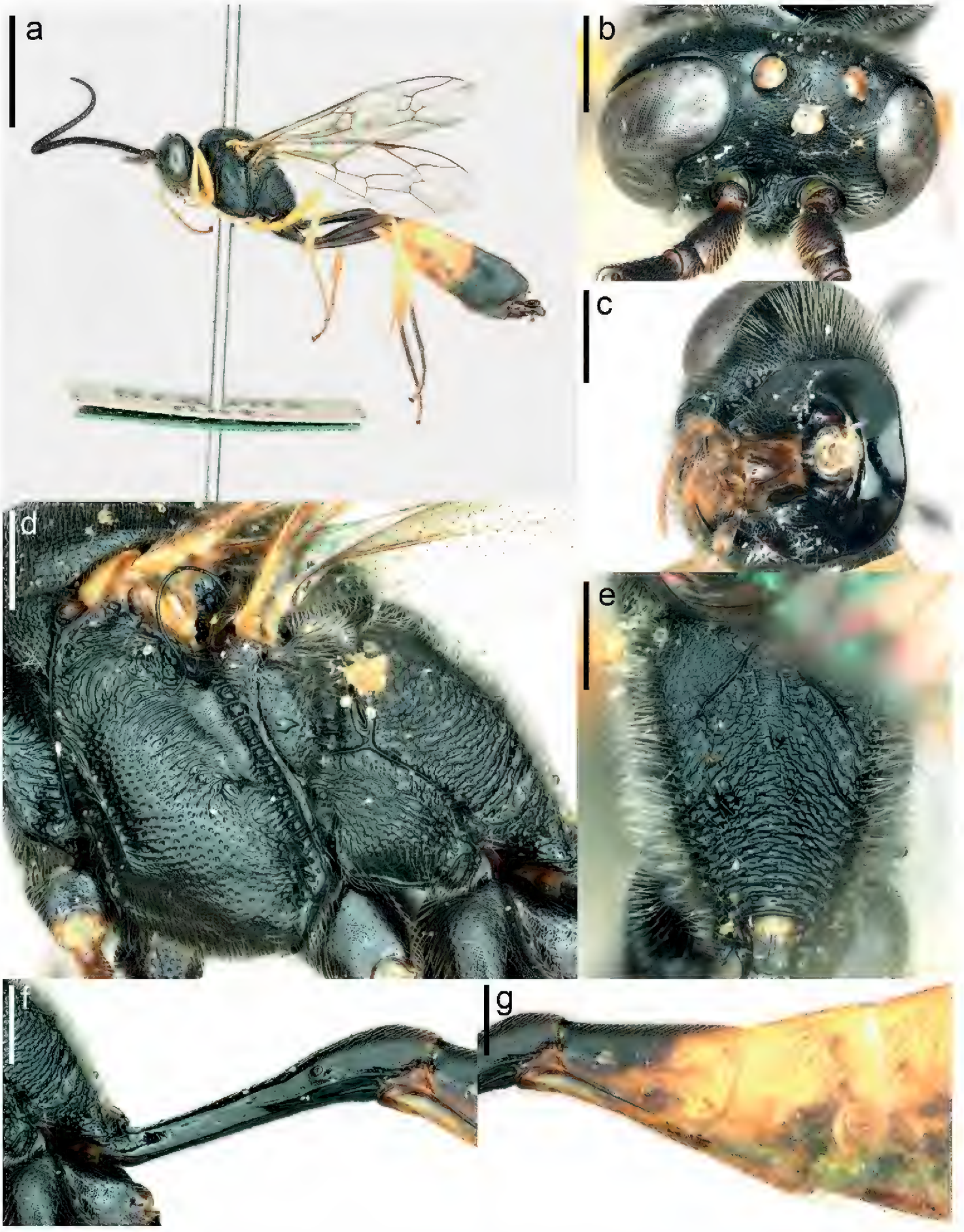

Figure 31. *D. dubitor* Hinz, 1977, ♂ Switzerland. **a** habitus **b** antennal carina **c** junction of genal and hypostomal carina **d** mesopleuron **e** propodeum **f** first gastral tergite **g** 2nd and 3rd gastral tergites. Scale bars: 3 mm (**a**); 0.5 mm (**b–g**). https://doi.org/10.5281/zenodo.6370139.

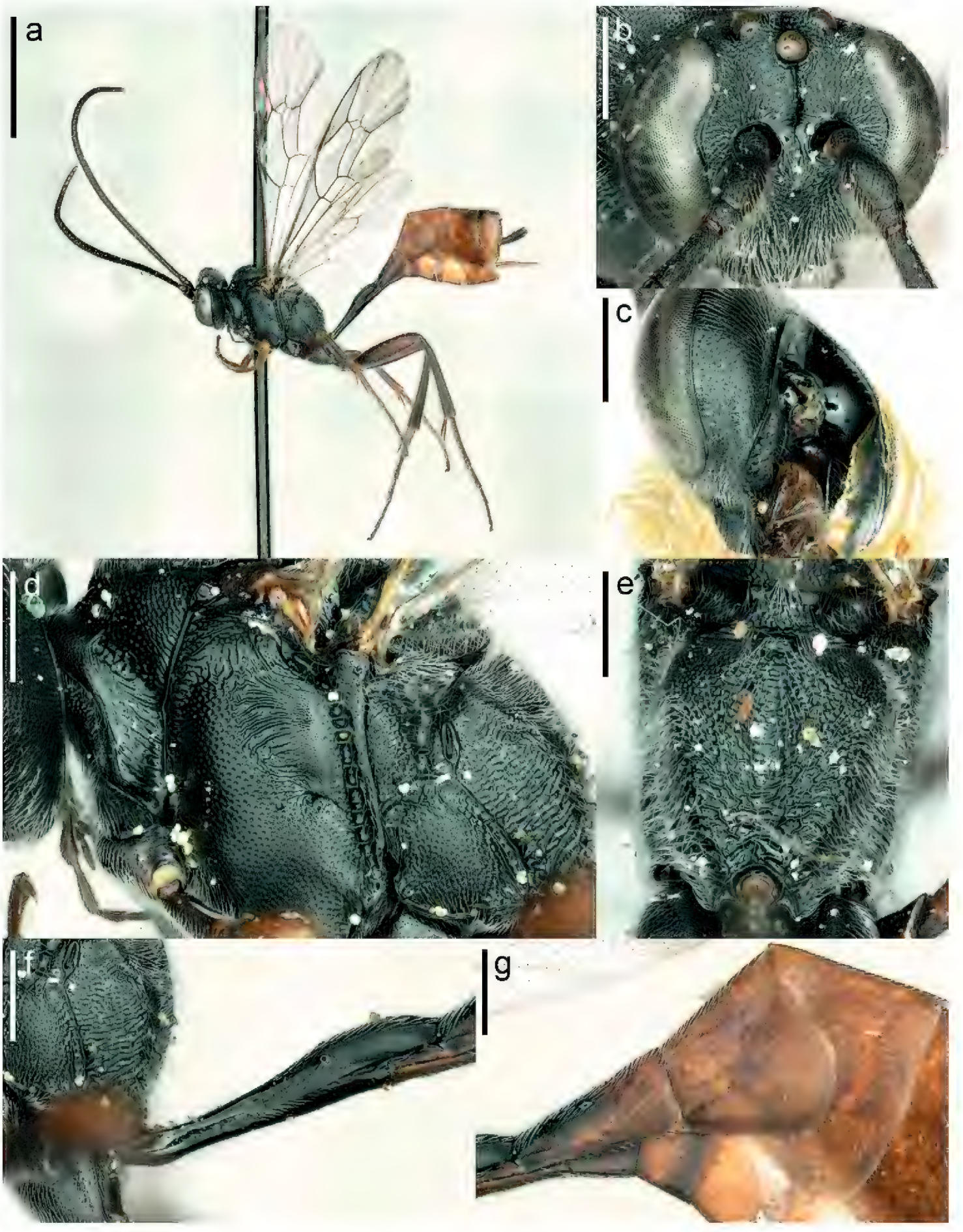

Figure 32. *D. erythrogaster* (Förster, 1868), ♀ Switzerland. **a** habitus. **b** antennal carina. **c** junction of genal and hypostomal carina. **d** mesopleuron. **e** propodeum. **f** first gastral tergite. **g** 2nd and 3rd gastral tergites. Scale bars: 3 mm (**a**); 0.5 mm (**b–g**). https://doi.org/10.5281/zenodo.6370145.

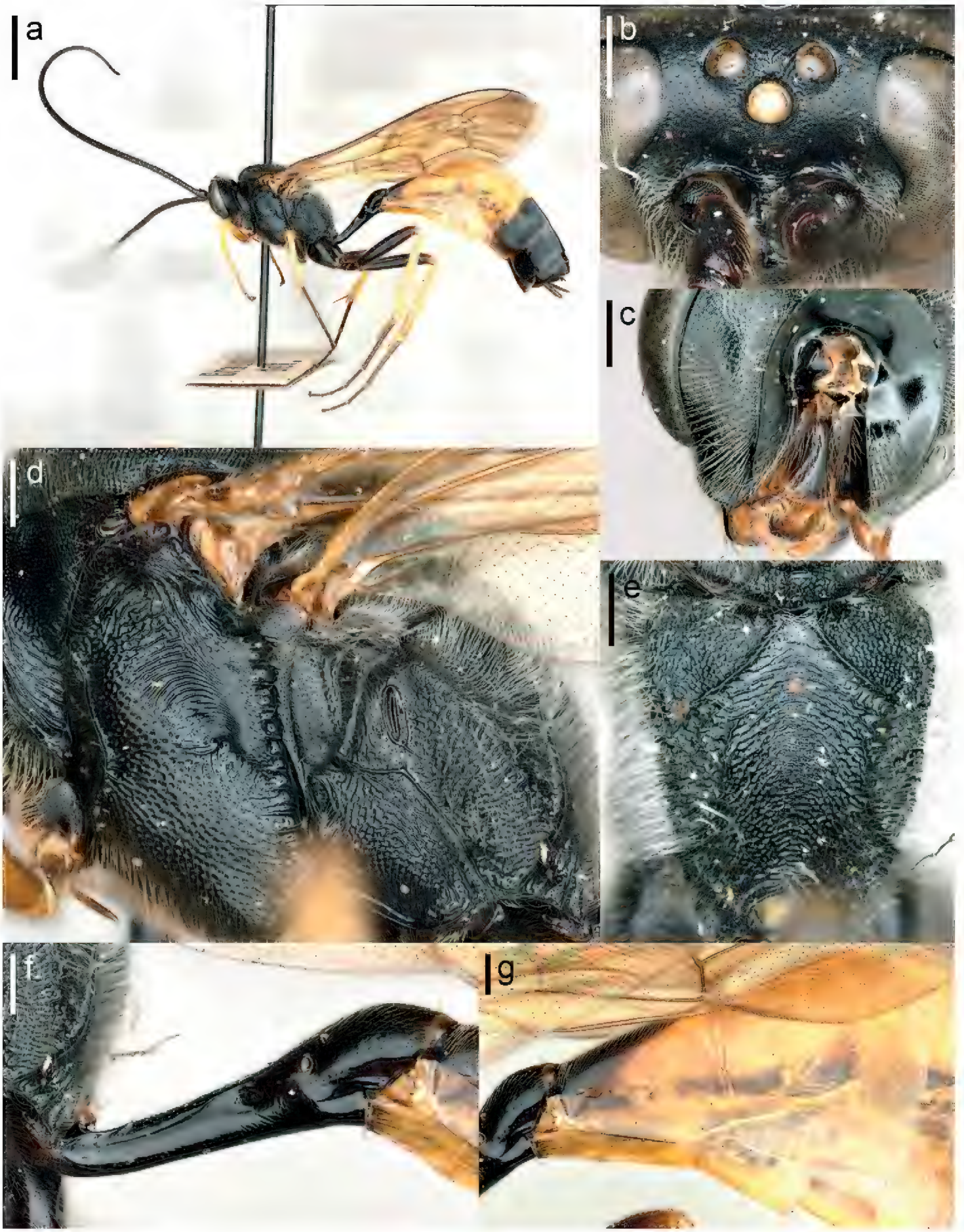

Figure 33. *D. falcator* (Fabricius, 1775), ♀ Switzerland. **a** habitus **b** antennal carina **c** junction of genal and hypostomal carina **d** mesopleuron **e** propodeum **f** first gastral tergite **g** 2nd and 3rd gastral tergites. Scale bars: 3 mm (**a**); 0.5 mm (**b–g**). https://doi.org/10.5281/zenodo.6370158.

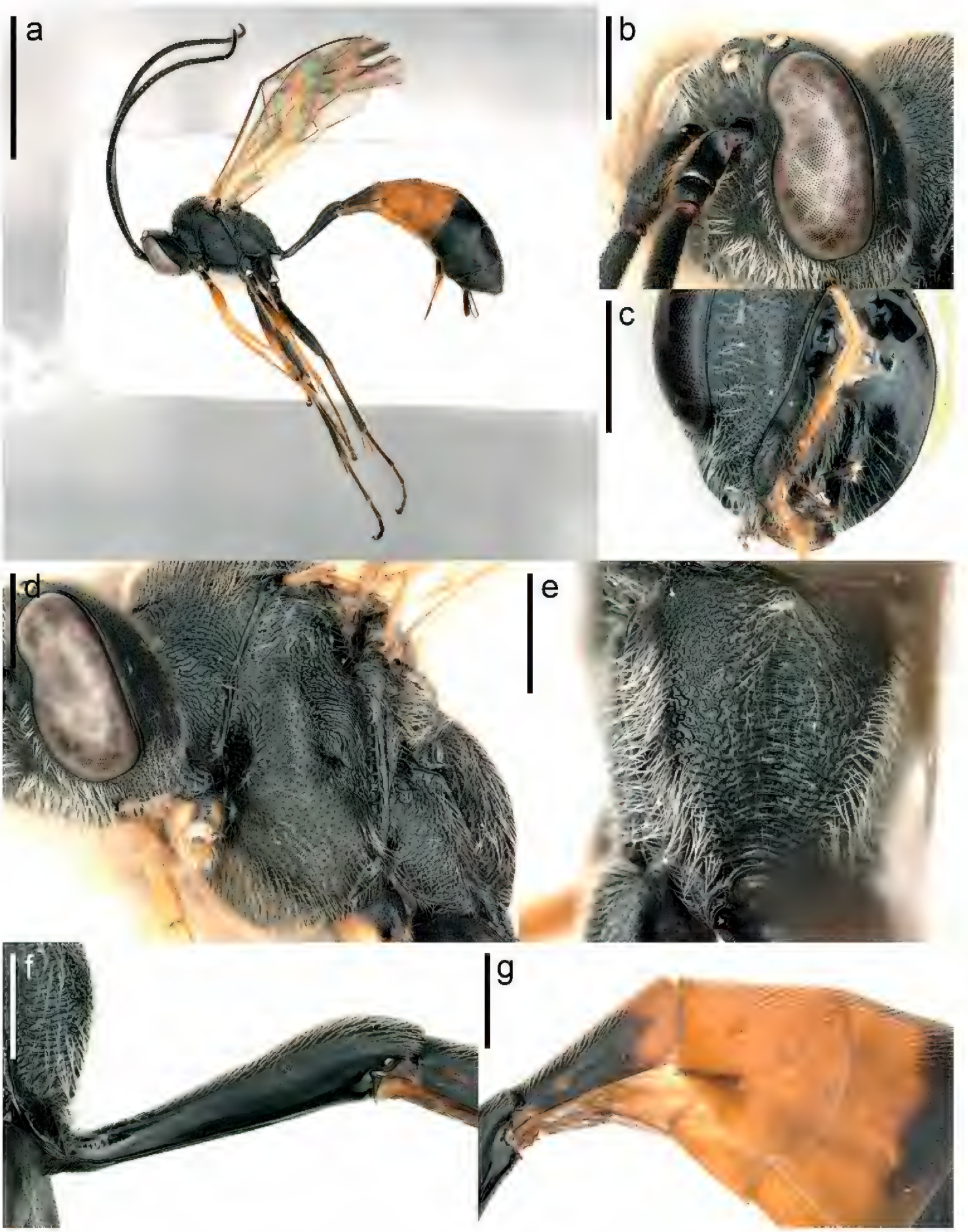

Figure 34. *D. flagellator* (Fabricius, 1793), ♀ Switzerland. **a** habitus **b** antennal carina **c** junction of genal and hypostomal carina **d** mesopleuron **e** propodeum **f** first gastral tergite **g** 2nd and 3rd gastral tergites. Scale bars: 3 mm (**a**); 0.5 mm (**b–g**). https://doi.org/10.5281/zenodo.6370164.

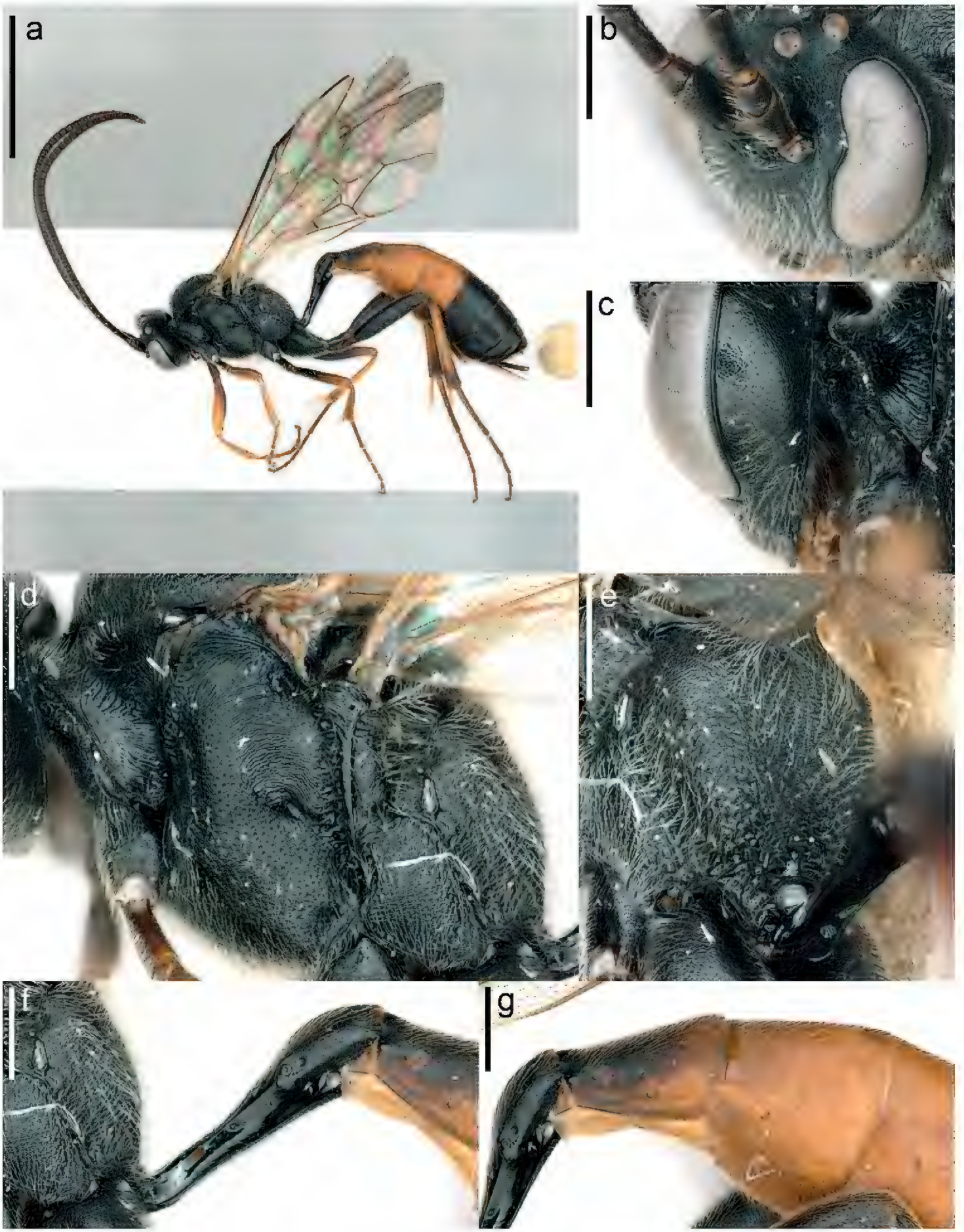

Figure 35. *D. humilis* (Förster, 1868), ♀ Switzerland. **a** habitus **b** antennal carina **c** junction of genal and hypostomal carina **d** mesopleuron **e** propodeum **f** first gastral tergite **g** 2nd and 3rd gastral tergites. Scale bars: 3 mm (**a**); 0.5 mm (**b–g**). https://doi.org/10.5281/zenodo.6370179.

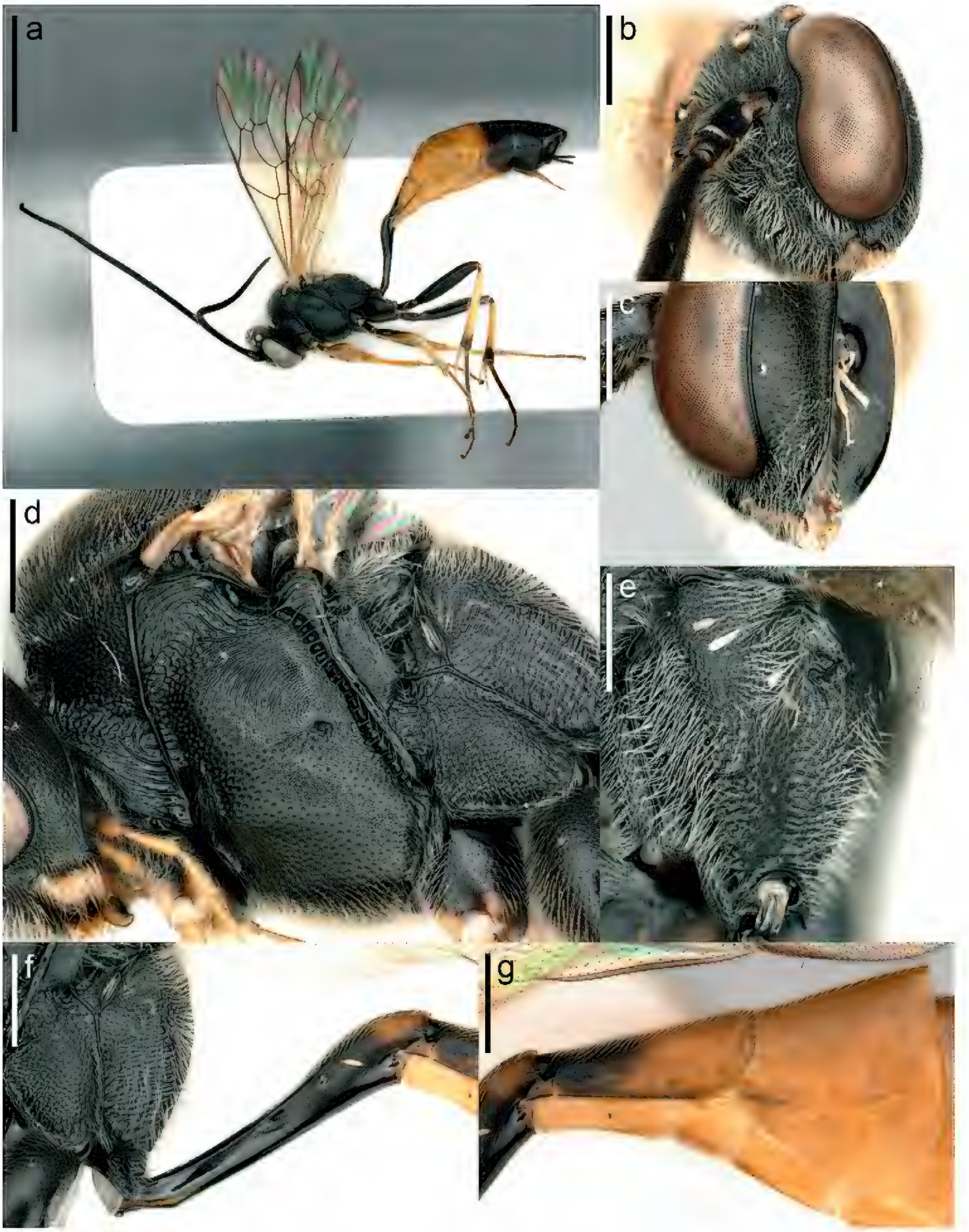

Figure 36. *D. inermis* (Förster, 1868), ♀ Sweden. **a** habitus **b** antennal carina **c** junction of genal and hypostomal carina **d** mesopleuron **e** propodeum **f** first gastral tergite **g** 2nd and 3rd gastral tergites. Scale bars: 3 mm (**a**); 0.5 mm (**b–g**). https://doi.org/10.5281/zenodo.6370190.

Figure 37. *D. infesta* (Förster, 1868), ♀ Switzerland. **a** habitus **b** antennal carina **c** junction of genal and hypostomal carina **d** mesopleuron **e** propodeum **f** first gastral tergite **g** 2nd and 3rd gastral tergites. Scale bars: 3 mm (**a**); 0.5 mm (**b–g**). https://doi.org/10.5281/zenodo.6370198.

Figure 38. *D. insignita* (Förster, 1868), ♀ Sweden. **a** habitus **b** antennal carina **c** junction of genal and hypostomal carina **d** mesopleuron **e** propodeum **f** first gastral tergite **g** 2nd and 3rd gastral tergites. Scale bars: 3 mm (**a**); 0.5 mm (**b–g**). https://doi.org/10.5281/zenodo.6370208.

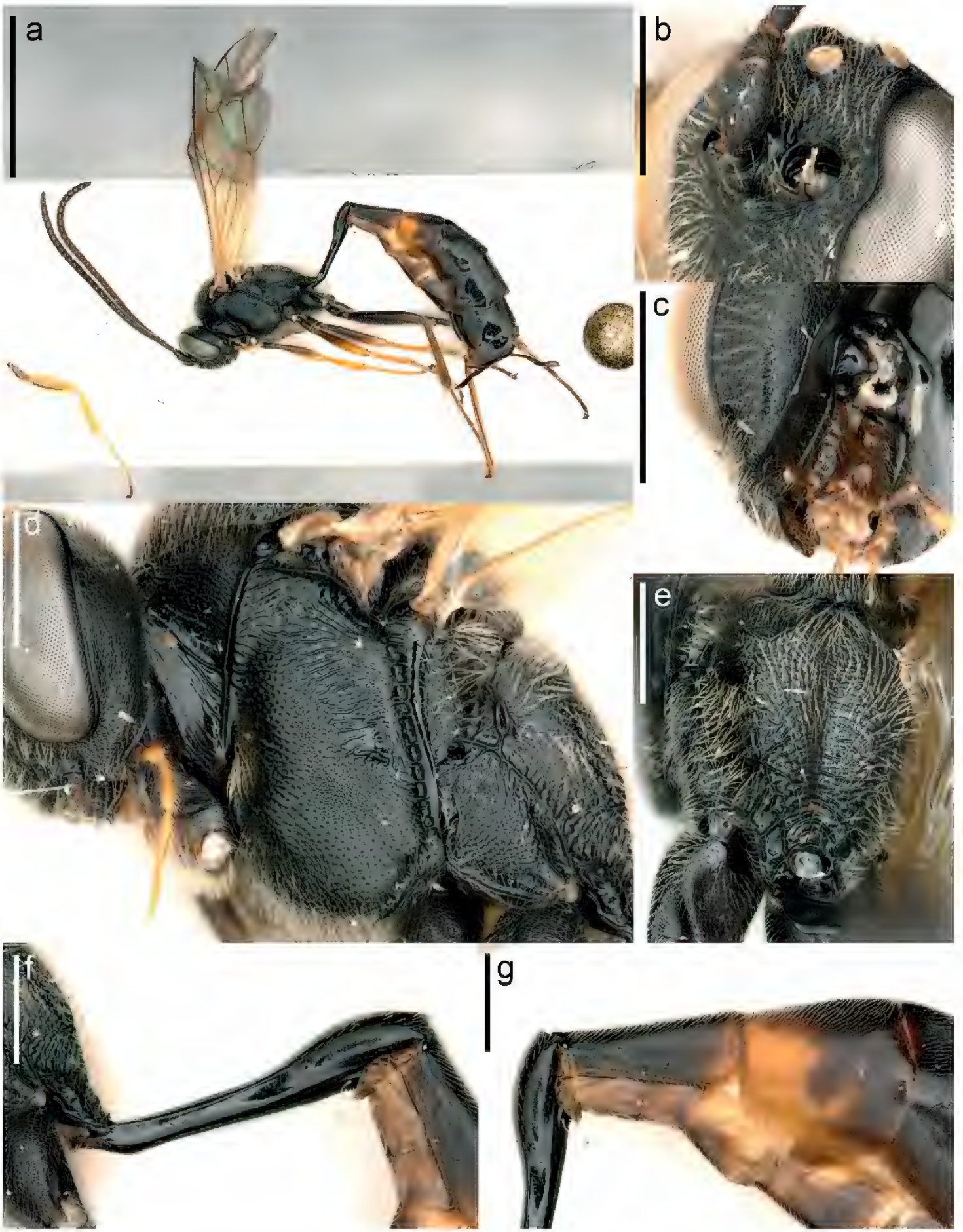

Figure 39. *D. juvenilis* (Förster, 1868), ♀ Switzerland. **a** habitus **b** antennal carina **c** junction of genal and hypostomal carina **d** mesopleuron **e** propodeum **f** first gastral tergite **g** 2nd and 3rd gastral tergites. Scale bars: 3 mm (**a**); 0.5 mm (**b–g**). https://doi.org/10.5281/zenodo.6370232.

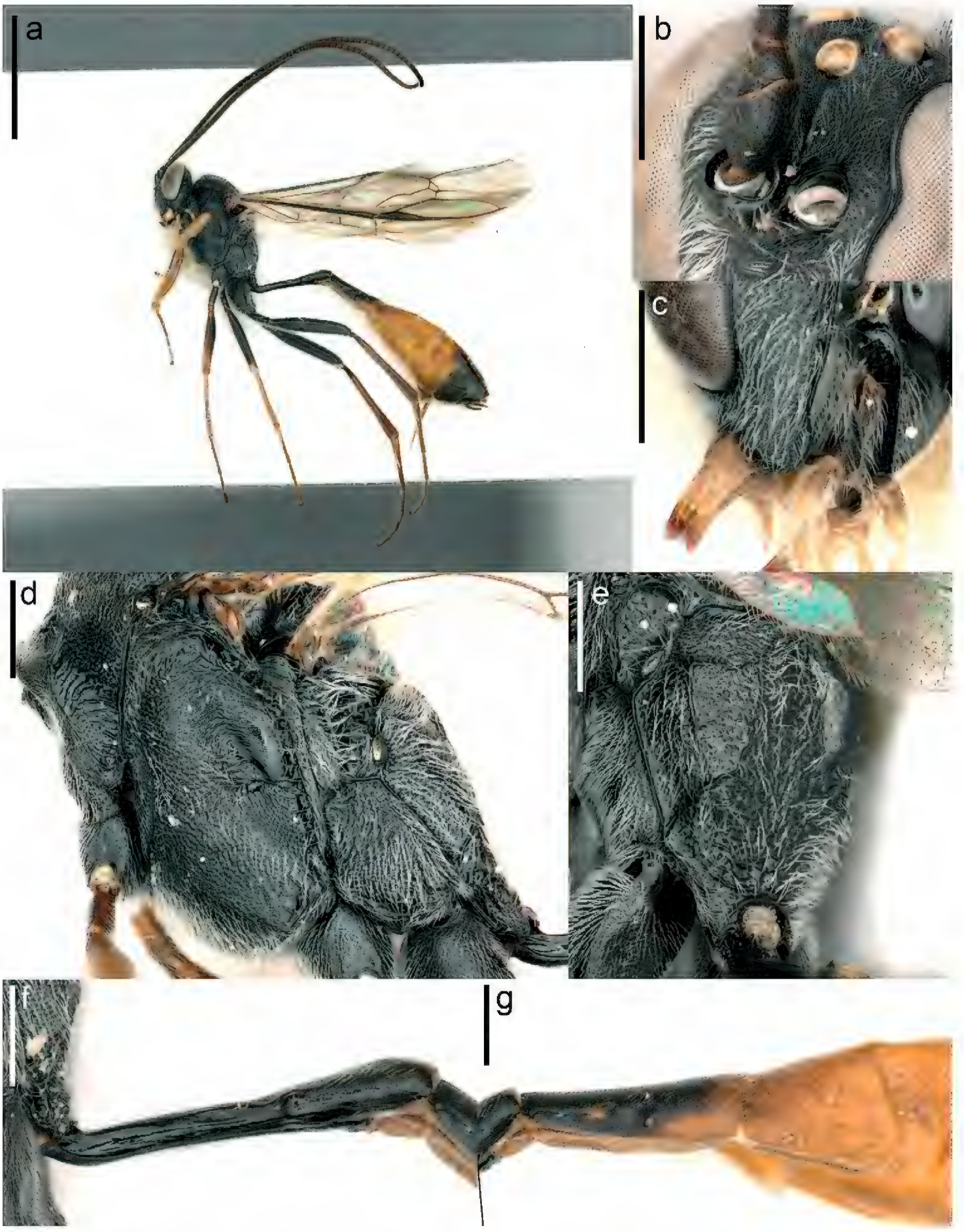

Figure 40. *D. leptogaster* (Holmgren, 1860), ♀ Sweden. **a** habitus **b** antennal carina **c** junction of genal and hypostomal carina **d** mesopleuron **e** propodeum **f** first gastral tergite **g** 2nd and 3rd gastral tergites. Scale bars: 3 mm (**a**); 0.5 mm (**b–g**). https://doi.org/10.5281/zenodo.6370357.

Figure 41. *D. libertatis* (Teunissen, 1947), ♀ Sweden. **a** habitus **b** antennal carina **c** junction of genal and hypostomal carina **d** mesopleuron **e** propodeum **f** first gastral tergite **g** 2nd and 3rd gastral tergites. Scale bars: 3 mm (**a**); 0.5 mm (**b–g**). https://doi.org/10.5281/zenodo.6370363.

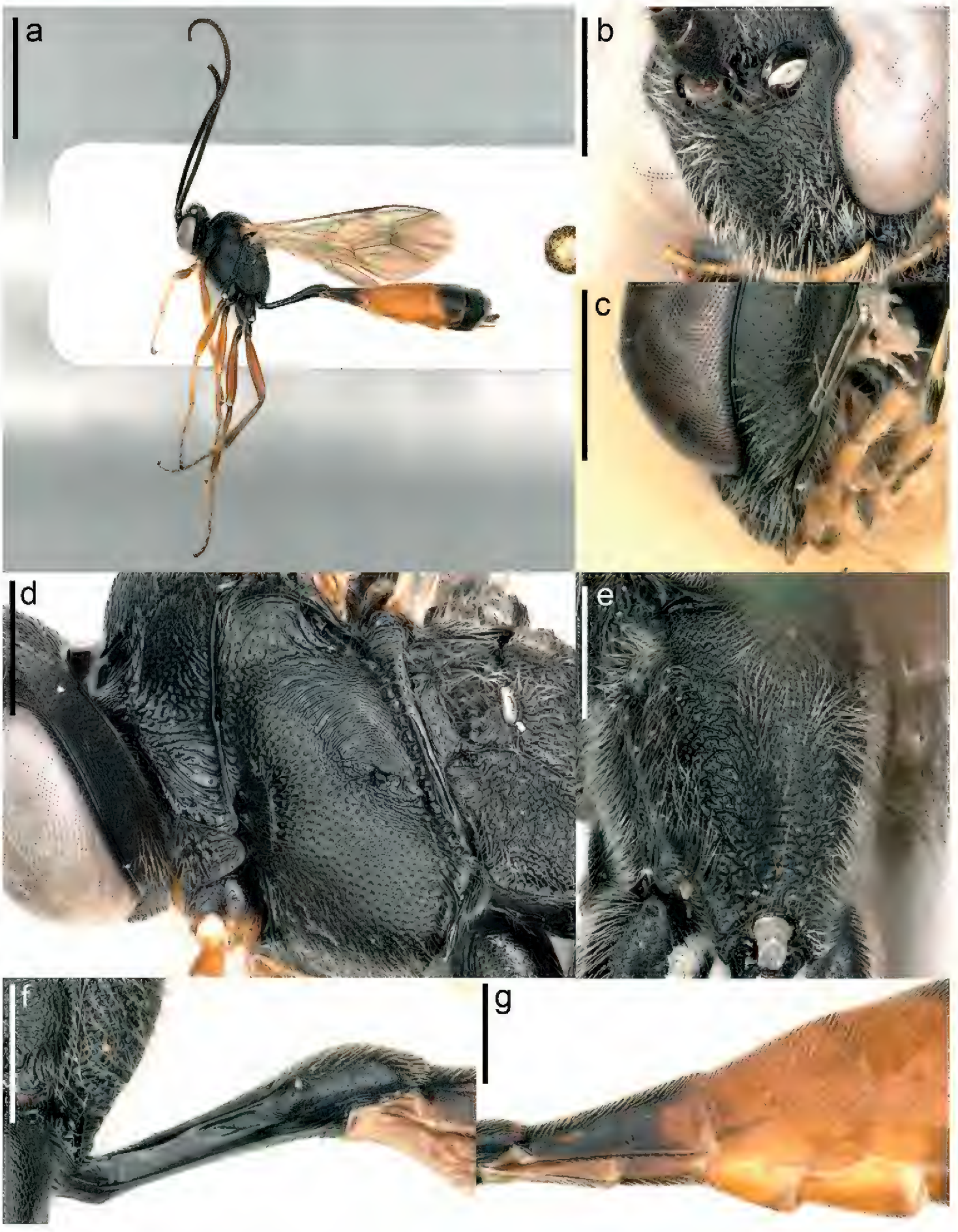

Figure 42. *D. limnobia* (Thomson, 1887), ♀ Sweden. **a** habitus **b** antennal carina **c** junction of genal and hypostomal carina **d** mesopleuron **e** propodeum **f** first gastral tergite **g** 2nd and 3rd gastral tergites. Scale bars: 3 mm (**a**); 0.5 mm (**b–g**). https://doi.org/10.5281/zenodo.6370379.

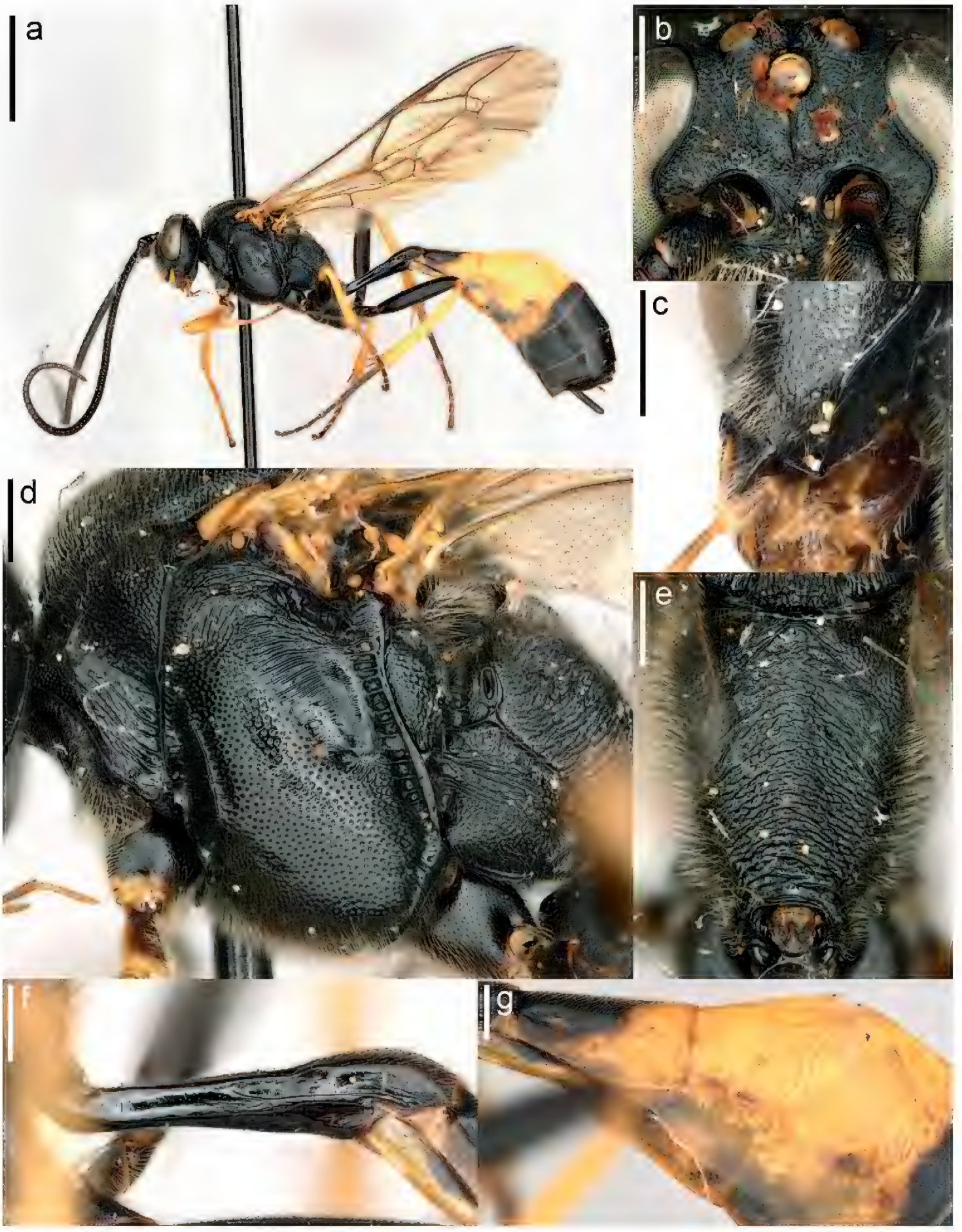

Figure 43. *D. mercator* (Fabricius, 1793), ♀ Switzerland. **a** habitus **b** antennal carina **c** junction of genal and hypostomal carina **d** mesopleuron **e** propodeum **f** first gastral tergite **g** 2nd and 3rd gastral tergites. Scale bars: 3 mm (**a**); 0.5 mm (**b–g**). https://doi.org/10.5281/zenodo.6370394.

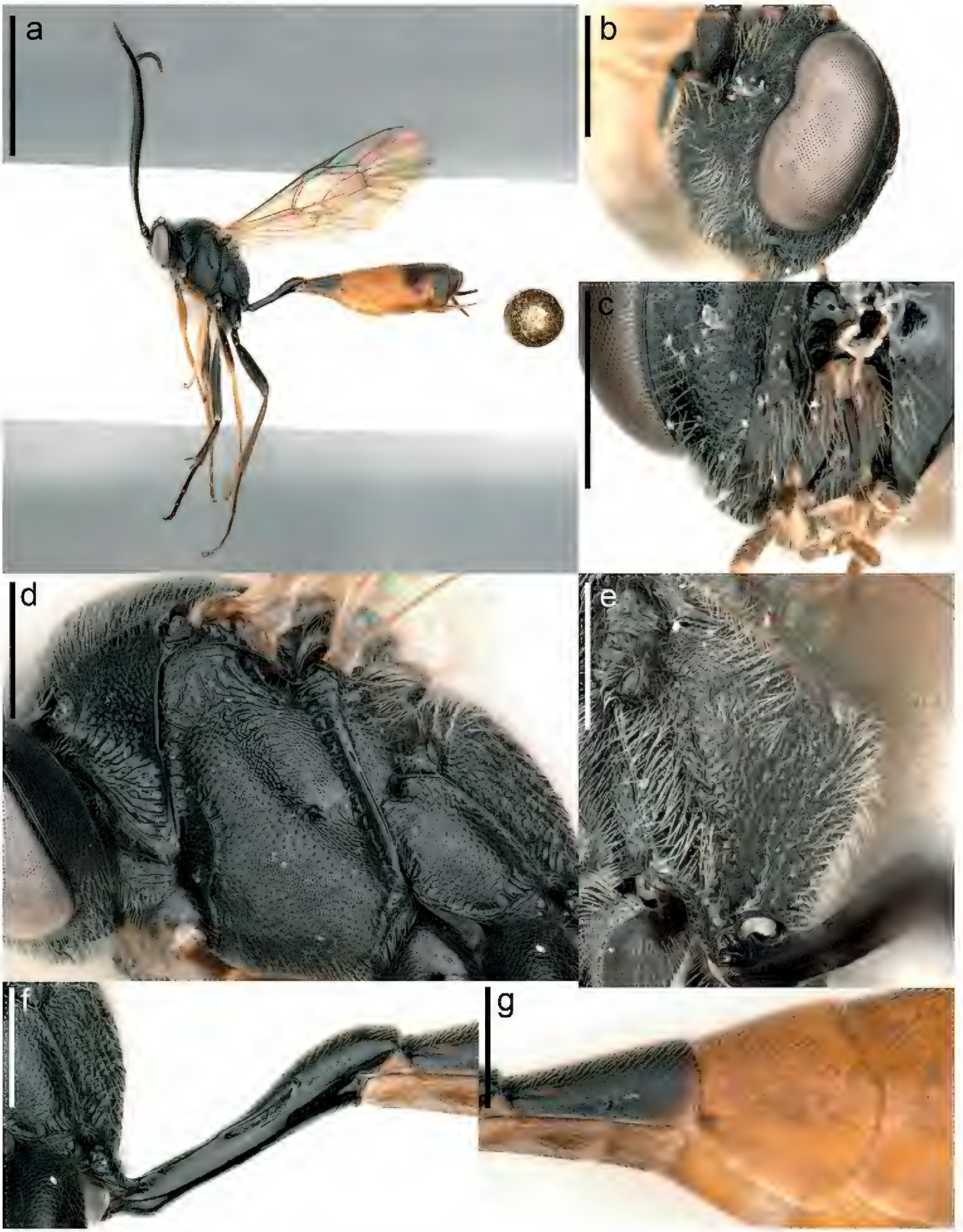

Figure 44. *D. minor* (Provancher, 1879), ♀ Sweden. **a** habitus **b** antennal carina **c** junction of genal and hypostomal carina **d** mesopleuron **e** propodeum **f** first gastral tergite **g** 2nd and 3rd gastral tergites. Scale bars: 3 mm (**a**); 0.5 mm (**b–g**). https://doi.org/10.5281/zenodo.6370397.

Figure 45. *D.* cf. *nebulosa* Horstmann, 2009, ♂ Sweden. **a** habitus **b** antennal carina **c** junction of genal and hypostomal carina **d** mesopleuron **e** propodeum **f** first gastral tergite **g** 2nd and 3rd gastral tergites. Scale bars: 3 mm (**a**); 0.5 mm (**b–g**). https://doi.org/10.5281/zenodo.6370415.

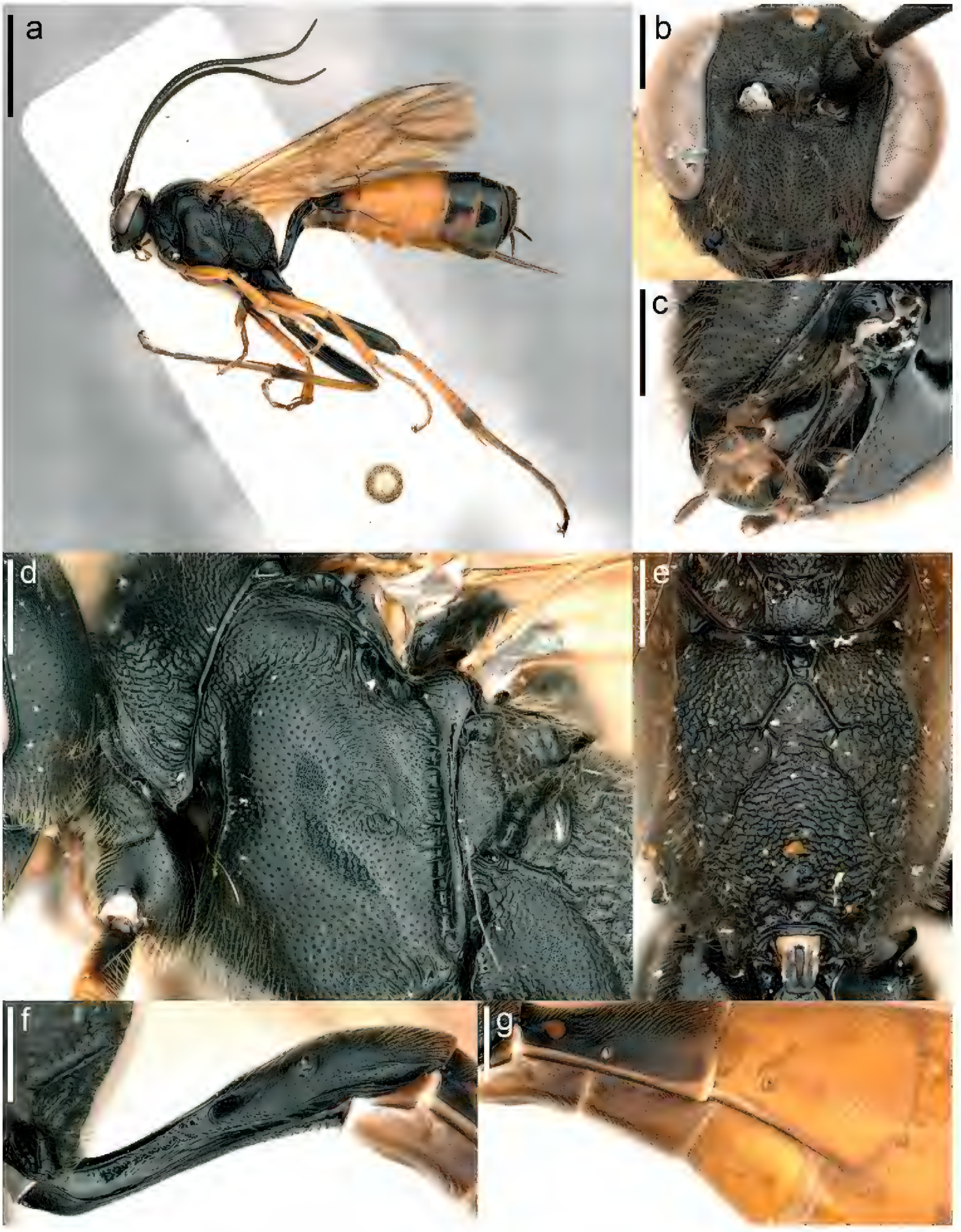

Figure 46. *D. nidulator* (Fabricius, 1804), ♀ Sweden. **a** habitus **b** antennal carina **c** junction of genal and hypostomal carina **d** mesopleuron **e** propodeum **f** first gastral tergite **g** 2nd and 3rd gastral tergites. Scale bars: 3 mm (**a**); 0.5 mm (**b–g**). https://doi.org/10.5281/zenodo.6370425.

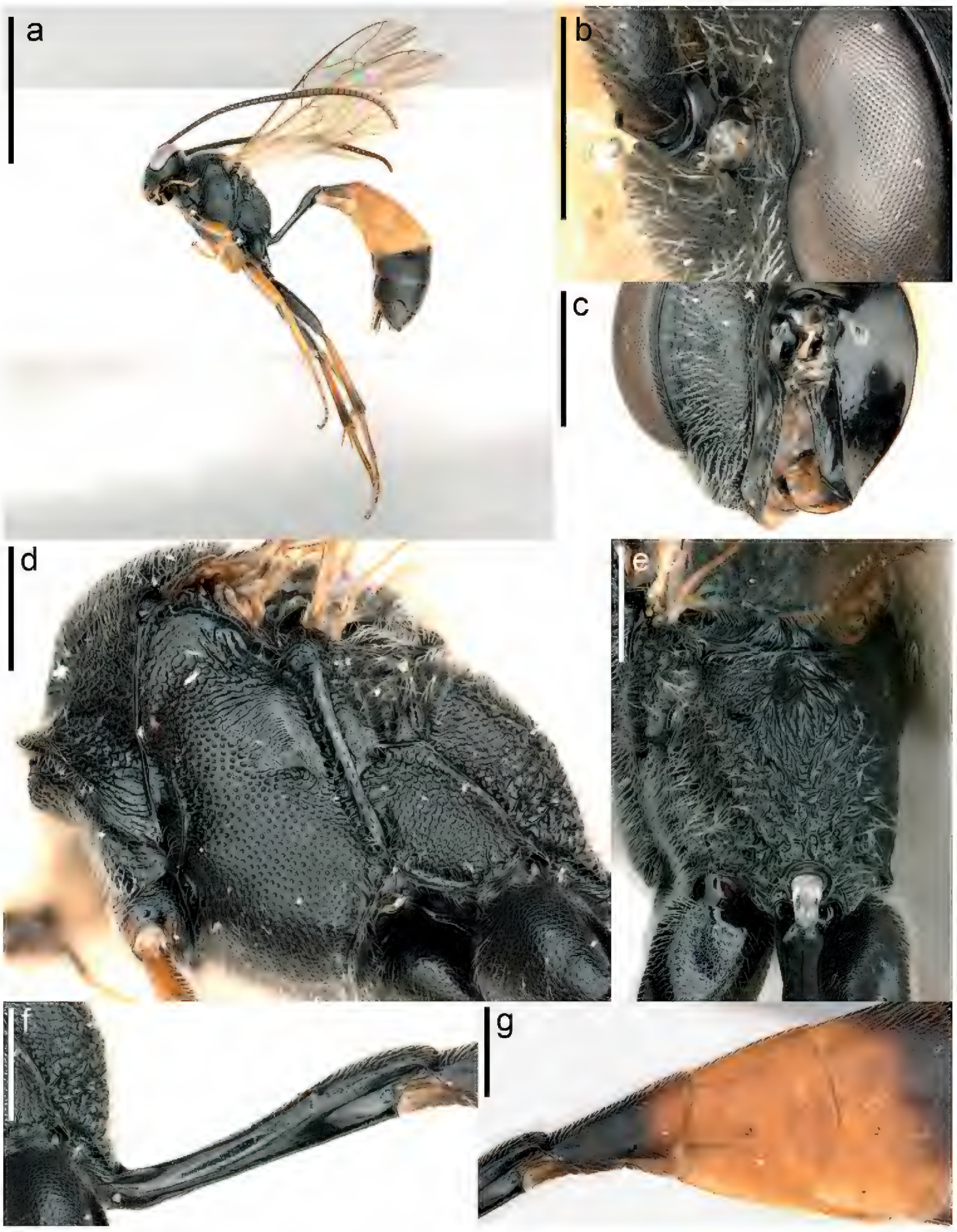

Figure 47. *D. notabilis* (Förster, 1868), ♀ Sweden. **a** habitus **b** antennal carina **c** junction of genal and hypostomal carina **d** mesopleuron **e** propodeum **f** first gastral tergite **g** 2nd and 3rd gastral tergites. Scale bars: 3 mm (**a**); 0.5 mm (**b–g**). https://doi.org/10.5281/zenodo.6370489.

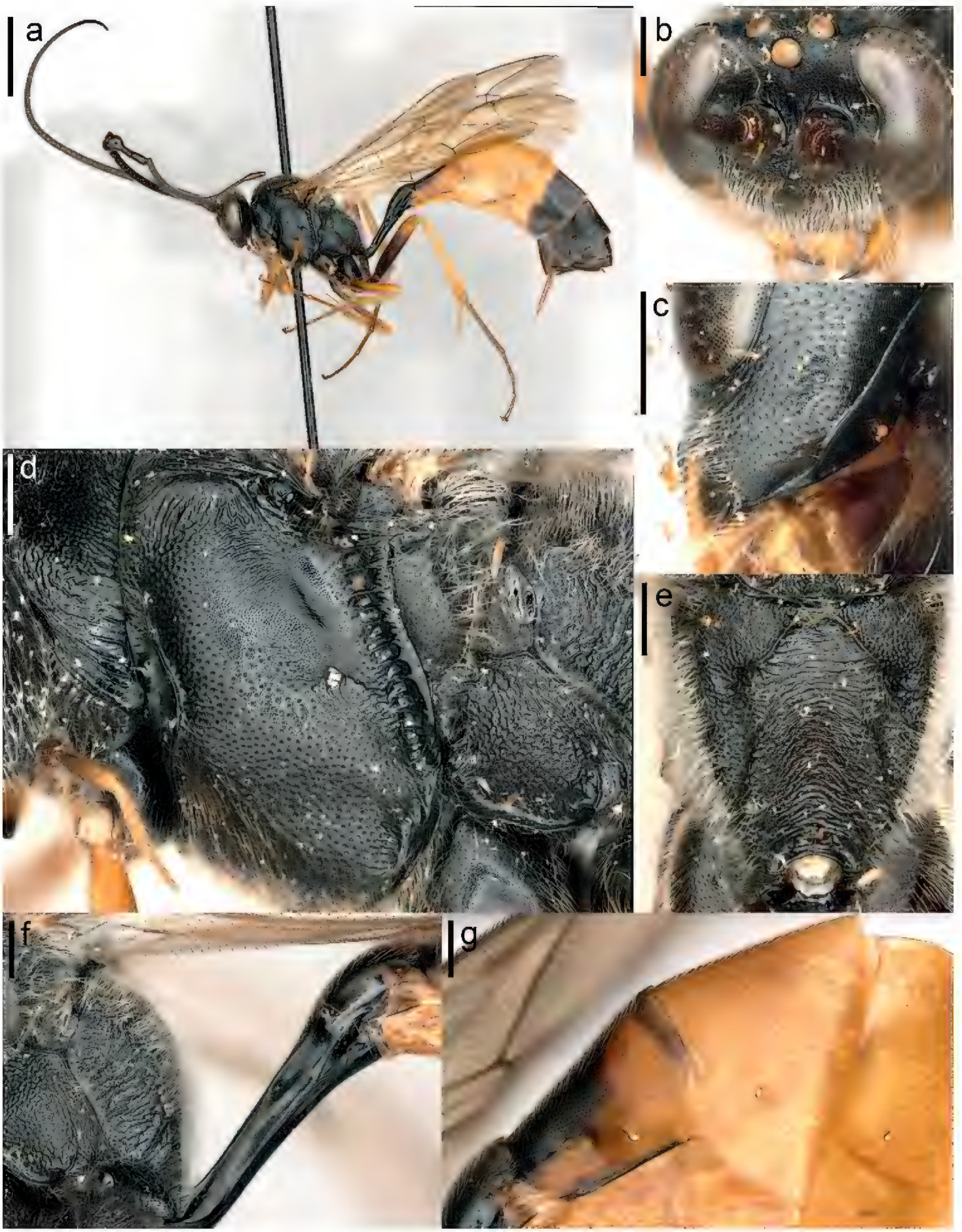

Figure 48. *D. obliterata* (Holmgren, 1872), ♀ Sweden. **a** habitus **b** antennal carina **c** junction of genal and hypostomal carina **d** mesopleuron **e** propodeum **f** first gastral tergite **g** 2nd and 3rd gastral tergites. Scale bars: 3 mm (**a**); 0.5 mm (**b–g**). https://doi.org/10.5281/zenodo.6370522.

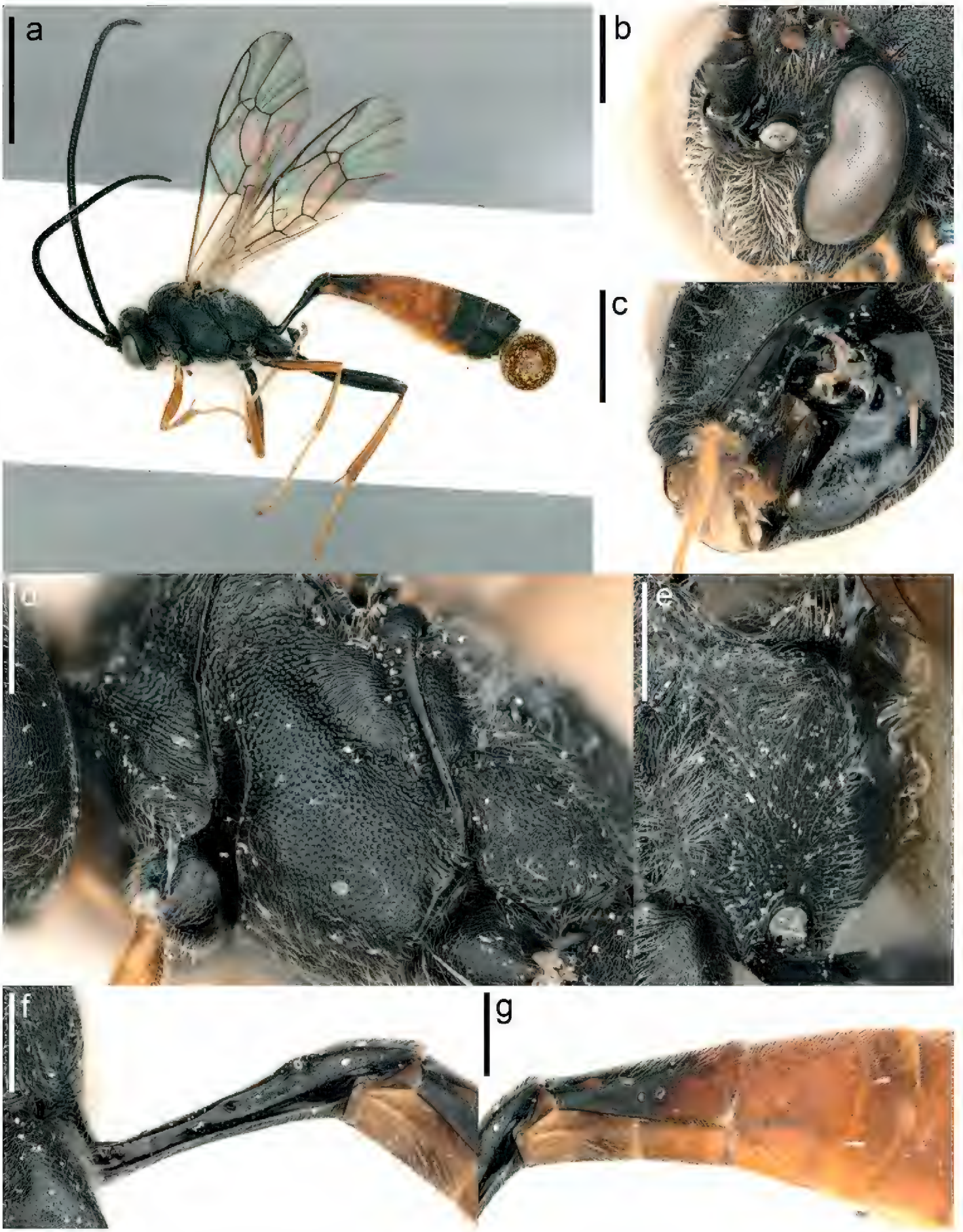

Figure 49. *D. opaca* (Thomson, 1887), ♀ Sweden. **a** habitus **b** antennal carina **c** junction of genal and hypostomal carina **d** mesopleuron **e** propodeum **f** first gastral tergite **g** 2nd and 3rd gastral tergites. Scale bars: 3 mm (**a**); 0.5 mm (**b–g**). https://doi.org/10.5281/zenodo.6370545.

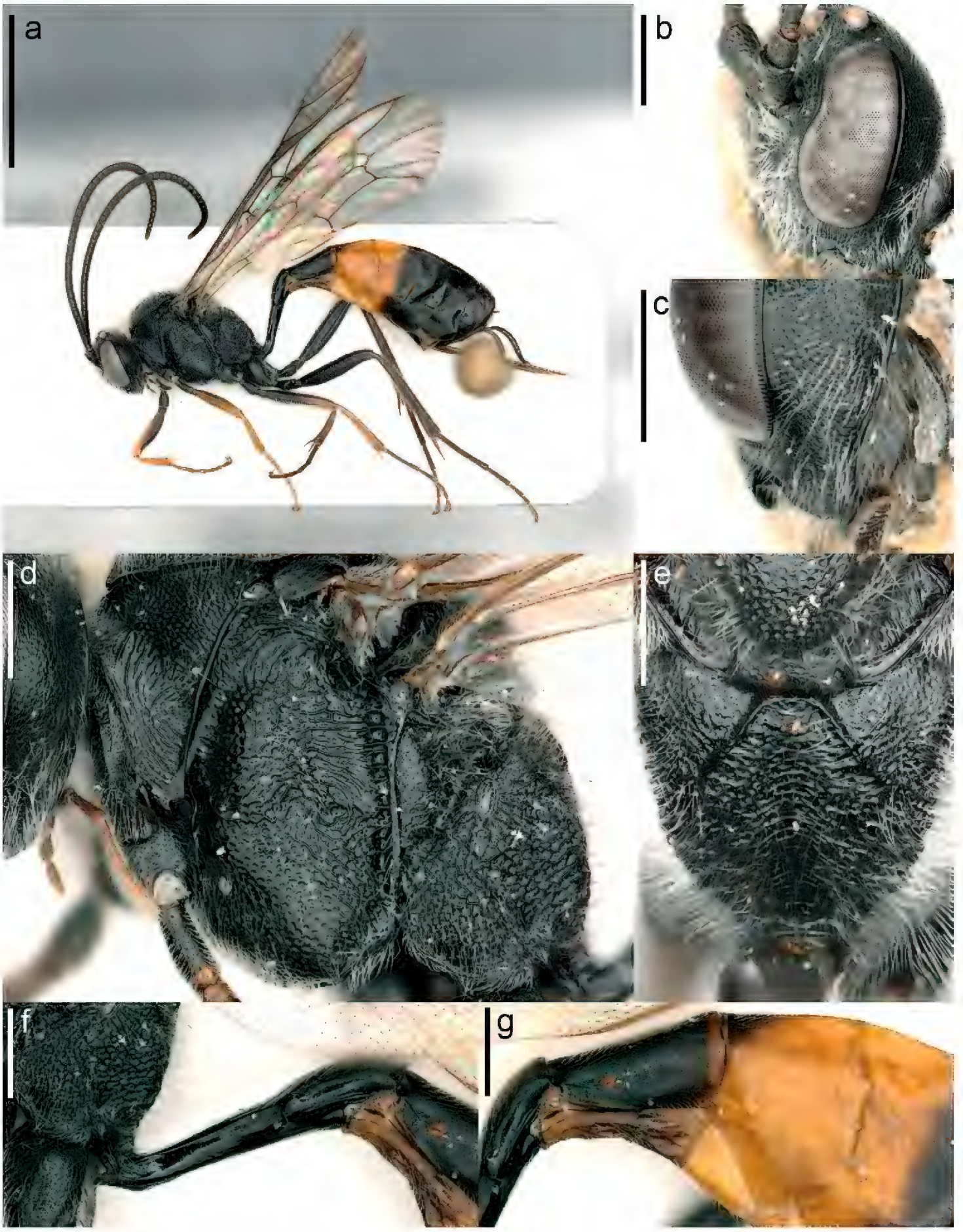

Figure 50. *D. petiolator* (Fabricius, 1804), ♀ Sweden. **a** habitus **b** antennal carina **c** junction of genal and hypostomal carina **d** mesopleuron **e** propodeum **f** first gastral tergite **g** 2nd and 3rd gastral tergites. Scale bars: 3 mm (**a**); 0.5 mm (**b–g**). https://doi.org/10.5281/zenodo.6370570.

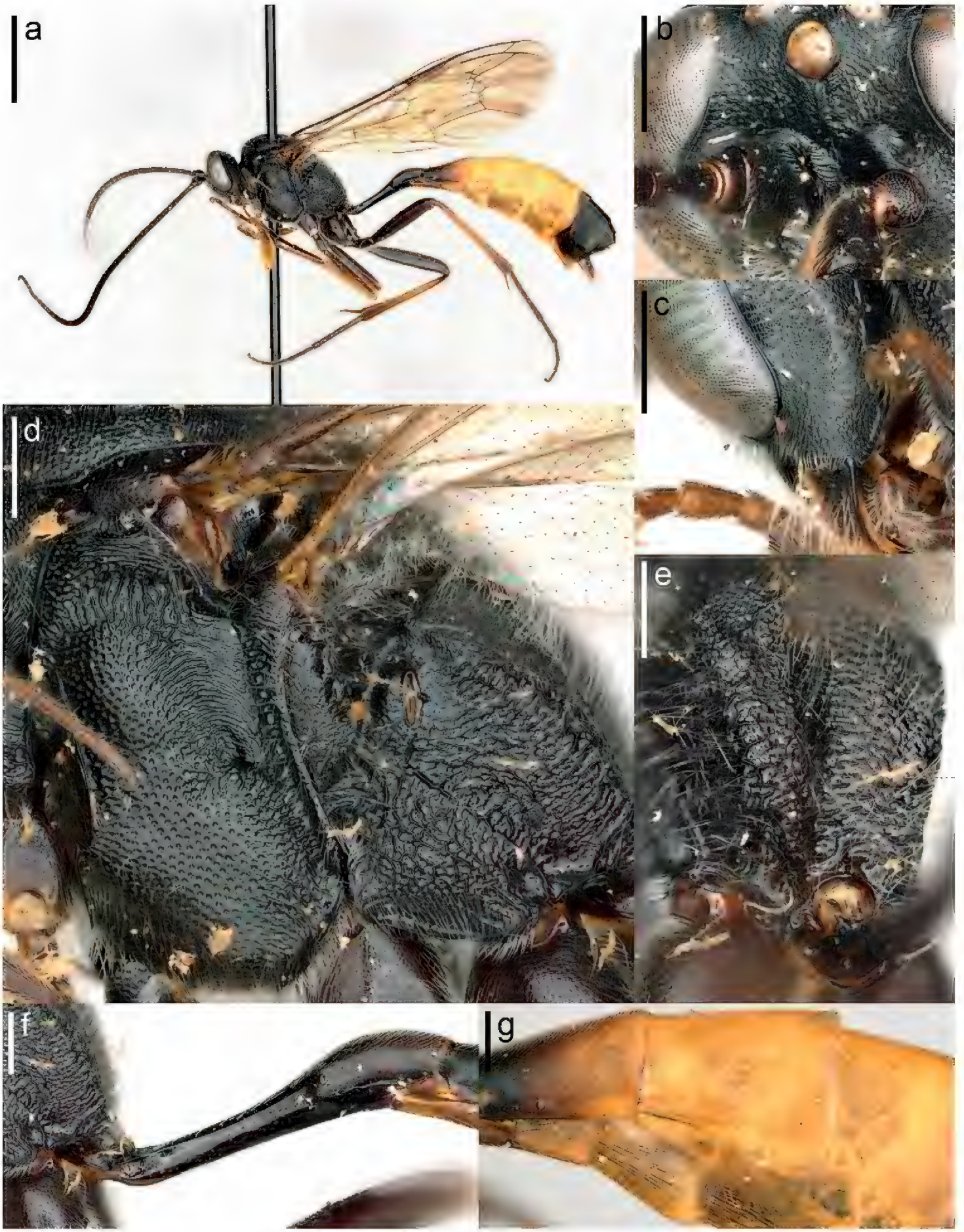

Figure 51. *D. pineticola* (Holmgren, 1872), ♀ Switzerland. **a** habitus **b** antennal carina **c** junction of genal and hypostomal carina **d** mesopleuron **e** propodeum **f** first gastral tergite **g** 2nd and 3rd gastral tergites. Scale bars: 3 mm (**a**); 0.5 mm (**b–g**). https://doi.org/10.5281/zenodo.6370593.

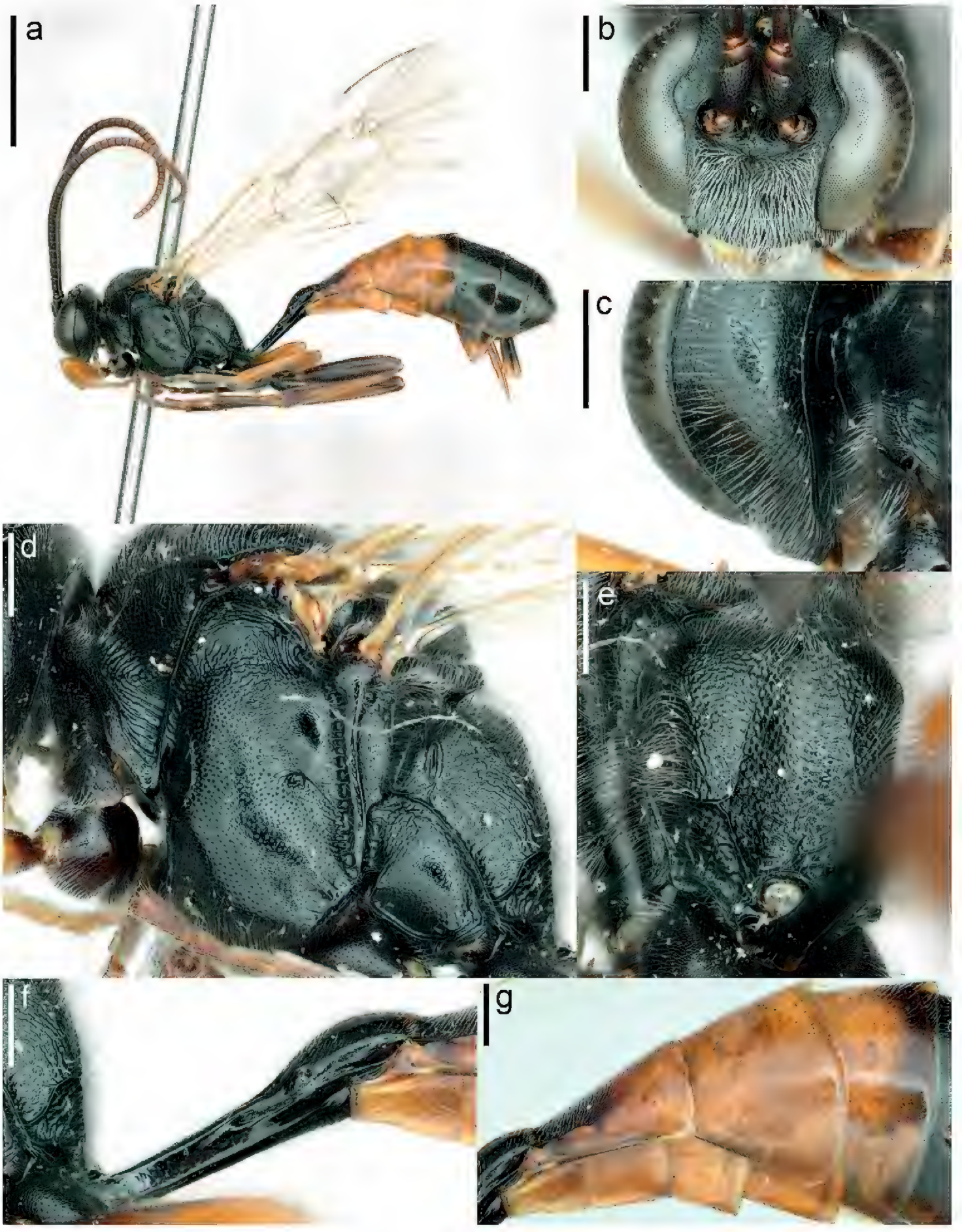

Figure 52. *D. polita* (Förster, 1868), ♀ Switzerland. **a** habitus **b** antennal carina **c** junction of genal and hypostomal carina **d** mesopleuron **e** propodeum **f** first gastral tergite **g** 2nd and 3rd gastral tergites. Scale bars: 3 mm (**a**); 0.5 mm (**b–g**). https://doi.org/10.5281/zenodo.6370620.

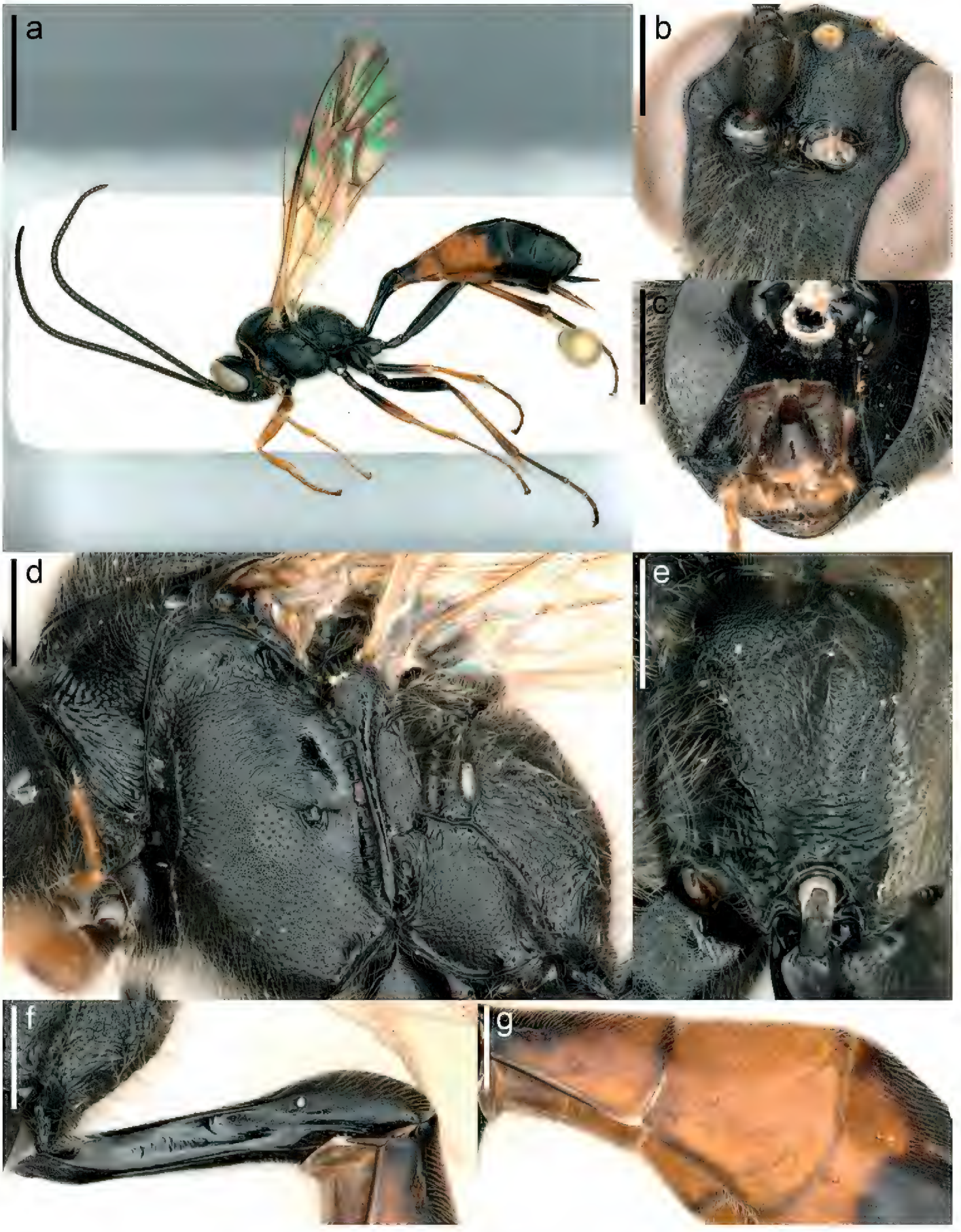

Figure 53. *D. prominula* (Förster, 1868), ♀ Sweden. **a** habitus **b** antennal carina **c** junction of genal and hypostomal carina **d** mesopleuron **e** propodeum **f** first gastral tergite **g** 2nd and 3rd gastral tergites. Scale bars: 3 mm (**a**); 0.5 mm (**b–g**). https://doi.org/10.5281/zenodo.6370633.

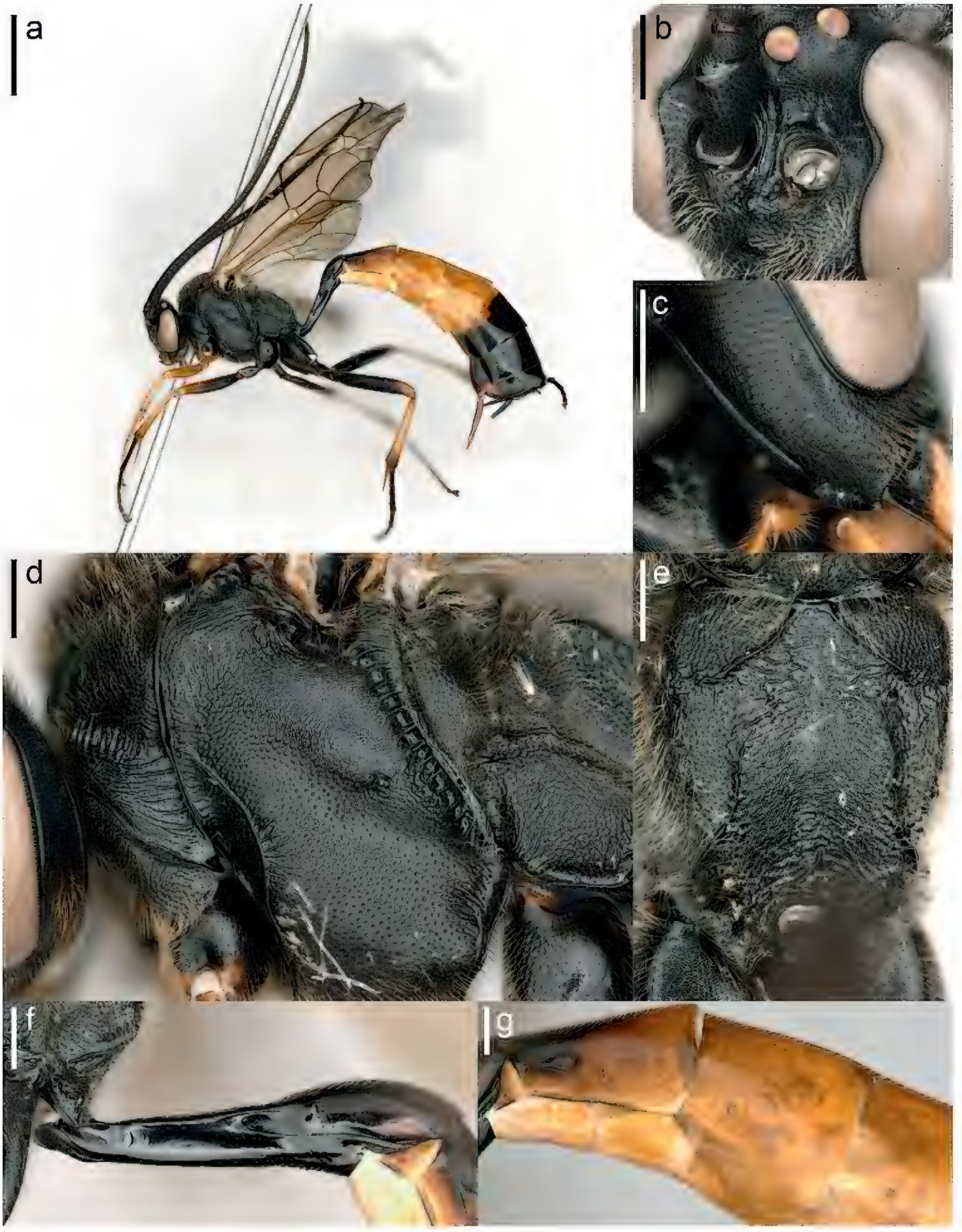

Figure 54. *D. pugillator* (Linnaeus, 1758), ♀ Sweden. **a** habitus **b** antennal carina **c** junction of genal and hypostomal carina **d** mesopleuron **e** propodeum **f** first gastral tergite **g** 2nd and 3rd gastral tergites. Scale bars: 3 mm (**a**); 0.5 mm (**b–g**). https://doi.org/10.5281/zenodo.6370641.

Figure 55. *D. pulchripes* (Holmgren, 1872), ♀ Sweden. **a** habitus **b** antennal carina **c** junction of genal and hypostomal carina **d** mesopleuron **e** propodeum **f** first gastral tergite **g** 2nd and 3rd gastral tergites. Scale bars: 3 mm (**a**); 0.5 mm (**b–g**). https://doi.org/10.5281/zenodo.6370652.

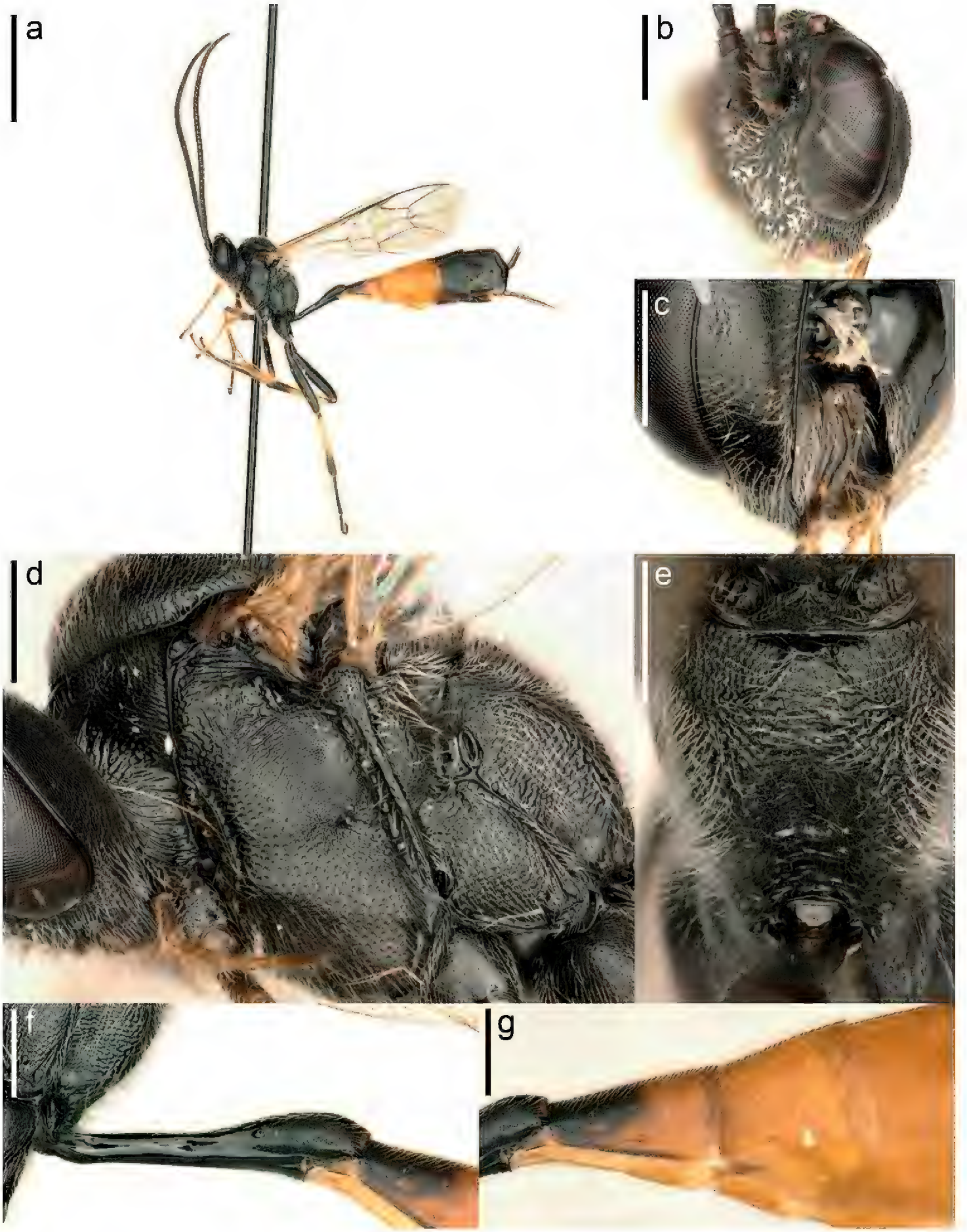

Figure 56. *D. recta* (Thomson, 1887), ♀ Sweden. **a** habitus **b** antennal carina **c** junction of genal and hypostomal carina **d** mesopleuron **e** propodeum **f** first gastral tergite **g** 2nd and 3rd gastral tergites. Scale bars: 3 mm (**a**); 0.5 mm (**b–g**). https://doi.org/10.5281/zenodo.6370667.

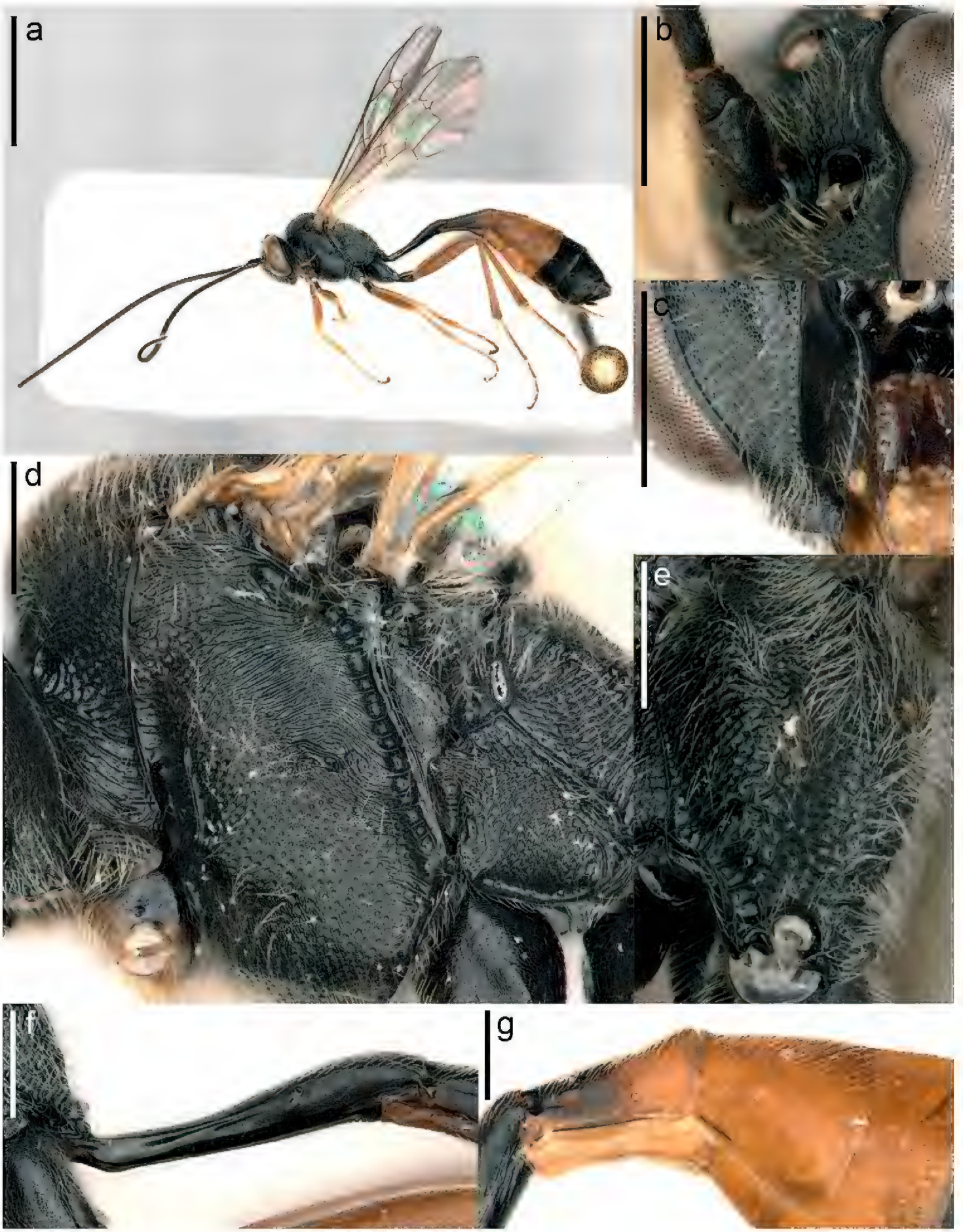

Figure 57. *D. rubidatae* Horstmann, 2009, ♀ Sweden. **a** habitus **b** antennal carina **c** junction of genal and hypostomal carina **d** mesopleuron **e** propodeum **f** first gastral tergite **g** 2nd and 3rd gastral tergites. Scale bars: 3 mm (**a**); 0.5 mm (**b–g**). https://doi.org/10.5281/zenodo.6370676.

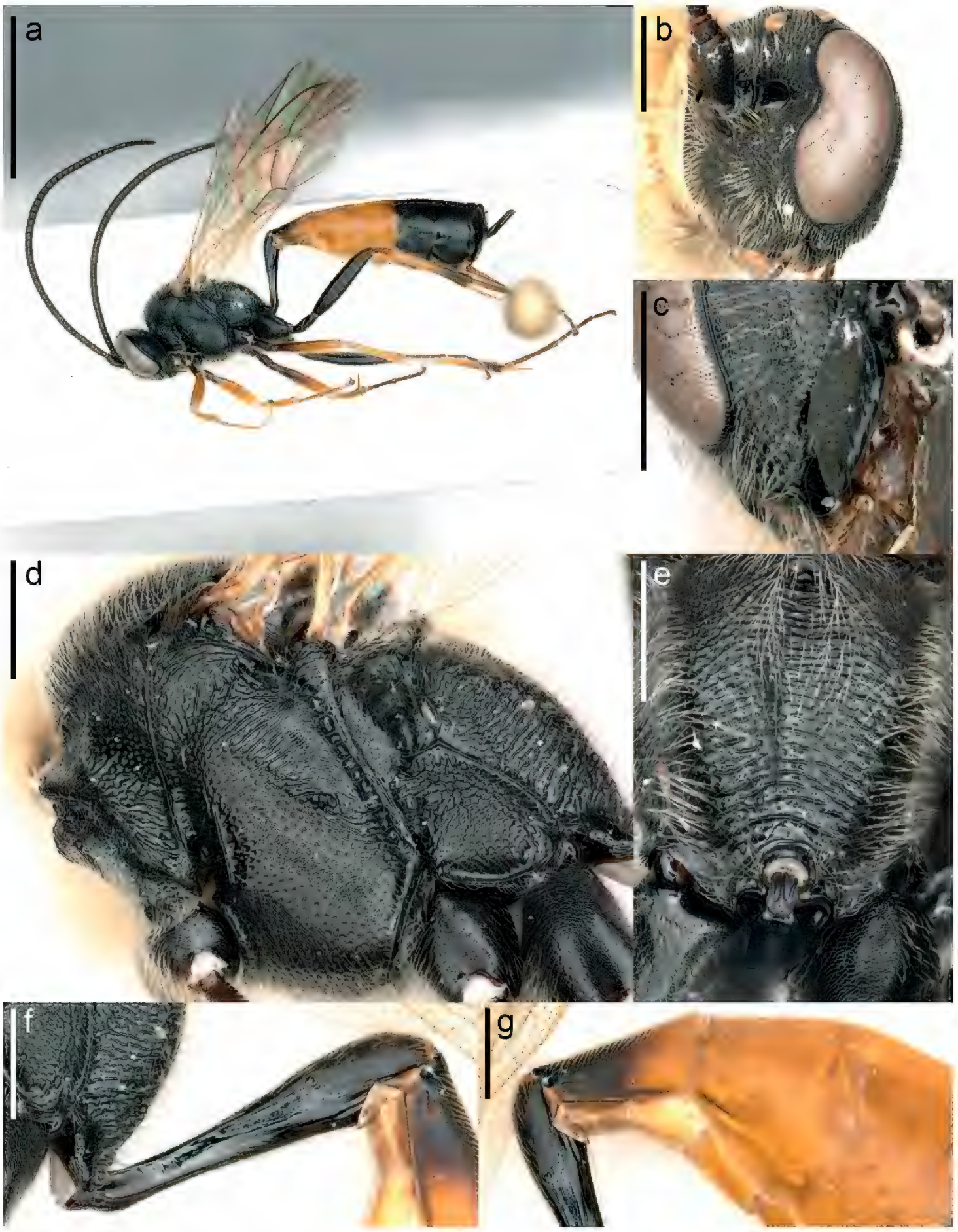

Figure 58. *D. sobolicida* (Förster, 1868), ♀ Sweden. **a** habitus **b** antennal carina **c** junction of genal and hypostomal carina **d** mesopleuron **e** propodeum **f** first gastral tergite **g** 2nd and 3rd gastral tergites. Scale bars: 3 mm (**a**); 0.5 mm (**b–g**). https://doi.org/10.5281/zenodo.6370684.

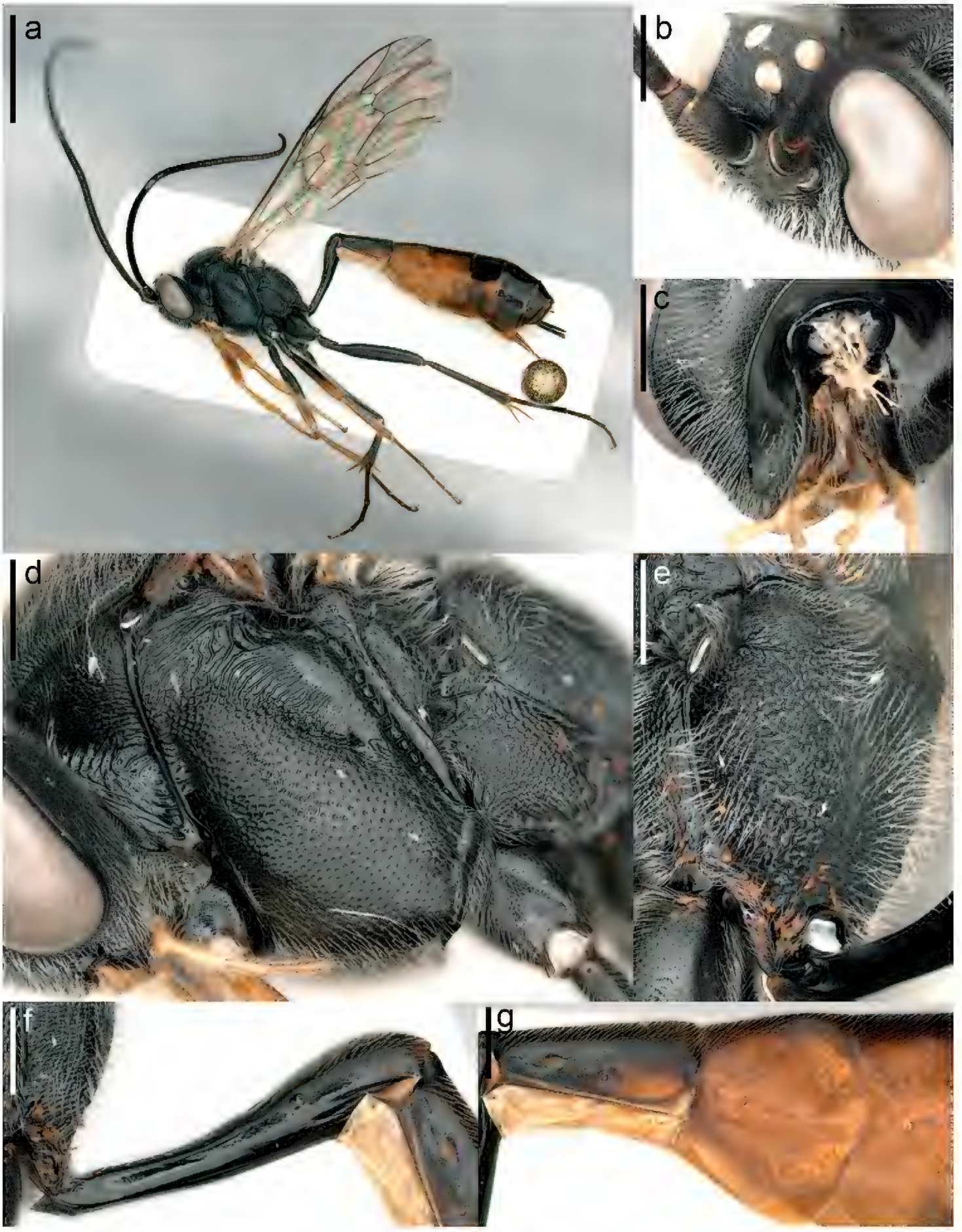

Figure 59. *D. spinipes* (Förster, 1868), ♀ Sweden. **a** habitus **b** antennal carina **c** junction of genal and hypostomal carina **d** mesopleuron **e** propodeum **f** first gastral tergite **g** 2nd and 3rd gastral tergites. Scale bars: 3 mm (**a**); 0.5 mm (**b–g**). https://doi.org/10.5281/zenodo.6370695.

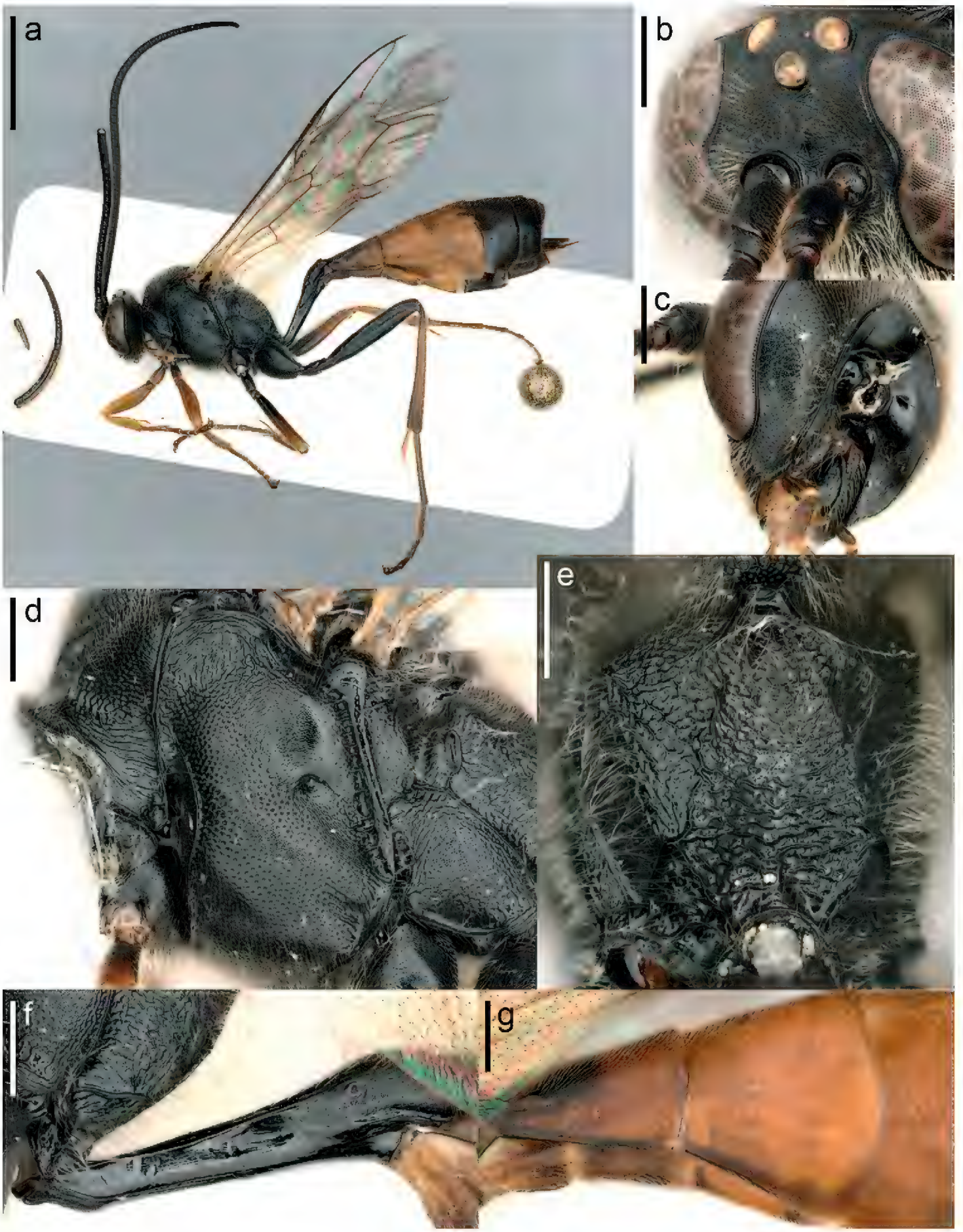

Figure 60. *D. stragifex* (Förster, 1868), ♀ Sweden. **a** habitus **b** antennal carina **c** junction of genal and hypostomal carina **d** mesopleuron **e** propodeum **f** first gastral tergite **g** 2nd and 3rd gastral tergites. Scale bars: 3 mm (**a**); 0.5 mm (**b–g**). https://doi.org/10.5281/zenodo.6370705.

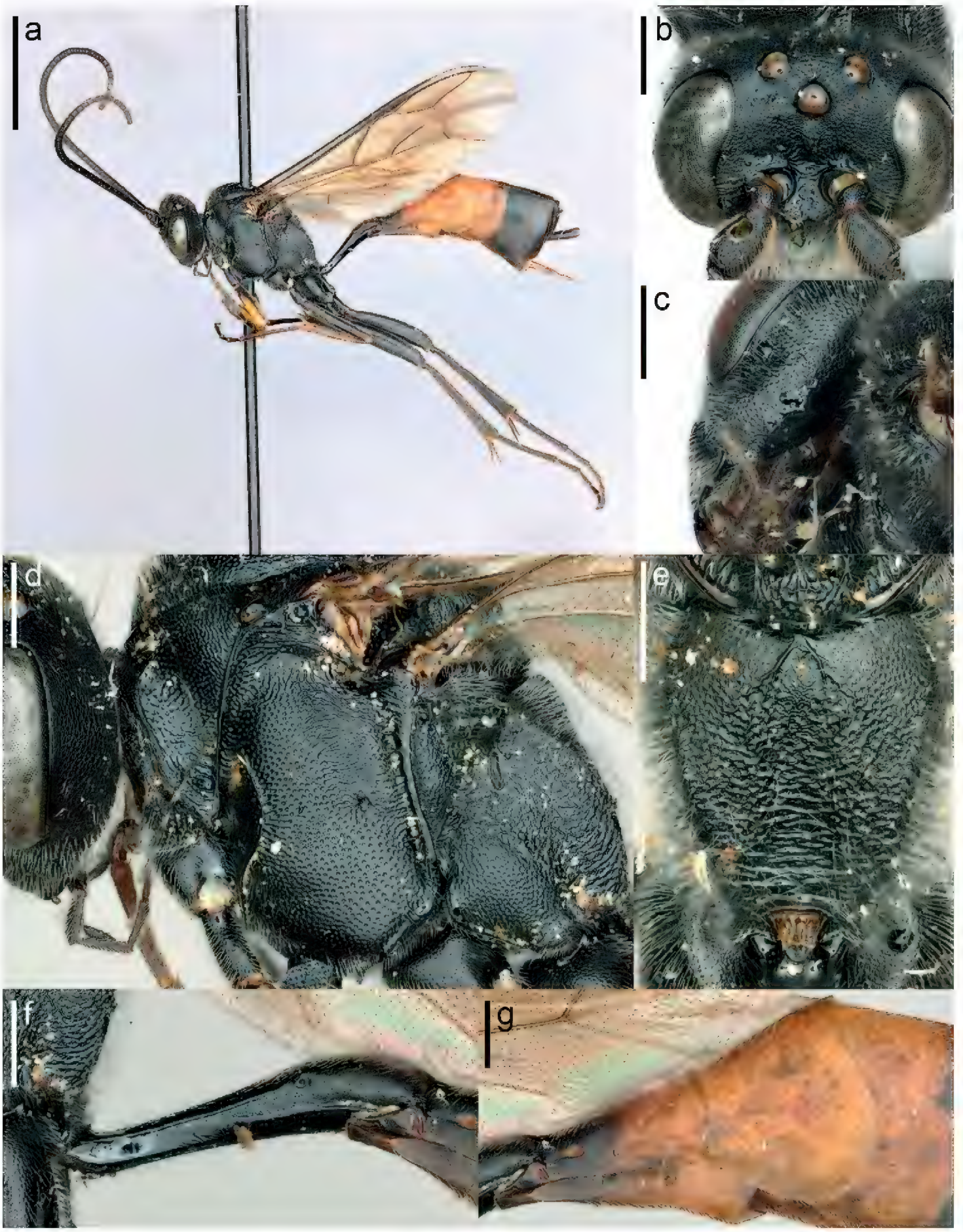

Figure 61. *D. stygia* (Förster, 1868), ♀ Switzerland. **a** habitus **b** antennal carina **c** junction of genal and hypostomal carina **d** mesopleuron **e** propodeum **f** first gastral tergite **g** 2nd and 3rd gastral tergites. Scale bars: 3 mm (**a**); 0.5 mm (**b–g**). https://doi.org/10.5281/zenodo.6370719.

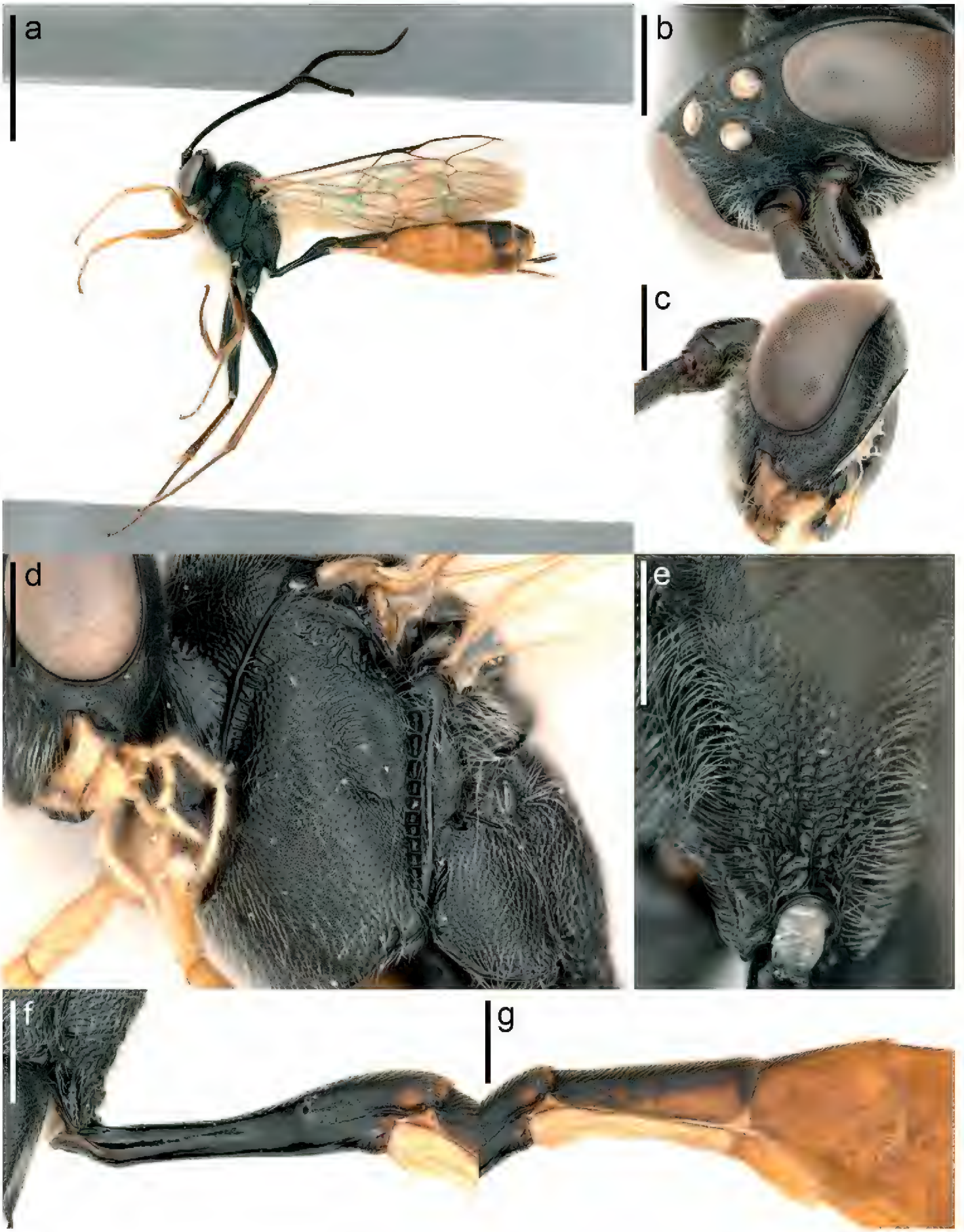

Figure 62. *D. subimpressa* (Förster, 1868), ♀ Sweden. **a** habitus **b** antennal carina **c** junction of genal and hypostomal carina **d** mesopleuron **e** propodeum **f** first gastral tergite **g** 2nd and 3rd gastral tergites. Scale bars: 3 mm (**a**); 0.5 mm (**b–g**). https://doi.org/10.5281/zenodo.6370729.

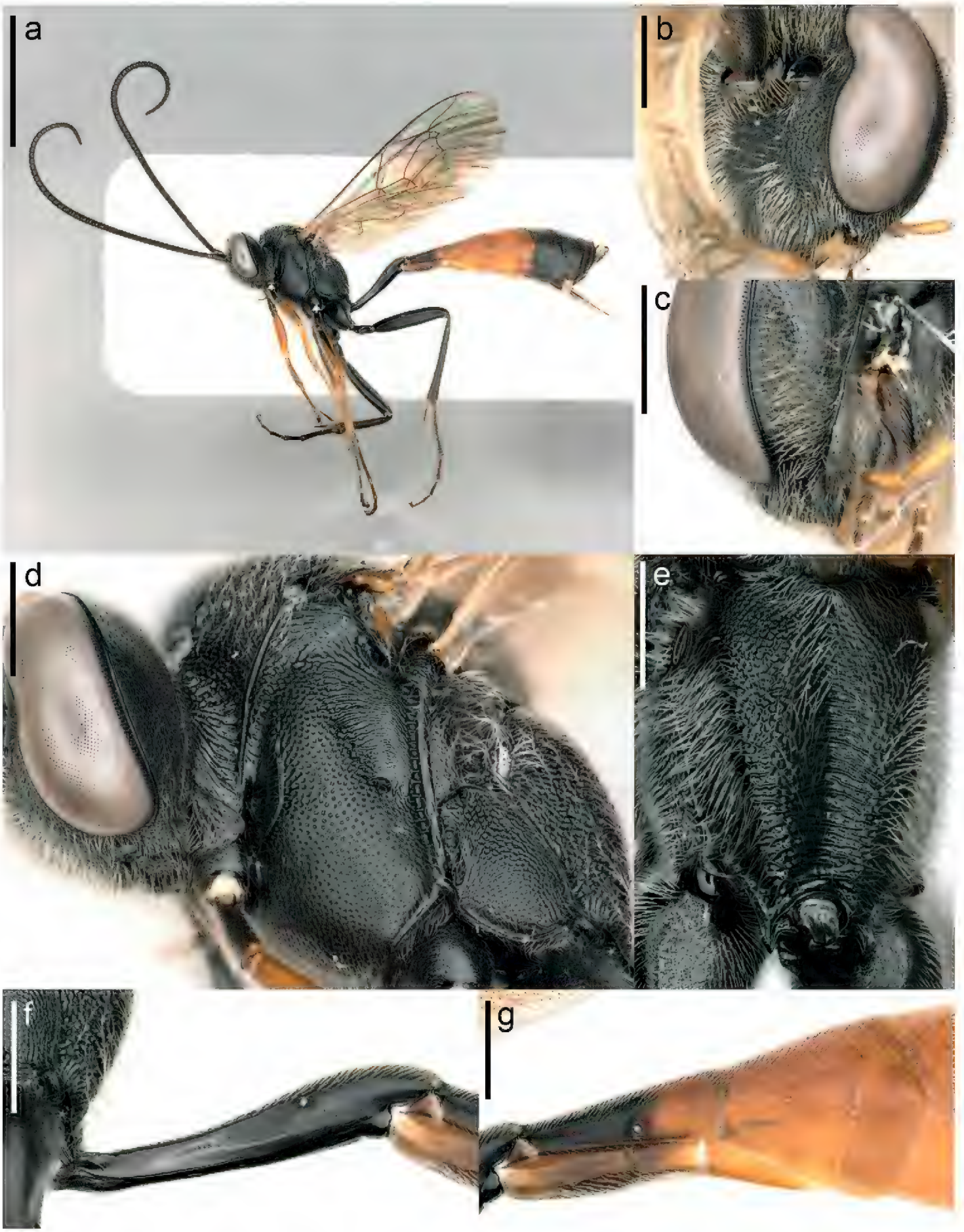

Figure 63. *D. tenuis* (Förster, 1868), ♀ Sweden. **a** habitus **b** antennal carina **c** junction of genal and hypostomal carina **d** mesopleuron **e** propodeum **f** first gastral tergite **g** 2nd and 3rd gastral tergites. Scale bars: 3 mm (**a**); 0.5 mm (**b–g**). https://doi.org/10.5281/zenodo.6370741.

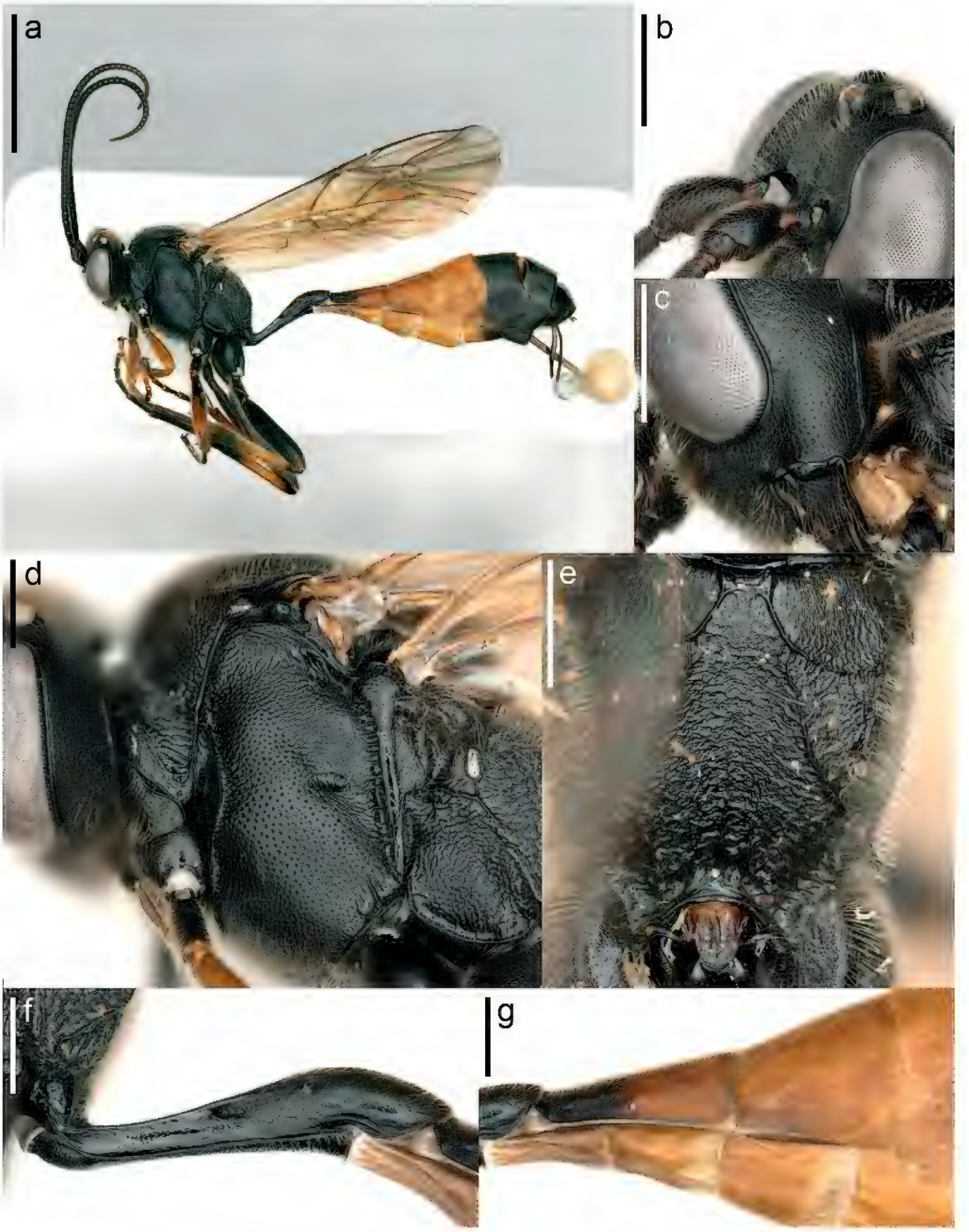

Figure 64. *D. terebrator* (Förster, 1868), ♀ Sweden. **a** habitus **b** antennal carina **c** junction of genal and hypostomal carina **d** mesopleuron **e** propodeum **f** first gastral tergite **g** 2nd and 3rd gastral tergites. Scale bars: 3 mm (**a**); 0.5 mm (**b–g**). https://doi.org/10.5281/zenodo.6370750.

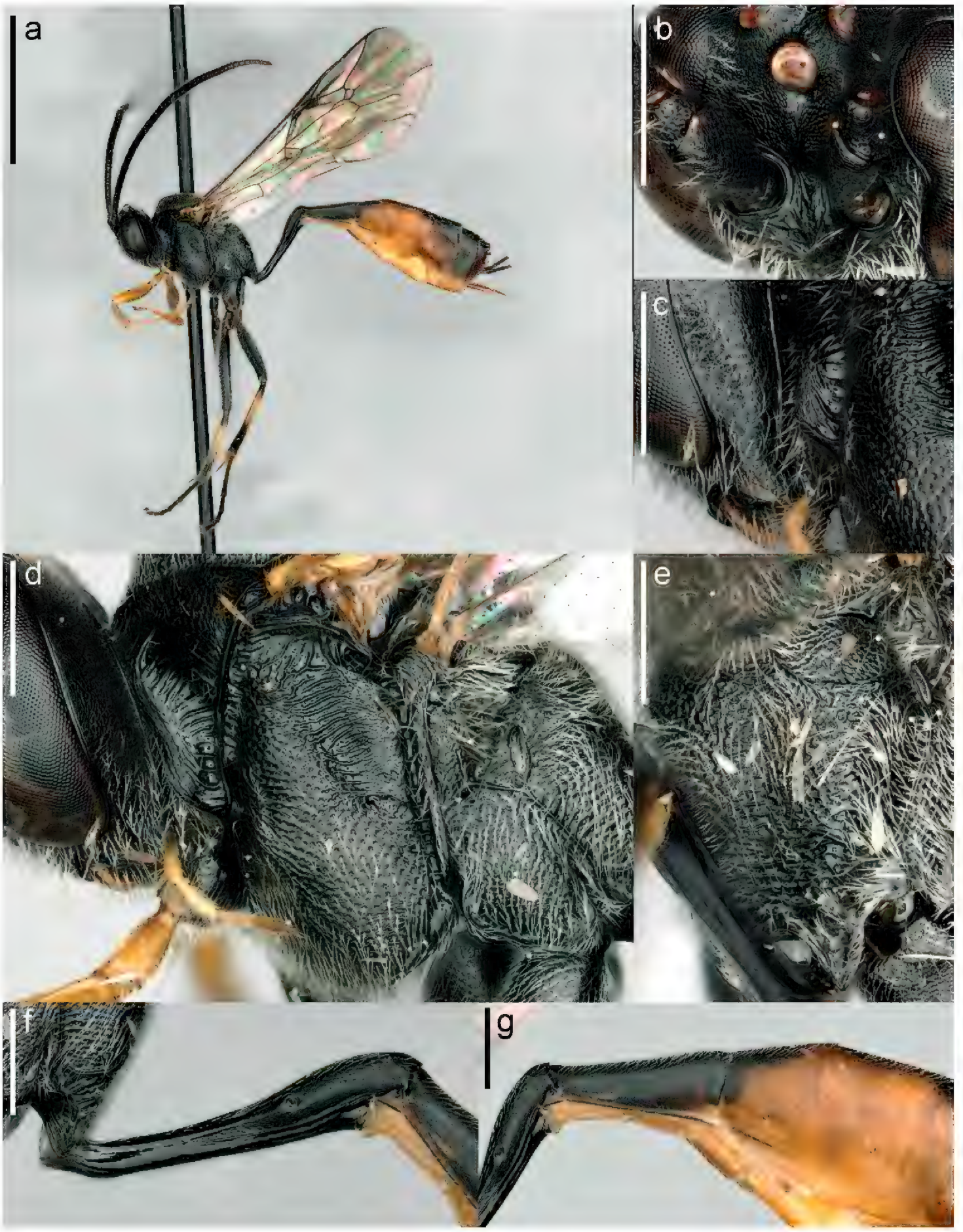

Figure 65. *D. thomsoni* Hinz, 1963, ♀ Norway. **a** habitus **b** antennal carina **c** junction of genal and hypostomal carina **d** mesopleuron **e** propodeum **f** first gastral tergite **g** 2nd and 3rd gastral tergites. Scale bars: 3 mm (**a**); 0.5 mm (**b–g**). https://doi.org/10.5281/zenodo.6370754.

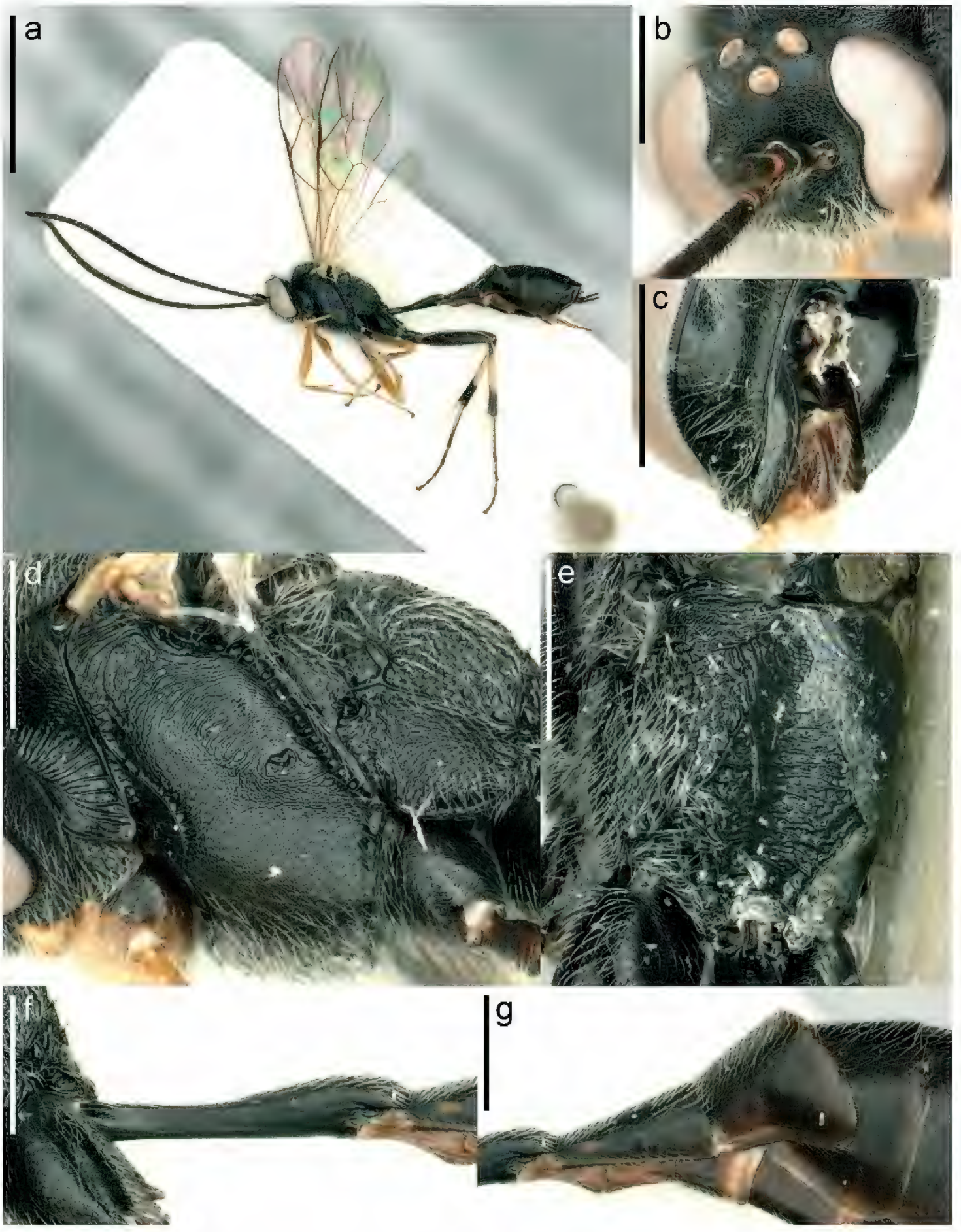

Figure 66. *D. vidua* (Gravenhorst, 1828), ♀ Sweden. **a** habitus **b** antennal carina **c** junction of genal and hypostomal carina **d** mesopleuron **e** propodeum **f** first gastral tergite **g** 2nd and 3rd gastral tergites. Scale bars: 3 mm (**a**); 0.5 mm (**b–g**). https://doi.org/10.5281/zenodo.6370761.

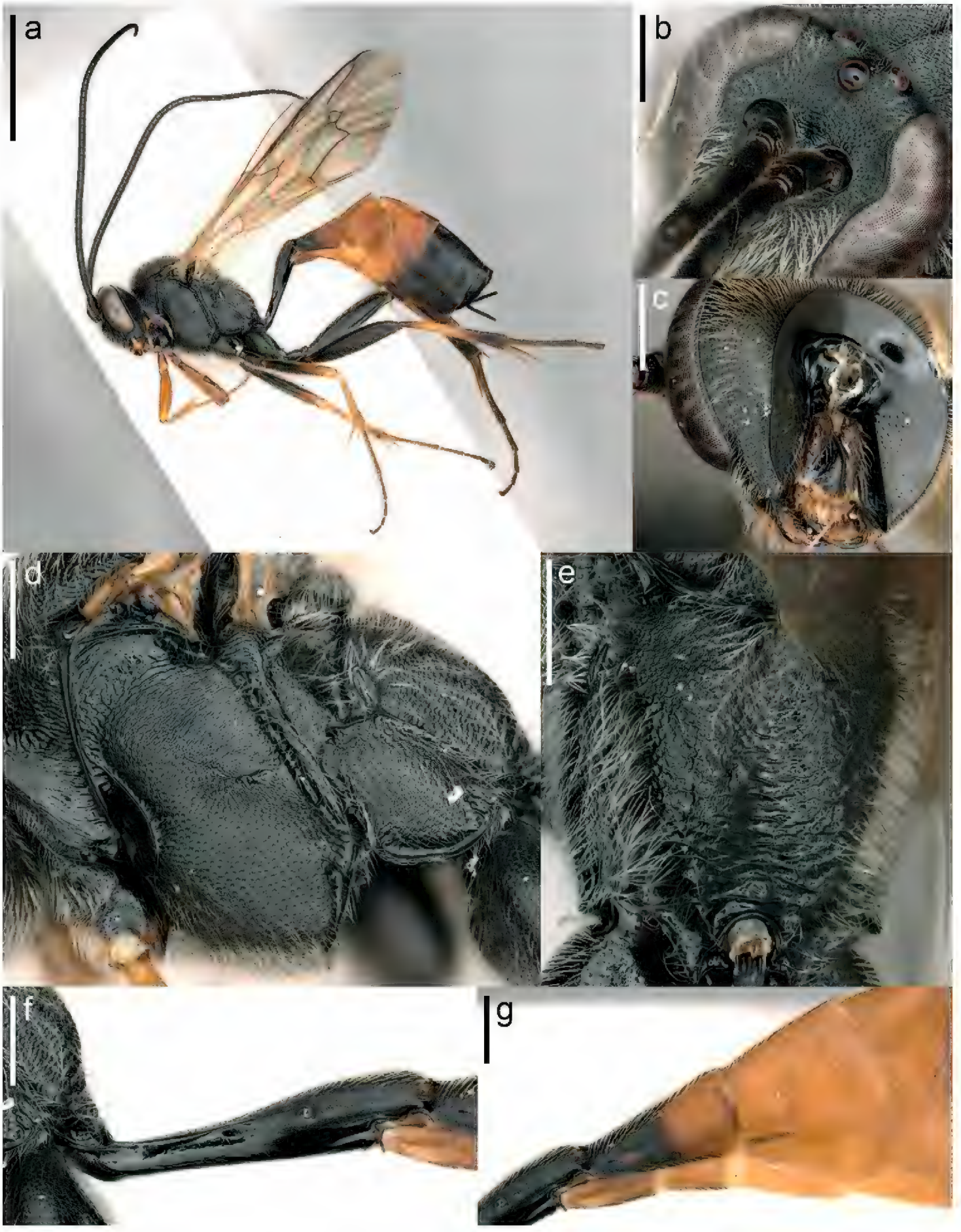

Figure 67. *D. xenocampta* (Förster, 1868), ♀ Sweden. **a** habitus **b** antennal carina **c** junction of genal and hypostomal carina **d** mesopleuron **e** propodeum **f** first gastral tergite **g** 2nd and 3rd gastral tergites. Scale bars: 3 mm (**a**); 0.5 mm (**b–g**). https://doi.org/10.5281/zenodo.6370765.

Molecular analyses

The 658 bp alignment of COI contained 101 sequences of 46 *Dusona* species plus the eight outgroup species, although we only managed to obtain shorter fragments for 18 of them. For the phylogenetic analysis, this data was complemented by three genes (Suppl. material 3, https://doi.org/10.5281/zenodo.6535230). For 28S, we in total obtained 63 sequences of an aligned length of 644 bp, for ITS2 51 sequences of 875 bp, and for CAD, which as a single-copy nuclear gene was the most difficult to amplify, 29 sequences of 433 bp each. The final alignment for the phylogenetic study included 65 specimens from 45 *Dusona* and eight outgroup species and was 2587 bp long. Sequences from Swiss and Swedish material were uploaded to GenBank, sequences from Norwegian material were mostly uploaded to BOLD (Table 3 and Suppl. material 3, https://doi.org/10.5281/zenodo.6535230).

Uncorrected p-distances based on COI sequences were in most cases above 4% between different *Dusona* species and below 1% within each species (Suppl. material 6, https://doi.org/10.5281/zenodo.6535253). However, between three pairs and one triplet of *Dusona* species, the p-distances were rather low, between 0.3% and 1.7%, and one species, *D. mercator* is paraphyletic with respect to *D. angustata* (Table 4). As we consider all these species as morphologically distinct, we do not propose any new synonyms based on similar barcode sequences.

The Bayesian phylogenetic analysis shows a well-supported backbone based on the multilocus-alignment (Fig. 68). However, the phylogeny based on COI alone has a much less supported backbone, which is shown by the large number of polytomies (= support values < 50%; Fig. 69).

In order to test whether it could be useful to split *Dusona* into subgenera, we have tested the phylogenetic distribution of various character states, covering the characters from the section *Assessment and illustration of diagnostic characters*. We have found that the character states dealing with the third laterotergite (fused with tergite or separated by crease of variable length), has a strong phylogenetic signal. Our phylogeny based on four genes reveals that most species that have the third laterotergite completely fused with the tergite cluster together in a distal clade within *Dusona*, and most species that have the third laterotergite separated from the tergite by a crease form a paraphyletic basal group within *Dusona* (Figs 68, 69). However, the length of the crease, i.e., the epipleural index, is is a continuous character. Hence, the division of the genus into two groups (epipleular index equals zero; epipleural index larger than zero), as proposed in the key of Horstmann (2009), does not reflect the true evolutionary history and comes with several outliers, such as *D. xenocampta*, *D. vidua* and *D. carinifrons*. In fact, there seems to be a strong trend from long creases in most basally branching *Dusona* species which form the paraphyletic "*nidulator* group" (*D. nidulator*, *D. leptogaster*, *D. admontina* and *D. terebrator*) towards short creases and completely fused third laterotergites in the distal clade. Given the lacking discriminatory characters and paraphyletic relationship of the basal species group, we do not support the subdivision of *Dusona* into subgenera (Yu et al. 2016).

Table 3. List of *Dusona* specimens examined for this study. For each species the number of males and females for each depository, the countries where the specimens originated from (CH = Switzerland, NO = Norway, SE = Sweden,), the references that were studied for each species and the COI barcodes obtained are indicated. The asterisk (*) indicates first observations of a species for the country. Abbreviations of collections for the material and references studied correspond to the institutions and private collectors listed in Table 1. NMBh stands for the historical collection of the Naturhistorisches Museum Basel, which was treated separately, since no molecular analyses were executed due to the age of this material. Barcodes beginning with "OM…" are published on GenBank, barcodes beginning with "COLLHH…" are published on BOLDsystems.

Species	Country	Material studied	Reference studied	Barcode
D. admontina (Speiser, 1908)	SE*	1♀4♂♂ SMTP	2♀♀ det. Hinz ZSM	
D. aemula (Förster, 1868)	CH*	1♀ NMB; 3♀♀ NJ		OM912312
D. alpigena Hinz, 1972	CH	1♀1♂ NMBh	1♀1♂ Paratypes, det. Hinz MZL	
D. alpina (Strobl, 1904)	SE*	1♀1♂ SMTP	1♀ det. Hinz MZL	OM912313
D. alticola (Gravenhorst, 1829)	SE	1♀ SMTP		OM912314
D. anceps (Holmgren, 1860)			1♂ det. Hinz MZL	
D. angustata (Thomson, 1887)	NO, SE	1♀ HH; 2♀♀1♂ NJ		COLHH2039-18
D. angustifrons (Förster, 1868)	NO, SE	2♀♀ HH; 4♀♀ NJ; 4♀♀2♂♂ SMTP	1♀1♂ det. Hinz MZL	OM912315, COLHH1330-18, COLHH1331-18
D. annexa (Förster, 1868)	CH, SE	5♀♀5♂♂ NMBh; 1♀1♂ SMTP	1♀1♂ det. Hinz MZL	OM912316
D. aurita (Kriechbaumer, 1883)	CH*	1♂ NMB	1♀ det. Aubert JF. MZL; 1♀2♂ det. Hinz ZSM	
D. baueri Hinz, 1973	SE*	2♂♂ SMTP	1♀1♂ Holotype, det. Hinz ZSM	OM912317
D. bellipes (Holmgren, 1872)	CH, SE	1♂ NJ; 17♀♀1♂ NMBh; 1♀ SMTP	1♂ det. Hinz MZL	OM912318
D. bicoloripes (Ashmead, 1906)	CH, NO, SE	3♀♀ HH; 15♀♀1♂ NHRS; 14♀♀ NJ; 21♀♀ NMBh; 84♀♀ SMTP	1♀1♂ det. Hinz MZL	OM912319, OM912320, OM912351, COLHH1316-18, COLHH1317-18, COLHH1318-18
D. blanda (Förster, 1868)	CH, NO, SE	3♀♀ HH; 9♀♀1♂ NJ; 24♀♀29♂♂ NMB; 7♀♀ NMBh; 1♀ NMSG; 26♀♀30♂♂ SMTP	1♀1♂ det. Hinz MZL	COLHH1346-18, COLHH1347-18, COLHH1348-18
D. bucculenta (Holmgren, 1860)	CH, SE	1♀ NJ; 5♀♀12♂♂ NMBh; 2♀♀1♂ SMTP	1♀1♂ det. Hinz MZL	OM912321
D. calceata (Brauns, 1895)	CH*	4♂♂ NMBh	2♀♀ det. Hinz ZSM	
D. carinifrons (Holmgren, 1860)	CH, NO, SE	3♀♀ HH; 3♀♀ NMBh; 1♀ SMTP		OM912322, COLHH1324-18, COLHH1325-18, COLHH1326-18
D. carpathica (Szépligeti, 1916)	CH, NO, SE	1♂ HH; 1♀ NJ; 2♀♀4♂♂ NMB; 1♀1♂ NMBh; 1♀ NMSG; 1♀ SMTP		OM912323, COLHH1320-18
D. circumcinctus (Förster, 1868)	SE	3♀♀1♂ NJ; 3♀♀1♂ SMTP	1♀1♂ det. Hinz MZL	OM912324
D. circumspectans (Förster, 1868)	SE	25♂♂ SMTP	1♂ det. Hinz MZL	OM912325
D. confusa (Förster, 1868)	CH, SE	7♀♀ NJ; 40♀♀ NMBh; 3♀♀ SMTP	1♀1♂ det. Hinz MZL	OM912326, OM912327
D. cultrator (Gravenhorst, 1829)	CH, SE	2♀♀ NJ; 3 ♀♀ NMBh; 2♀♀ SMTP	1♀1♂ det. Hinz MZL	OM912328
D. disclusa (Förster, 1868)			1♂ det. Hinz MZL; 2♀♀2♂♂ det. Hinz ZSM	
D. dubitor Hinz, 1977	CH, SE	5♂♂ NJ; 1♀1♂ NMBh	1♀ det. Hinz MZL	
D. einbecki, Hinz 1977	SE	1♀ NJ		
D. erythrogaster (Förster, 1868)	CH	2♀♀1♂ NMBh	1♀1♂ det. Hinz MZL	
D. falcator (Fabricius, 1775)	CH, SE	3♀♀ NJ; 13♀♀2♂♂ NMBh	1♀ det. Hinz MZL	

Species	Country	Material studied	Reference studied	Barcode
D. flagellator (Fabricius, 1793)	CH, SE	15♀♀ NJ; 7♀♀5♂♂ NMB; 1♀4♂♂ NMBh; 1♀♀3♂♂ NHRS; 6♀♀2♂♂ SMTP	1♀1♂ det. Hinz MZL	
D. habermehli (Kriechbaumer, 1898)			1♂ det. Hinz MZL	
D. humilis (Förster, 1868)	CH, SE	11♀♀ NJ; 3♀♀4♂♂ NMB; 1♂ NMBh; 1♂ NMSG; 3♀♀1♂ SMTP;	1♀1♂ det. Hinz MZL	OM912330
D. inermis (Förster, 1868)	NO, SE	3♀♀ HH; 3♀♀1♂ NJ; 16♀♀4♂♂ SMTP	1♀1♂ det. Hinz MZL	OM912331, COLHH1335-18, COLHH1336-18, COLHH1337-18
D. infesta (Förster, 1868)	CH, NO, SE	1♀ HH; 2♀♀ NJ; 37♀♀9♂♂ NMBh; 2♂♂ SMTP	1♀1♂ det. Hinz MZL	OM912331, COLHH1328-18
D. insignita (Förster, 1868)	CH, NO, SE	2♀♀ HH; 4♀♀1♂ NJ; 2♀♀ NMBh; 4♀♀ SMTP	1♀1♂ det. Hinz MZL	OM912333, COLHH2777-19, COLHH2778-19
D. juvenilis (Förster, 1868)	CH, SE	1♀ NJ; 2♀♀ NMB; 1♀ NMBh	1♀1♂ det. Hinz MZL	OM912334
D. leptogaster (Holmgren, 1860)	SE	5♀♀5♂♂ NJ; 9♀♀4♂♂ SMTP	1♀1♂ det. Hinz MZL	OM912335
D. libertatis (Teunissen, 1947)	SE*	1♀ NHRS	1♀ det. Hinz NHRS	
D. limnobia (Thomson, 1887)	CH, NO, SE	5♀♀ HH; 5♀♀ NJ; 1♂NMB; 1♂ NMBh; 9♀♀7♂♂ SMTP	1♀2♂♂ det. Hinz ZSM	OM912336, COLHH1344-18, COLHH1349-18, COLHH1350-18, COLHH1351-18, COLHH2042-18
D. mercator (Fabricius, 1793)	CH, NO, SE	1♂ HH; 7♀♀ NMBh; 1♀ SMTP	1♀ det. Hinz MZL	OM912337, COLHH1319-18
D. minor (Provancher, 1879)	SE	2♀♀ SMTP		OM912338
D. montana (Roman, 1929)	SE		1♀1♂ det. Hinz MZL	
D. cf. nebulosa (Horstmann, 2004)	SE*	1♂ SMTP		
D. nidulator (Fabricius, 1804)	CH, SE	1♀ NJ; 4♀♀2♂♂ NMBh; 2♀♀4♂♂ SMTP	1♀1♂ det. Hinz MZL	OM912339
D. notabilis (Förster, 1868)	CH, SE	1♀ NJ; 1♂NMB; 2♀♀8♂♂ SMTP	1♀1♂ det. Hinz MZL	OM912340, OM912341, OM912342, OM912343
D. obliterata (Holmgren, 1872)	CH, NO, SE	1♀ HH; 5♀♀ NJ; 6♀♀2♂♂ NMBh; 5♀♀1♂ SMTP	1♀ det. Hinz MZL	COLHH1311-18
D. opaca (Thomson, 1887)	CH, SE*	1♀1♂ NMB; 1♂ SMTP	1♀1♂ det. Hinz MZL	OM912344
D. petiolator (Fabricius, 1804)	CH, SE	10♀♀ NJ; 2♀♀ NMB; 7♀♀2♂♂ NMBh	1♀1♂ det. Hinz MZL	
D. pineticola (Holmgren, 1872)	CH	1♀ NMBh	1♀ det. Hinz MZL	
D. polita (Förster, 1868)	CH, SE	1♀ NJ 4♀♀; NMBh	1♀1♂ det. Hinz MZL	
D. prominula (Förster, 1868)	CH, NO, SE	3♀♀ HH; 4♀♀1♂ NJ; 4♀♀2♂♂ NMBh; 40♀♀7♂♂ SMTP		OM912345, COLHH1312-18, COLHH1332-18, COLHH1333-18
D. pugillator (Linnaeus, 1758)	CH, NO, SE	2♀♀ HH; 21♀♀3♂♂ NHRS; 6♀♀ NJ; 4♀♀2♂♂1♀ NMBh; 2♀♀ SMTP	1♀1♂ det. Hinz MZL	OM912346, COLHH1327-18, COLHH1329-18
D. pulchripes (Holmgren, 1872)	SE	1♀ NJ; 2♀♀4♂♂ SMTP		OM912347
D. recta (Thomson, 1887)	SE*	1♀ NHRS; 1♀ NJ		
D. rugifer (Förster, 1868)	CH, NO	1♂ HH; 1♀ NMBh	1♀1♂ det. Hinz MZL	COLHH1334-18
D. rubidatae Horstmann, 2009	CH, SE*	1♀ NJ; 2♀♀1♂ NMB; 6♀♀3♂♂ SMTP	2♀♀2♂♂ det. Hinz ZSM	OM912348
D. sobolicida (Förster, 1868)	CH, SE	3♀♀ NJ; 2♀♀ NMB; 3♀♀2♂♂ NMBh; 4♀♀2♂♂ SMTP	1♀1♂ det. Hinz MZL	OM912349, OM912350
D. spinipes (Thomson, 1887)	CH, NO, SE*	3♀♀ HH; 4♀♀ NJ; 1♀NMSG; 1♀ SMTP	1♂ det. Hinz MZL; 2♀♀1♂ det. Hinz ZSM	OM912352, COLHH1313-18, COLHH1314-18, COLHH1315-18
D. stragifex (Förster, 1868)	CH, NO, SE	3♀♀ HH; 9♂♂1♂ NJ; 1♀ NMB; 15♀♀3♂♂ NMBh; 2♀ NMSG; 36♀♀12♂♂ SMTP;	1♀1♂ det. Hinz MZL	OM912353, COLHH1321-18, COLHH1322-18, COLHH1323-18
D. stygia (Förster, 1868)	SE*	2♀♀1♂ NJ	1♀ det. Hinz MZL	

Species	Country	Material studied	Reference studied	Barcode
D. subimpressa (Förster, 1868)	CH, NO, SE*	3♂♂ HH; 1♀ NMB; 5♀♀12♂♂ SMTP; 3♀♀1♂ NJ	1♀1♂ det. Hinz MZL	OM912354, COLHH1338-18, COLHH1339-18, COLHH1340-18
D. tenuis (Förster, 1868)	SE	4♀♀ NJ; 3♀♀9♂♂ SMTP	1♀1♂ det. Hinz MZL	OM912356, OM912355
D. terebrator (Förster, 1868)	CH, SE	11♀♀3♂♂ NJ; 1♀ NMB; 6♀♀ NMBh; 4♀♀1♂ SMTP	1♀1♂ det. Hinz MZL	OM912357
D. thomsoni Hinz, 1963	NO	1♀1♂ HH		COLHH1341-18, COLHH2040-18
D. vidua (Gravenhorst, 1869)	NO, SE	1♀1♂ HH; 1♀ SMTP		OM912358, COLHH2043-18, COLHH2779-19
D. xenocampta (Förster, 1868)	CH, SE	6♀♀ NJ; 1♀ NMB; 2♀♀2♂♂ NMBh; 14♀♀5♂♂ SMTP	1♀ det. Hinz MZL	OM912358

Table 4. *Dusona* species with p-distances below 2%. Diagnostic characters differentiating each species. The complete list of p-distances is given in Suppl. material 6, https://doi.org/10.5281/zenodo.6535253.

P-distance	Species	Diagnostic characters (species 1 / species 2 / species 3)
0.33%	*D. annexa* / *D. rubidatae*	Mesopleuron: sculpture (smooth between punctures / coriaceous and dull between the punctures)
1.70%	*D. aemula* / *D. juvenilis*	Ovipositor index (0.6 / 1.3)
1.30%	*D. mercator* / *D. angustata*	Gena: shape behind eyes (distinctly narrowed / widened)
0.35%	*D. angustifrons* / *D. minor* / *D.* cf. *carpathica*	Hind corner of pronotum: distinctly elongate (- / + / -); propodeum: with distinct transverse wrinkles in the median longitudinal furrow (+ / - / -); hind legs: completely black or dark brown (+ / + / -); for *D.* cf. *carpathica,* see also section *species treatments*

Instead of proposing subgenera, we present a number of species groups that clustered together in the phylogenetic analyses and can be easily described by morphological characters. The first to mention is the *mercator* group which consists of *D. mercator*, *D. angustata*, *D. sobolicida* and *D. aurita* within our phylogeny (Figs 68, 69) and was already mentioned by Hinz and Horstmann (2004). The species of this group can be identified by the following synapomorphy: the genal and hypostomal carinae form a lopsided triangular pyramid. Furthermore, most of the species of this group show a conspicuous light yellow metasomal colouration (Hinz 1977). Further species for which we have no molecular data, but likely belong to the *mercator* group based on morphology are *D. calceata* and *D. dubitor.* Then there are two species groups, the *flagellator* group (*D. flagellator*, *D. inermis* and *D. notabilis*) and the *angustifrons* group (*D. angustifrons*, *D. minor*, *D. carpathica*, *D. aemula*, and *D. juvenilis*), that are best described by the homoplastic character of the genal carina meeting the hypostomal carina at the base of the mandible; however, this character state also occurs in *D. pulchripes*, which does not cluster with either of these groups (Figs 68, 69). Generally, the *angustifrons*-group differs from the flagellator-group by having only the second and third metasomal segments marked with red (except for D. minor which differs from the *flagellator*-group by the transverse carina being low) in combination with usually fewer flagellomeres. The *subimpressa* group (*D. subimpressa*, *D. circumcinctus*, *D. spinipes*,

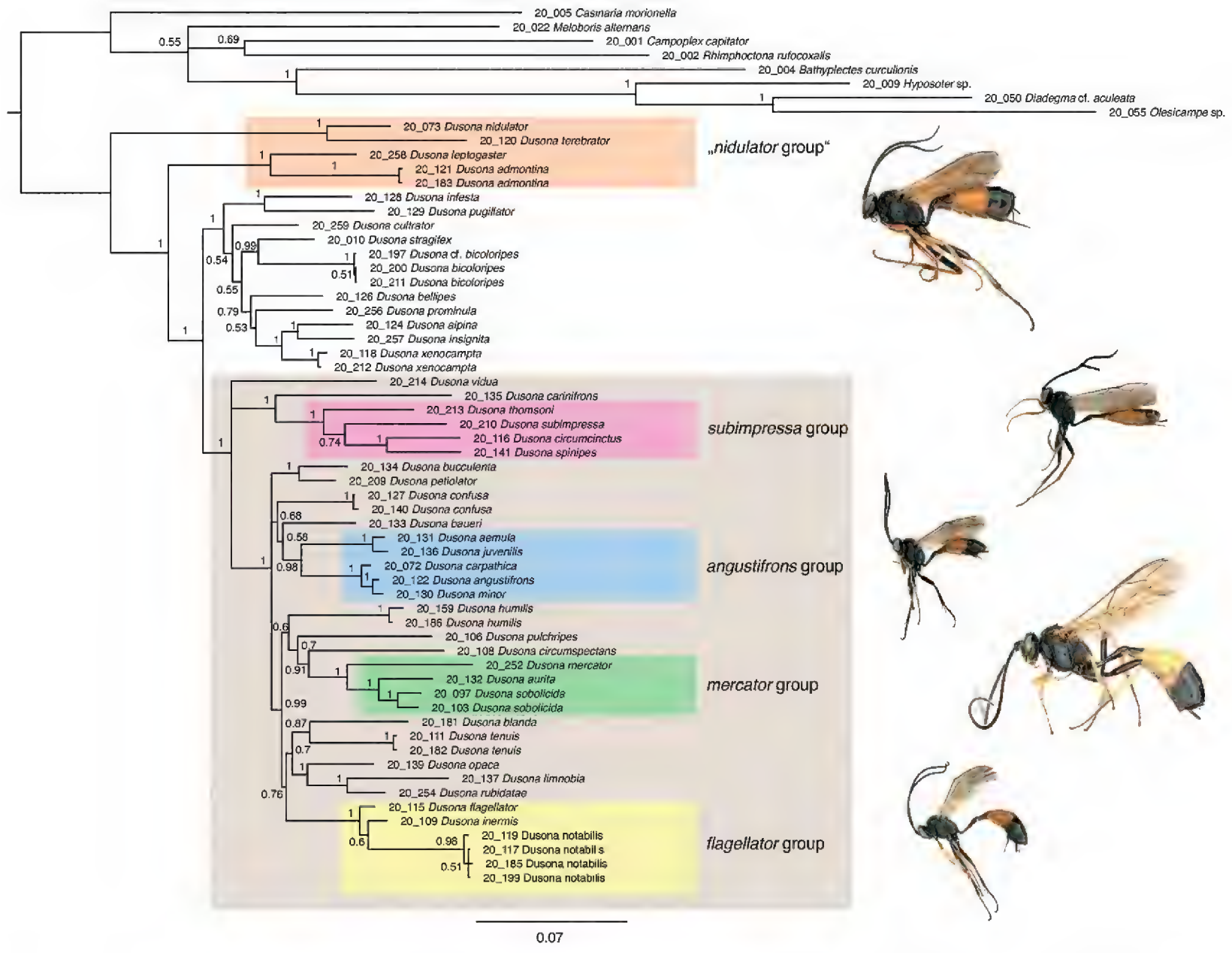

Figure 68. Majority-rule consensus tree as obtained from the Bayesian phylogenetic analysis, based on 4 molecular markers of 45 *Dusona* species and 8 outgroup taxa. Node support values indicate posterior probabilities. Morphologically distinct species groups are indicated by different colours. Pictures show the representative species after which the groups are named.

Figure 69. Majority-rule consensus tree from the Bayesian phylogenetic analysis, based on the barcoding portion of COI of 46 *Dusona* species and 8 outgroup taxa. Node support values indicate posterior probabilities.

D. carinifrons and *D. thomsoni*) is best characterized by the second metasomal tergite being black on the dorsal posterior edge, the transverse carina of the mesopleuron being distinct, and the pleural part of the epicnemial carina being obliterated to a variable extent. Often, the posterior gastral tergites are marked with or completely red in these species. The morphological similarity of the species belonging to the *subimpressa* group (Figs 68, 69) was also reported by Hinz (1977).

Discussion

The role of Darwin wasps in the biodiversity inventory of Sweden

This study reveals the presence of 11 previously unrecorded *Dusona* species for Sweden. However, so far, we have examined only a third of the Campopleginae material from the SMTP and some of the individuals in the collections of the NHRS and of Niklas Johansson. There is certainly much more Swedish material present in other natural history museum and private collections, such as at the Lund Museum of Zoology. The presence of multiple species represented only by a single specimen in our data set and the clearly unsaturated species accumulation curve (Fig. 10c) indicate that the occurrence of additional *Dusona* species is certainly to be expected for Sweden. Furthermore, there might be habitat types that have not been covered extensively by SMTP (Johansson 2020), hence additional sampling might be necessary to complete the faunistic records for this genus. This result lends support to other studies that showed major knowledge gaps for parasitoid wasps and Diptera, even in the faunistic record of well-studied countries such as Sweden (Johansson and Cederberg 2019; Johansson 2020; Johansson and Klopfstein 2020; Riedel 2020; Ronquist et al. 2020). Several of the newly recorded species were restricted to southern and coastal areas (Fig. 9). Hence, it is plausible that in addition to previously overlooked species, some of the newly discovered species could represent recent faunistic changes as a by-product of climate change. Effects of climate change on faunistic assemblages are already observable (Cerini 2020) and expected to lead to immigration of species into higher latitudinal (Dortel et al. 2013) and altitudinal (Gilgado et al. 2022) regions. To further evaluate this aspect, additional sampling is needed in diverse habitats and main collections need to be more thoroughly revised. Even though *Dusona* is the largest genus of Campopleginae, it experienced rather recent revisions in the Palaearctic (Hinz and Horstmann 2004; Horstmann 2009). Interestingly, the proportion of *Dusona* specimens in our sample (8%) was distinctly lower than the proportion of *Dusona* species in the Western Palaearctic fauna of Campopleginae (12%). Maybe *Dusona* species are less abundant or less likely to be caught by Malaise traps than other Campopleginae, but more likely, this indicates that other Campopleginae genera, such as the four next largest genera, *Diadegma* Förster, 1869, *Hyposoter* Förster, 1869, *Olesicampe* Förster, 1869, and *Campoplex* Gravenhorst, 1829, are still much less intensively investigated than *Dusona*. Hence, even more faunistic and taxonomic novelties can be expected for these genera.

Open access to taxonomic knowledge

Since the identification of *Dusona* species and Campopleginae in general has been considered a challenge in taxonomy (Townes 1969b; Broad et al. 2018), one major goal of this study was to improve the applicability of existing keys and to facilitate species identifications for a wide target audience. The photographic guide to diagnostic characters we provide (Figs 1–7) will allow for a better understanding of the different character states mentioned in the keys of Hinz and Horstmann (2004) and Horstmann (2009). Furthermore, the illustrations of almost half of the 125 Western Palaearctic *Dusona* species (n = 57, Figs 11–67) with highly resolved colour plates provides a solid, though incomplete basis for a reference-based species identification. We consider these species plates a highly valuable supplement to the dichotomous keys, as many species have highly distinctive traits in coloration, which are only partly addressed in the existing keys (Hinz and Horstmann 2004; Horstmann 2009). However, in order to be aware of the intraspecific variability of characters and especially of colour traits, the species descriptions in Hinz and Horstmann (2004) and Horstmann (2009) should also be checked. Some species need to be considered as even more variable than previously assumed. In the future, the figures used for the character guide and species plates could even be used to create an interactive key, which again would simplify the species identification compared to strictly dichotomous keys. However, in ecological studies, time and expertise for morphological species determination is often limited. Even though the species treated in this study are generally morphologically distinct, cryptic species also occur in Darwin wasps (Smith et al. 2011; Veijalainen et al. 2011; Johansson and Cederberg 2019). Hence, we have also provided a first extensive reference set of barcodes for 46 *Dusona* species based on reliably identified specimens that are deposited in public collections (Suppl. material 3). Barcodes allow for ecological studies, such as food-web, pollination, or community analysis, with species-level data (Smith et al. 2011; Joly et al. 2014). But also systematics benefits from species-level ecological studies as they can contribute ecological data to strengthen species boundaries (Van Valen 1976; Smith et al. 2011). The completeness of reference barcode libraries is crucial for their value in applied studies (Pinna et al. 2021). In the future, these resources should both be expanded to cover an increasing proportion of the diversity of the genus.

A first glimpse of unknown relationships

We have proposed a first phylogeny of Western Palaearctic *Dusona* species, which is based on a multilocus dataset with 45 *Dusona* species. Many morphological characters were found to be highly homoplastic, and it was thus not possible to define well-supported subgenera. Instead, the evolution of *Dusona* appears to have led to a plethora of parallel evolution of several traits, which means that the genus has to be treated in its entirety in identification keys. Nevertheless, we have recovered several closely related species groups with distinct, unique characters or combinations thereof, such as the *mercator* group or the *subimpressa* group that correspond to species groups suggested already by Hinz (1977). Interestingly, the basal "*nidulator* group" shares the same characters dif-

ferentiating it from the rest of the examined *Dusona* species as the former genus *Kartika* from India (Gupta and Gupta 1976): complete separation of the third laterotergite from the tergite (epipleural index = 0) and a complete petiolar suture. Because these character states are plesiomorphic for Campopleginae, Wahl (1991) declared *Kartika* as a synonym of *Dusona*. Further molecular analyses of Indian *Dusona* species belonging to the former *Kartika* are necessary to evaluate their relatedness to the "*nidulator* group". Even though our data does not suggest to split *Dusona* into subgenera, studying these species groups can help to understand the evolution of characters and maybe host adaptations.

Based on the p-distances, we found that the barcodes were able to differentiate most of the *Dusona* species well (<1% intraspecifically, > 4% interspecifically). However, there were some notable exceptions, with closely related species that showed distances of about 1% or that even turned out as paraphyletic. As these species are morphologically distinct, we suggest this might be evidence either for rapid evolution or mtDNA introgression within *Dusona*, and thus a limitation of barcoding in separating these species. Indeed, barcoding has been shown in the past to have a limited discriminatory power in some Darwin wasp groups, such as Diplazontinae, *Ichneumon* Linnaeus, 1758 and *Enicospilus* Stevens, 1835 (Tschopp et al. 2013; Klopfstein et al. 2016; Shimizu et al. 2020).

Outlook

Future taxonomic work on the genus *Dusona* should aim to complete the barcode library for the well-established Palaearctic fauna, but also focus on the genus diversity in regions lacking recent revisions. Since many *Dusona* species are described from the Nearctic and the Oriental (Yu et al. 2016), these regions appear especially relevant for future revisions. However, the southern hemisphere is still massively under-researched and its diversity of *Dusona* most likely heavily underestimated (Vas and Di Giovanni 2021). Further research is needed to understand the complex evolutionary history of *Dusona*, the processes leading to the rapid radiation within this genus, and the factors driving its host adaptation. Complementing our phylogenetic framework with an extended taxon sampling, including the global diversity of *Dusona,* would be a very ambitious approach but could certainly deliver answers to some of these questions. Based on our study, we hope that the determination of *Dusona* specimens has become more accessible and that more people will be encouraged to work with the genus.

Acknowledgements

We would like to thank everybody who contributed to this study in some way. We are especially grateful to the people who entrusted us with various loans enabling the study of extensive material from Sweden, Switzerland, and some of the reference collection of R. Hinz and K. Horstmann: Dave Karlsson and Carina Romero Ugarph from Station Linné (Öland, SE), Anne Freitag from the Musée Cantonale de Zoology (Lausanne, CH), Stefan Schmidt from the Zoologische Staatssammlung (Munich, DE) and Nik-

las Johansson (Habo, SE). Moreover, we thank the collection assistants at the Naturhistorisches Museum Basel who contributed valuable support in the digitization, labelling and imaging of the specimens: Anina Wacker, Tabia Stoffel, Sarah Müller, and Lara Asady. We thank Anthony Galsworthy, Niklas Johansson and Gavin Broad for reviewing our manuscript and providing excellent suggestions for improvements.

DNA barcode data in this publication were in part generated in collaboration with the Norwegian Barcode of Life Network (NorBOL) funded by the Research Council of Norway and the Norwegian Biodiversity Information Centre. This study was financially supported by the Swedish Taxonomy Initiative (Artdatabanken, grant dha 2019-221). Bioinformatic computations were performed on the HPC cluster UBELIX of the University of Bern, Switzerland (http://www.id.unibe.ch/hpc).

References

Belshaw R, Quicke DLJ (1997) A Molecular Phylogeny of the Aphidiinae (Hymenoptera: Braconidae). Molecular Phylogenetics and Evolution 7: 281–293. https://doi.org/10.1006/mpev.1996.0400

Bennett AMR, Cardinal S, Gauld ID, Wahl DB (2019) Phylogeny of the subfamilies of Ichneumonidae (Hymenoptera). Journal of Hymenoptera Research 71: 1–156. https://doi.org/10.3897/jhr.71.32375

Broad GR, Shaw MR, Fitton MG (2018) 7 Ichneumonid Wasps (Hymenoptera: Ichneumonidae) their Classification and Biology. Field Studies Council for the Royal Entomological Society, Telford.

Cardinale BJ, Duffy JE, Gonzalez A, Hooper DU, Perrings C, Venail P, Narwani A, Mace GM, Tilman D, Wardle DA, Kinzig AP, Daily GC, Loreau M, Grace JB, Larigauderie A, Srivastava DS, Naeem S (2012) Biodiversity loss and its impact on humanity. Nature 486: 59–67. https://doi.org/10.1038/nature11148

Cerini F (2020) Long-term shifts in the communities of Odonata: effect of chance or climate change? North-Western Journal of Zoology 16: 1–6.

Choi J-K, Lee J-W (2014) Addition to the study of the genus *Dusona* (Hymenoptera, Ichneumonidae, Campopleginae) in Korea with description of a new species and key to the Korean species. ZooKeys 424: 58–89. https://doi.org/10.3897/zookeys.424.7546

Di Giovanni F, Reshchikov A, Riedel M, Diller E, Schwarz M (2015) New records of Ichneumonidae (Hymenoptera) for the Italian fauna. Biodiversity Data Journal 3: e5057. https://doi.org/10.3897/BDJ.3.e5057

Dortel E, Thuiller W, Lobo JM, Bohbot H, Lumaret JP, Jay-Robert P (2013) Potential effects of climate change on the distribution of Scarabaeidae dung beetles in Western Europe. Journal of Insect Conservation 17: 1059–1070. https://doi.org/10.1007/s10841-013-9590-8

Dyntaxa (2022) Dyntaxa, Svensk taxonomisk databas. SLU Artdatabanken. www.dyntaxa.se

Folmer O, Black M, Hoeh W, Lutz R, Vrijenhoek R (1994) DNA primers for amplification of mitochondrial cytochrome c oxidase subunit I from diverse metazoan invertebrates. Molecular Marine Biology and Biotechnology 3: 294–299.

Gilgado JD, Rusterholz H, Baur B (2022) Millipedes step up: species extend their upper elevational limit in the Alps in response to climate warming. Insect Conservation and Diversity 15: 61–72. https://doi.org/10.1111/icad.12535

Gupta VK, Gupta ML (1976) A new porizontine genus *Kartika* from India and Burma (Hymenoptera: Ichneumonidae). Oriental Insects 10: 459–496. https://doi.org/10.1080/00305316.1976.10434519

Haraldseide H (2015) Five ichneumonid wasps (Hymenoptera, Ichneumonidae) new to Norway. Norwegian Journal of Entomology 62: 133–134.

Hinz R (1963) Über einige Typen der Gattung *Dusona* Cameron (Hymenoptera: Ichneumonidae). Beiträge zur Entomologie 13: 335–346.

Hinz R (1977) Über einige Arten der Gattung *Dusona* Cameron (Hymenoptera, Ichneumonidae). Nachrichtenblatt der Bayerischen Entomologen 26: 47–54.

Hinz R (1985) Neue sibirische *Dusona*-Arten (Hymenoptera, Ichneumonidae). Deutsche Entomologische Zeitschrift 32: 297–317. https://doi.org/10.1002/mmnd.19850320408

Hinz R (1990) Beiträge zur Taxonomie der Gattung *Delopia* Cameron, 1903 (*Dusona* auct.) (Hymenoptera, Ichneumonidae). Zeitschrift für Entomologie 11: 261–271.

Hinz R (1994) Neue Arten der Gattung *Dusona* Cameron, 1903, aus der östlichen Palearktis (Hymenoptera, Ichneumonidae). Zeitschrift für Entomologie 15: 29–38.

Hinz R, Horstmann K (2004) Revision of the eastern Palearctic species of *Dusona* Cameron: Insecta, Hymenoptera, Ichneumonidae, Campopleginae. Pfeil, München, 183 pp.

Holmgren AE (1872) Om de scandinaviska arterna af ophionidslägtet *Campoplex*. Bihang till Kungliga Svenska Vetenskapsakademiens handlingar 1: 89.

Horstmann K (1995) Typenrevision einiger Ichneumonidae aus der Sammlung Strobl (Hymenoptera). Zeitschrift der Arbeitsgemeinschaft Österreichischer Entomologen 47: 31–35.

Horstmann K (2009) Revision of the western Palearctic species of *Dusona* Cameron. Spixiana 32: 45–110.

Horstmann K (2011) Verbreitung und Wirte der *Dusona*-Arten in der Westpaläarktis (Hymenoptera, Ichneumonidae, Campopleginae). Linzer biologische Beiträge 43: 1295–1330.

Johansson N (2020) Additions to the Swedish fauna of Diplazontinae (Hymenoptera: Ichneumonidae) with the descriptions of five new species. European Journal of Taxonomy 724: e 1159. https://doi.org/10.5852/ejt.2020.724.1159

Johansson N, Cederberg B (2019) Review of the Swedish species of *Ophion* (Hymenoptera: Ichneumonidae: Ophioninae), with the description of 18 new species and an illustrated key to Swedish species. European Journal of Taxonomy 550: 1–136. https://doi.org/10.5852/ejt.2019.550

Johansson N, Klopfstein S (2020) Revision of the Swedish species of *Neoxorides* Clément, 1938 (Ichneumonidae: Poemeniinae) with the description of a new species and an illustrated key to species. European Journal of Taxonomy 680: 1–29. https://doi.org/10.5852/ejt.2020.680

Joly S, Davies TJ, Archambault A, Bruneau A, Derry A, Kembel SW, Peres-Neto P, Vamosi J, Wheeler TA (2014) Ecology in the age of DNA barcoding: the resource, the promise and the challenges ahead. Molecular Ecology Resources 14: 221–232. https://doi.org/10.1111/1755-0998.12173

Karlsson D, Forshage M, Holston K, Ronquist F (2020a) The data of the Swedish Malaise Trap Project, a countrywide inventory of Sweden's insect fauna. Biodiversity Data Journal 8: e56286. https://doi.org/10.3897/BDJ.8.e56286

Karlsson D, Hartop E, Forshage M, Jaschhof M, Ronquist F (2020b) The Swedish Malaise Trap Project: A 15 Year Retrospective on a Countrywide Insect Inventory. Biodiversity Data Journal 8: e47255. https://doi.org/10.3897/BDJ.8.e47255

Katoh K, Rozewicki J, Yamada KD (2019) MAFFT online service: multiple sequence alignment, interactive sequence choice and visualization. Briefings in Bioinformatics 20: 1160–1166. https://doi.org/10.1093/bib/bbx108

Klopfstein S, Kropf C, Baur H (2016) *Wolbachia* endosymbionts distort DNA barcoding in the parasitoid wasp genus *Diplazon* (Hymenoptera: Ichneumonidae). Zoological Journal of the Linnean Society 177: 541–557. https://doi.org/10.1111/zoj.12380

Klopfstein S, Langille B, Spasojevic T, Broad GR, Cooper SJB, Austin AD, Niehuis O (2019b) Hybrid capture data unravels a rapid radiation of pimpliform parasitoid wasps (Hymenoptera: Ichneumonidae: Pimpliformes). Systematic Entomology 44: 361-383. https://doi.org/10.1111/syen.12333

Klopfstein S, Riedel M, Schwarz M (2019c) Checklist of ichneumonid parasitoid wasps in Switzerland (Hymenoptera, Ichneumonidae): 470 species new for the country and an appraisal of the alpine diversity. Alpine Entomology 3: 51–81. https://doi.org/10.3897/alpento.3.31613

Klopfstein S, Santos BF, Shaw MR, Alvarado M, Bennett AMR, Dal Pos D, Giannotta M, Herrera Florez AF, Karlsson D, Khalaim AI, Lima AR, Mikó I, Sääksjärvi IE, Shimizu S, Spasojevic T, Van Noort S, Vilhelmsen L, Broad GR (2019a) Darwin wasps: a new name heralds renewed efforts to unravel the evolutionary history of Ichneumonidae. Entomological Communications 1: ec01006. https://doi.org/10.37486/2675-1305.ec01006

Klopfstein S, Vilhelmsen L, Heraty JM, Sharkey M, Ronquist F (2013) The Hymenopteran Tree of Life: Evidence from Protein-Coding Genes and Objectively Aligned Ribosomal Data. Janke A (Ed.). PLoS ONE 8: e69344. https://doi.org/10.1371/journal.pone.0069344

Kumar S, Stecher G, Tamura K (2016) MEGA7: Molecular Evolutionary Genetics Analysis Version 7.0 for Bigger Datasets. Molecular Biology and Evolution 33: 1870–1874. https://doi.org/10.1093/molbev/msw054

Lue C, Buffington ML, Scheffer S, Lewis M, Elliott TA, Lindsey ARI, Driskell A, Jandova A, Kimura MT, Carton Y, Kula RR, Schlenke TA, Mateos M, Govind S, Varaldi J, Guerrieri E, Giorgini M, Wang X, Hoelmer K, Daane KM, Abram PK, Pardikes NA, Brown JJ, Thierry M, Poirié M, Goldstein P, Miller SE, Tracey WD, Davis JS, Jiggins FM, Wertheim B, Lewis OT, Leips J, Staniczenko PPA, Hrcek J (2021) DROP: Molecular voucher database for identification of *Drosophila* parasitoids. Molecular Ecology Resources 21: 2437–2454. https://doi.org/10.1111/1755-0998.13435

Mardulyn P, Whitfield JB (1999) Phylogenetic Signal in the COI, 16S, and 28S Genes for Inferring Relationships among Genera of Microgastrinae (Hymenoptera; Braconidae): Evidence of a High Diversification Rate in This Group of Parasitoids. Molecular Phylogenetics and Evolution 12: 282–294. https://doi.org/10.1006/mpev.1999.0618

Matsumoto R (2016) Molecular phylogeny and systematics of the *Polysphincta* group of genera (Hymenoptera, Ichneumonidae, Pimplinae): Molecular phylogeny of the *Polysphincta* group. Systematic Entomology 41: 854–864. https://doi.org/10.1111/syen.12196

Mazor T, Doropoulos C, Schwarzmueller F, Gladish DW, Kumaran N, Merkel K, Di Marco M, Gagic V (2018) Global mismatch of policy and research on drivers of biodiversity loss. Nature Ecology & Evolution 2: 1071–1074. https://doi.org/10.1038/s41559-018-0563-x

Mora C, Tittensor DP, Adl S, Simpson AGB, Worm B (2011) How Many Species Are There on Earth and in the Ocean? Mace GM (Ed.). PLoS Biology 9(8): e1001127. https://doi.org/10.1371/journal.pbio.1001127

Oksanen J, Blanchet FG, Friendly M, Mindt R, Legendre P, McGlinn D, Minchin RP, O'Hara RB, Simpson GL, Solymos P, Stevens MHH, Szoecs E, Wagner H (2020) Package "vegan". Community Ecology Package. https://cran.r-project.org, https://github.com/vegandevs/vegan

Pinna M, Saccomanno B, Marini G, Zangaro F, Kabayeva A, Khalaj M, Shaimardan L, D'Attis S, Tzafesta E, Specchia V (2021) Testing the Influence of Incomplete DNA Barcode Libraries on Ecological Status Assessment of Mediterranean Transitional Waters. Biology 10: e1092. https://doi.org/10.3390/biology10111092

QGIS.org (2022) QGIS Geographic Information System. QGIS Association. http://www.qgis.org

Quicke DLJ, Laurenne NM, Fitton MG, Broad GR (2009) A thousand and one wasps: a 28S rDNA and morphological phylogeny of the Ichneumonidae (Insecta: Hymenoptera) with an investigation into alignment parameter space and elision. Journal of Natural History 43: 1305–1421. https://doi.org/10.1080/00222930902807783

Quicke DLJ, Mori M, Zaldivar-Riverón A, Laurenne NM, Shaw MR (2006) Suspended mummies in *Aleiodes* species (Hymenoptera: Braconidae: Rogadinae) with descriptions of six new species from western Uganda based largely on DNA sequence data. Journal of Natural History 40: 2663–2680. https://doi.org/10.1080/00222930601121288

R Core Team (2017) R: A language and environment for statistical computing. R Foundation for Statistical Computing, Vienna. https://www.R-project.org/

Riedel M (2020) Contribution to the Mesochorinae of Sweden (Hymenoptera: Ichneumonidae). Entomologisk Tidskrift 141: 95–120. http://et-online.nu/index.php/contents/article/view/36 [January 29, 2022]

Ronquist F, Forshage M, Häggqvist S, Karlsson D, Hovmöller R, Bergsten J, Holston K, Britton T, Abenius J, Andersson B, Buhl PN, Coulianos C-C, Fjellberg A, Gertsson C-A, Hellqvist S, Jaschhof M, Kjærandsen J, Klopfstein S, Kobro S, Liston A, Meier R, Pollet M, Riedel M, Roháček J, Schuppenhauer M, Stigenberg J, Struwe I, Taeger A, Ulefors S-O, Varga O, Withers P, Gärdenfors U (2020) Completing Linnaeus's inventory of the Swedish insect fauna: Only 5,000 species left? Cerretti P (Ed.). PLoS ONE 15(3): e0228561. https://doi.org/10.1371/journal.pone.0228561

Ronquist F, Teslenko M, van der Mark P, Ayres DL, Darling A, Höhna S, Larget B, Liu L, Suchard MA, Huelsenbeck JP (2012) MrBayes 3.2: Efficient Bayesian Phylogenetic Inference and Model Choice Across a Large Model Space. Systematic Biology 61: 539–542. https://doi.org/10.1093/sysbio/sys029

Sharanowski BJ, Ridenbaugh RD, Piekarski PK, Broad GR, Burke GR, Deans AR, Lemmon AR, Moriarty Lemmon EC, Diehl GJ, Whitfield JB, Hines HM (2021) Phylogenomics of Ichneumonoidea (Hymenoptera) and implications for evolution of mode of parasitism and viral endogenization. Molecular Phylogenetics and Evolution 156: e107023. https://doi.org/10.1016/j.ympev.2020.107023

Shaw MR, Hochberg ME (2001) The Neglect of Parasitic Hymenoptera in Insect Conservation Strategies: The British Fauna as a Prime Example. Journal of Insect Conservation 5: 253–263. https://doi.org/10.1023/A:1013393229923

Shaw MR, Horstmann K, Whiffin AL (2016) Two hundred and twenty-five species of reared western Palaearctic Campopleginae (Hymenoptera: Ichneumonidae) in the National Museums of Scotland, with descriptions of new species of *Campoplex* and *Diadegma*, and records of fifty-five species new to Britain. 67: 47.

Shimizu S, Broad GR, Maeto K (2020) Integrative taxonomy and analysis of species richness patterns of nocturnal Darwin wasps of the genus *Enicospilus* Stephens (Hymenoptera, Ichneumonidae, Ophioninae) in Japan. ZooKeys 990: 1–144. https://doi.org/10.3897/zookeys.990.55542

Sigovini M, Keppel E, Tagliapietra D (2016) Open Nomenclature in the biodiversity era. Isaac N (Ed.). Methods in Ecology and Evolution 7: 1217–1225. https://doi.org/10.1111/2041-210X.12594

Smith MA, Eveleigh ES, McCann KS, Merilo MT, McCarthy PC, Van Rooyen KI (2011) Barcoding a Quantified Food Web: Crypsis, Concepts, Ecology and Hypotheses. Romanuk TN (Ed.). PLoS ONE 6(7): e14424. https://doi.org/10.1371/journal.pone.0014424

Teunissen HGM (1947) Het genus *Campoplex* (Subfam. Ophioninae. Fam. Ichneumonidae). Tijdschrift voor Entomologie 88: 249–270.

Thomson CG (1887) Försök till uppställning och beskrifning af arterna inom slägtet *Campoplex* (Grav.). Opuscula entomologica (Lund) Fasc. XI: 1043–1182.

Townes H (1969a) The Genera of Ichneumonidae, Part 1. Memoirs of the American Entomological Institute 11.

Townes H (1969b) The Genera of Ichneumonidae, Part 3. Memoirs of the American Entomological Institute 13.

Tschopp A, Riedel M, Kropf C, Nentwig W, Klopfstein S (2013) The evolution of host associations in the parasitic wasp genus Ichneumon (Hymenoptera: Ichneumonidae): convergent adaptations to host pupation sites. BMC Evolutionary Biology 13: e74. https://doi.org/10.1186/1471-2148-13-74

United Nations (2015) Transforming our world: The 2030 Agenda for Sustainable Development. [United Nations General Assembly, 2015]

Van Valen L (1976) Ecological species, multispecies and oaks. TAXON 25: 233–239. https://doi.org/10.2307/1219444

Varga O (2021) First record of the genus *Dusona* (Hymenoptera: Ichneumonidae: Campopleginae) from the Ukrainian Carpathians. https://doi.org/10.5281/ZENODO.5749467

Vas Z, Di Giovanni F (2021) New species and records of Afrotropical Campopleginae II. (Hymenoptera: Ichneumonidae). Folia Entomologica Hungarica 82: 7–22. https://doi.org/10.17112/FoliaEntHung.2021.82.7

Veijalainen A, Broad G, Wahlberg N, Longino J, Sääksjärvi I (2011) DNA barcoding and morphology reveal two common species in one: *Pimpla molesta* stat. rev. separated from *P. croceipes* (Hymenoptera, Ichneumonidae). ZooKeys 124: 59–70. https://doi.org/10.3897/zookeys.124.1780

Wahl D (1991) Article: A new species of *Dusona* from New Zealand, and the application of Dusona vs. Delopia (Hymenoptera: Ichneumonidae, Campopleginae). American Entomological Institute 93: 946–950.

Yu DSK, Van Achterberg K, Horstmann K (2016) Taxapad 2016, Ichneumonoidea 2015 (Biological and taxonomcal information), Taxapad Interactive Catalogue Database on flash-drive. Nepean, Ottawa. www.taxapad.com

Supplementary material 1

Taxon list SMTP

Authors: Noah Meier, Karin Urfer, Håkon Haraldseide, Hege Vårdal, Seraina Klopfstein

Data type: Occurence data

Explanation note: Collection data for the material from the SMTP (including coordinates, dates, habitat and species identification), https://doi.org/10.5281/zenodo.6535195.

Copyright notice: This dataset is made available under the Open Database License (http://opendatacommons.org/licenses/odbl/1.0/). The Open Database License (ODbL) is a license agreement intended to allow users to freely share, modify, and use this Dataset while maintaining this same freedom for others, provided that the original source and author(s) are credited.

Link: https://doi.org/10.3897/jhr.91.83318.suppl1

Supplementary material 2

Taxon list CH

Authors: Noah Meier, Karin Urfer, Håkon Haraldseide, Hege Vårdal, Seraina Klopfstein

Data type: Occurence data

Explanation note: Material list for specimens collected in Switzerland (including coordinates, dates and habitat information), https://doi.org/10.5281/zenodo.6535211.

Copyright notice: This dataset is made available under the Open Database License (http://opendatacommons.org/licenses/odbl/1.0/). The Open Database License (ODbL) is a license agreement intended to allow users to freely share, modify, and use this Dataset while maintaining this same freedom for others, provided that the original source and author(s) are credited.

Link: https://doi.org/10.3897/jhr.91.83318.suppl2

Supplementary material 3

Specimens with molecular data

Authors: Noah Meier, Karin Urfer, Håkon Haraldseide, Hege Vårdal, Seraina Klopfstein

Data type: Molecular database accesion numbers

Explanation note: Data for specimens that were used for molecular analyses. Accession numbers for GenBank and BOLD, https://doi.org/10.5281/zenodo.6535230.

Copyright notice: This dataset is made available under the Open Database License (http://opendatacommons.org/licenses/odbl/1.0/). The Open Database License (ODbL) is a license agreement intended to allow users to freely share, modify, and use this Dataset while maintaining this same freedom for others, provided that the original source and author(s) are credited.

Link: https://doi.org/10.3897/jhr.91.83318.suppl3

Supplementary material 4

PCR conditions

Authors: Noah Meier, Karin Urfer, Håkon Haraldseide, Hege Vårdal, Seraina Klopfstein

Data type: Methodology

Explanation note: PCR conditions, https://doi.org/10.5281/zenodo.6535284.

Copyright notice: This dataset is made available under the Open Database License (http://opendatacommons.org/licenses/odbl/1.0/). The Open Database License (ODbL) is a license agreement intended to allow users to freely share, modify, and use this Dataset while maintaining this same freedom for others, provided that the original source and author(s) are credited.

Link: https://doi.org/10.3897/jhr.91.83318.suppl4

Supplementary material 5

MrBayes Input file

Authors: Noah Meier, Karin Urfer, Håkon Haraldseide, Hege Vårdal, Seraina Klopfstein

Data type: Genomic

Explanation note: Input file with molecular data for MrBayes - Bayesian phylogenetic inference https://doi.org/10.5281/zenodo.6535309.

Copyright notice: This dataset is made available under the Open Database License (http://opendatacommons.org/licenses/odbl/1.0/). The Open Database License (ODbL) is a license agreement intended to allow users to freely share, modify, and use this Dataset while maintaining this same freedom for others, provided that the original source and author(s) are credited.

Link: https://doi.org/10.3897/jhr.91.83318.suppl5

Supplementary material 6

P-distances

Authors: Noah Meier, Karin Urfer, Håkon Haraldseide, Hege Vårdal, Seraina Klopfstein

Data type: Phylogenetic

Explanation note: P-distances calculated for all retrieved COI sequences, https://doi.org/10.5281/zenodo.6535253.

Copyright notice: This dataset is made available under the Open Database License (http://opendatacommons.org/licenses/odbl/1.0/). The Open Database License (ODbL) is a license agreement intended to allow users to freely share, modify, and use this Dataset while maintaining this same freedom for others, provided that the original source and author(s) are credited.

Link: https://doi.org/10.3897/jhr.91.83318.suppl6